NOVA SCHOOL OF SCIENCE & TECHNOLOGY

PHYSICS DEPARTMENT

INÊS ISABEL CANELAS NUNES JORGE

Bachelor's Degree in Biomedical Engineering Sciences

DEVELOPMENT OF AN OBJECTIVE MEASUREMENT SYSTEM FOR QUALITY ASSESSMENT OF CHEST COMPRESSIONS DURING CPR

DISSERTATION TO THE OBTENTION OF MASTER'S DEGREE ON BIOMEDICAL ENGINEERING

INTEGRATED MASTER'S ON BIOMEDICAL ENGINEERING

Universidade NOVA de Lisboa

November, 2021

NOVA SCHOOL OF SCIENCE & TECHNOLOGY

PHYSICS DEPARTMENT

DEVELOPMENT OF AN OBJECTIVE MEASUREMENT SYSTEM FOR QUALITY ASSESSMENT OF CHEST COMPRESSIONS DURING CPR

DISSERTATION TO THE OBTENTION OF MASTER'S DEGREE ON BIOMEDICAL ENGINEERING

INÊS ISABEL CANELAS NUNES JORGE

Bachelor's Degree in Biomedical Engineering Sciences

Supervisor: Prof. Dra. Carla Sá-Couto, Affiliated Professor and Director, Centro de Simulação Biomédica, Faculdade de Medicina da Universidade do Porto

Co-supervisor: Prof. Dr. Pedro Vieira, Assistant Professor, NOVA School of Science and Technology, Universidade NOVA de Lisboa

Jury Panel

President: Prof. Dra. Carla Maria Quintão Pereira, Auxiliar Professor, NOVA School of Science and Technology, Universidade NOVA de Lisboa

Arguer: Prof. Dr. Dawei Liang, Affiliated Professor, NOVA School of Science and Technology, Universidade NOVA de Lisboa

Vogal: Prof. Dra. Carla Sá-Couto, Affiliated Professor and Director, Centro de Simulação Biomédica, Faculdade de Medicina da Universidade do Porto (supervisor)

INTEGRATED MASTER'S ON BIOMEDICAL ENGINEERING

Universidade NOVA de Lisboa

November, 2021

Development of an Objective Measurement System for Quality Assessment of Chest Compressions during CPR

À minha mãe, Manuela,
ao meu pai, Jorge,
ao meu irmão, João
e à minha avó, Fortunata.

ACKNOWLEDGMENTS

It was a long and challenging way towards this achievement, but also a happy and rewarding one. As I often say, the greatest luck I have had in life is the people that have come across my path. In this end of chapter, that was, once more, the rule.

Success and great achievements are often in the end of a learning path made individually but guided by someone who tells us the best way to go. For this guidance, for all the help, advice and dedication invested in me and in this project, and for keeping me on track when I was getting lost in different treads, moved by curiosity, I have much to thank to Prof. Dr. Carla Sá-Couto. It was a privilege to work and to get to know such inspiring and brilliant person. You are an example of professionalism, and an inspiration for the type of biomedical engineer I hope to be someday. For the same guidance, I also thank to Eng. Abel Nicolau, who had an incredible relevance for the success of this achievement, and that invested so much energy and dedication in this project without expecting nothing in return, only moved by the passion for his work. Thank you for all the advisory, motivation and friendship. It was a pleasure to be your first apprentice. Both of you gifted me with the opportunity to experience simulation and, through your passion, turned it into an area that captivates and fascinates me.

To Dr. Nélia Alberto, Dr. Paulo Antunes and, in particular, Dr. Maria de Fátima Domingues, from *Instituto de Telecomunicações da Universidade de Aveiro*, I thank for the amazing collaboration and all the availability to help me in an area that I could never be able to explore without your help. From the first contact, my ideas were embraced and my curiosity motivated. Without your support, your guidance in an unfamiliar area for me, and your collaboration, a significant part of this work would not be possible.

Furthermore, I would like to thank to Prof. Dr. Pedro Vieira, one of the professors whose professionalism and teaching style most captivated me during my academic years, and that I have the privilege to have as co-supervisor of this project.

Beyond the professional component, this journey is also made by one's personality and posture towards challenges. The values that are the basis of my personality derive from my education. In that aspect, I owe so much to my family. To my parents, José Jorge and Manuela Jorge, thank you for all the support, constant care, and for believing in me more than I do. Thank you for giving me all the tools I needed to build my own way, the freedom to do so, and to become who I want to be. If today I am who I am, I owe it to you. To my older brother, João Jorge, thank you for always taking such good care of me, for being my best friend and the person I know I can always count on, for everything. And

finally, to my grandmother, Fortunata Canelas, thank you for help raising me, making me the person I am today, and, even without a full understanding of my professional adventures, always supporting, appreciating, and celebrating my achievements.

I could not end these acknowledgments without thanking one of the most important people of my life. Thank you, Francisco Formosinho, for being by my side and accompanying me, cherishing and loving me, and celebrating my achievements as yours, for almost eight years now. Thank you for every smile and for making me happy every day.

Many other friends I cherish were left to thank… Thank you for everything and for always having a smile to give me.

I hope I make all of you proud.

“Não tenhas medo da criatividade.”
(Jorge Enes)

ABSTRACT

Out-of-hospital cardiac arrest is the third leading cause of death in Europe, with an associated survival rate of only 8%. A rapid and effective intervention of the community with the application of the Basic Life Support (BLS) algorithm and the execution of Cardiopulmonary Resuscitation (CPR), emphasizing chest compressions, can double chances of victim survival. Being CPR of critical impact on victim survival and extremely accessible to all the community, it is important and necessary to guarantee the quality of BLS education, optimizing CPR skills acquisition and knowledge retention. In this context, the use of devices to support CPR training trough real-time feedback are considered by international guidelines an important tool for BLS education as they allow training monitorization and show improvement on CPR training performance and skills acquisition. Based on this educational need, this project presents several approaches, from electronic sensors to exploratory optical fiber technology, for the development of a low-cost feedback device for CPR training, focused on assessing chest compression quality, in order to facilitate a more objective and regular training, potentiating a more effective knowledge acquisition and retention. From all the technologies tested, the selected approaches for prototype development showed great response and robustness to chest compressions during CPR training, providing accurate assessment of specific parameters of chest compressions, according to current international guidelines. Thus, it is expected that the proposed solution could provide an alternative or a complementary tool for CPR skills acquisition and maintenance on BLS education. As future work, it is recommended the inclusion of ventilation related measurements and further development envisioning educational validation.

Keywords: Cardiopulmonary Resuscitation; Feedback devices; Chest compression quality.

RESUMO

A paragem cardíaca em contexto pré-hospitalar constitui a terceira causa de morte a nível europeu, com uma taxa de sobrevivência associada de apenas 8%. A intervenção rápida e eficaz da comunidade com a aplicação do algoritmo de Suporte Básico de Vida (SBV) e a execução da manobra de Ressuscitação Cardiopulmonar (RCP), com especial ênfase nas compressões torácicas, pode chegar a duplicar a probabilidade de sobrevivência das vítimas. Tendo esta manobra um impacto crucial na sobrevivência, e sendo extremamente acessível e exequível por qualquer membro da comunidade, é essencial e necessário garantir a qualidade da educação em SBV, otimizando a aquisição e retenção de competências de RCP. Neste contexto, o uso de dispositivos que apoiam o treino da manobra de RCP através de *feedback* em tempo real são considerados pelas diretrizes internacionais ferramentas importantes na educação em SBV, dado que permitem a monitorização do treino e mostram melhorias na performance da manobra e na aquisição de competências. Tendo por base esta necessidade educacional, este projeto apresenta várias abordagens (desde o uso de sensores eletrónicos à exploração do usa da fibra ótica enquanto sensor) para o desenvolvimento de um dispositivo de *feedback* de custo controlado, com foco na qualidade das compressões torácicas, de maneira a facilitar um treino mais objetivo e regular, que potencie a aquisição e retenção destas competências. De todas as abordagens testadas, a usada no desenvolvimento do protótipo de treino mostrou uma resposta muito adequada e robusta às compressões efetuadas durante o treino de RCP, fornecendo uma leitura e avaliação precisas de parâmetros específicos das compressões torácicas, de acordo com as atuais diretrizes internacionais. Posto isto, espera-se que a solução proposta providencie uma alternativa ou uma ferramenta complementar na aquisição e manutenção das competências de RCP na educação em SBV. Como trabalho futuro, recomenda-se a inclusão dos parâmetros de treino de RCP relacionados com a ventilação e desenvolvimento de estudos de validação educacional.

Palavras-chave: Ressuscitação Cardiopulmonar, Dispositivos de *feedback*; Qualidade das compressões torácicas.

TABLE OF CONTENTS

TABLE OF FIGURES

TABLE OF TABLES

ACRONYMS

AED	Automated external defibrillator
BLS	Basic Life Support
CPR	Cardiopulmonary Resuscitation
CSB-FMUP	Centro de Simulação Biomédica da Faculdade de Medicina da Universidade do Porto
EMS	Emergency medical services
ERC	European Resuscitation Council
FBG	Fiber Bragg grating
IDE	Integrated Development Environment
IMU	Inertial measurement unit
OHCA	Out-of-hospital cardiac arrest
RMSE	Root mean square error
SCA	Sudden cardiac arrest

1 INTRODUCTION

Out-of-hospital cardiac arrest (OHCA) is one of the major causes of death in developed countries [1]. High quality cardiopulmonary resuscitation (CPR), with emphasis on chest compressions, is proved to have a fundamental impact on OHCA victim survival [1]. Nevertheless, CPR is rarely provided in case of OHCA due to the lack of knowledge of the general population in Basic Life Support (BLS) and, when provided, is commonly performed ineffectively, due to unproductive training and low skill retention, leading to a decreased probability of victim survival. Thus, there is an important need of educating and training the community, and to do it effectively.

The traditional approach for BLS education and CPR training is based on isolated sessions with an extensive theoretical module and a practical training component on a manikin, with feedback on the performance provided subjectively by an instructor. However, there is evidence that instructors provide poor feedback, especially in the correction of chest compressions related parameters [2]. Additionally, the lack of frequent practice is associated with a rapid decay in skill quality and retention [2]. Several studies comparing the CPR training quality with, and without training feedback systems suggest that the use of these feedback devices and their integration on BLS education seems to significantly improve the quality of chest compressions, not only by providing objective feedback, but also by promoting frequent training.

The proposed project aligns with this educational and training need and consists in the design, implementation and testing of a system to objectively measure chest compressions quality during CPR training. More than promoting a more effective BLS education, this project aims to strengthen the quality of CPR training with higher skills acquisition and knowledge retention by supporting and encourage a more regular training, through an accurate and accessible feedback system.

This dissertation presents the work developed over ten months in *Centro de Simulação Biomédica da Faculdade de Medicina da Universidade do Porto*, and is organized in seven different chapters. In Chapter 2 this project is further contextualized by presenting the impact of the BLS algorithm in cardiac arrest, the available educational strategies and their limitations, and the importance of objective feedback devices in CPR training. Current technologies for CPR training feedback, included in market search and a literature review, are presented and discussed in Chapter 3, in order to overview the existing alternatives, their limitations, which this project intends to overcome, and emphasize the need to develop new technologies for CPR training and assessment. The next three

chapters present the core development work of this dissertation, referring to the technical description of the developed measurement systems, described in detail, and a critical analysis of the advantages and limitations of the methods used. Two parallel approaches were considered for development: one considering an operational approach using off-the-shelf sensors, presented in Chapter 4; and another with an exploratory and innovative approach using optical fiber technology as a sensory system, presented in Chapter 5. Chapter 6 applies the developed systems to CPR training and, through established metrics, assesses chest compressions quality, providing concept validity. The closing chapter, Chapter 7, provides an overall discussion of the selected approach and ends with recommendations and insights for future developments.

2

BASIC LIFE SUPPORT AND EDUCATIONAL STRATEGIES FOR CPR TRAINING

This chapter introduces relevant concepts on Basic Life Support (BLS) principles, according to the European Resuscitation Council (ERC) guidelines [1], emphasizing high-quality cardiopulmonary resuscitation (CPR) and the role of the community on out-of-hospital cardiac arrest (OHCA) victim survival. In-hospital cardiac arrest, despite of its importance, is not further explored as it is out of the scope of the proposed work. Beyond CPR and BLS fundamental research, educational strategies and effective training are also of major relevance [3], and are further explored in this contextualization chapter, as they are essential to the comprehension of the proposed work application.

2.1 Introductory Concepts: Sudden Cardiac Arrest, Chain of Survival and Basic Life Support Algorithm

Sudden cardiac arrest (SCA) is the third leading cause of death in Europe [4]. In particular, OHCA has an annual incidence between 67 to 170 per 100 000 individuals per year [4], [5], with an increasing number of reported OHCAs in recent years, and an estimated survival rate of only 8% [5]. In Portugal, according to the most recent data of National Institute of Medical Emergency, during the year of 2020, there were documented 21 992 OHCA occurrences [6].

This event can be defined as an unexpected failure in heart effective contraction which stops blood circulation [7] , primarily with cardiovascular (80%) or cardiac (60%) aetiology [8], and with victims tolerating several acute symptoms, most commonly angina and dyspnea, within one hour before collapse occurring [7]. Most of the victims present previously documented cardiac diseases or relevant risk factors, conditions which increase the risk of rhythmic disturbances and heart failure [8]. Among the non-cardiac causes, there is a spectrum of reported aetiologies being the most common stroke and pulmonary disease [8]. In 20% of the cases [5], SCA is triggered by initial shockable rhythms, (predominantly ventricular fibrillation with 76% of the cases [7]), which is one of the most important predictors of survival after an OHCA. Proceeding with immediate resuscitation in an OHCA victim, preferably while the initial shockable rhythm is still present, has a crucial impact in the return of

spontaneous circulation and, thus, victim survival [7]. After the collapse, cardiac rhythm tends to deteriorate to asystole, jeopardizing survival chances [7].

The Chain of Survival summarizes the links for an early and efficient resuscitation in the context of OHCA (Figure 2.1). This chain, and hence the victim survival, depends on a sequence of actions, including early recognition of cardiac arrest, through the detection of victim unresponsiveness and abnormal breathing (also called agonal breathing), activation of the Emergency Medical Services (EMS), early bystander CPR, early use of automated external defibrillator (AED), and effective Advanced Life Support and standardized post-resuscitation care, provided by EMS in order to improve patient outcomes [1], [7].

Even though the apparent emphasis of the impact of medical dependent elements of the Chain of Survival, the role of the community and its coordination with the EMS is of major importance, as those are the elements with greater impact on patient survival [9]. In fact, regarding OHCA recognition, while unresponsiveness is easily detectable, agonal breathing remains the biggest barrier to recognition of OHCA, being commonly misinterpreted as a sign of life by bystanders [1]. Early recognition of agonal breathing is a prerequisite for early CPR and defibrillation, and failure in the recognition of this symptom is highly associated with decreased survival [1]. Additionally, activating the EMS allows not only an earlier EMS arrival, but also creates the opportunity for faster recognition of OHCA and immediately start of CPR, assisted by the emergency medical dispatcher [7]. The mean time from emergency call to EMS arrival is 5 to 11 minutes, time during which the victim survival depends on bystander CPR and the use of an AED [7]. Regarding CPR, chest compressions are the key component of effective resuscitation, as they provide organ perfusion during cardiac arrest [1], allowing a more gradual decline in victim survival, and buying time for EMS arrival [7]. For every minute without CPR, survival from SCA decreases by 7 to 10% [10]. When bystander CPR is provided, the decrease in survival is more gradual and averages 3 to 4% per minute [10] . The effectiveness of chest compressions is dependent on four maneuver components, which are further detailed in section 2.2. Additionally, if the use of AEDs by bystanders is allowed, which depends on national legislation and regulatory boards, defibrillation attempts prior to EMS arrival [1] is recommended. This may increase survival rate up to 70% if performed within the first 3 to 5 minutes after collapse [7], when a shockable rhythm is present.

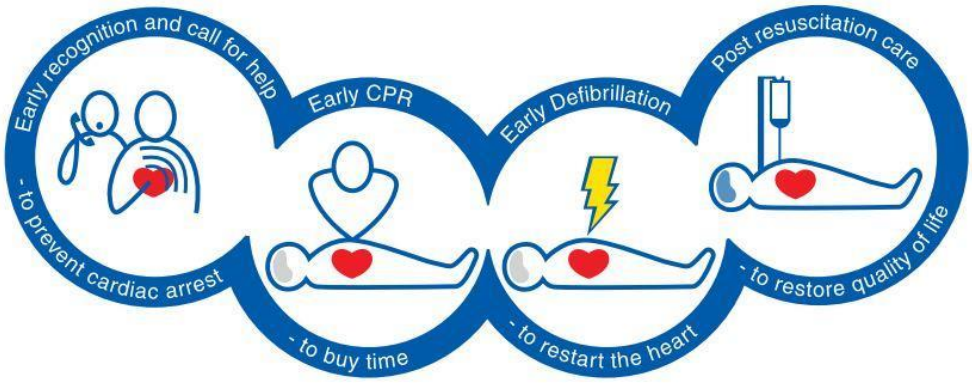

Figure 2.1. OHCA Chain of Survival [7].

In a more general view, early initiation of effective CPR, associated with early defibrillation, can double or quadruple survival from OHCA [7], being this value two-times higher when CPR is immediately started by a bystander than when it is only started after the arrival of EMS [5]. Thus, there is a critical need for bystanders to act, as the victim survival depends on their readiness to initiate resuscitation. Nevertheless, the proportion of OHCA cases where resuscitation is attempted is still not ideal. According to European data, bystanders initiated CPR in 58% of cases, and resuscitation was later commenced or continued in about 50% to 60% of cases attended by EMS [5].

In order to emphasize the importance of taking action in case of OHCA, and how to do it properly, a practical algorithm included in the steps of the Chain of Survival for effective resuscitation was created: the adult BLS sequence (Figure 2.2). It comprises a sequence of actions, which include the assessment of unresponsiveness and agonal breathing, EMS activation, high-quality CPR, and early, correct use of an AED, in a logical and concise manner designed to be easily learned, remembered and performed. Detailed step-by-step sequence can be found in [1]. Due to the direct impact in victim survival and the relevance for the developed work contextualization, within the BLS algorithm, high quality CPR is further detailed.

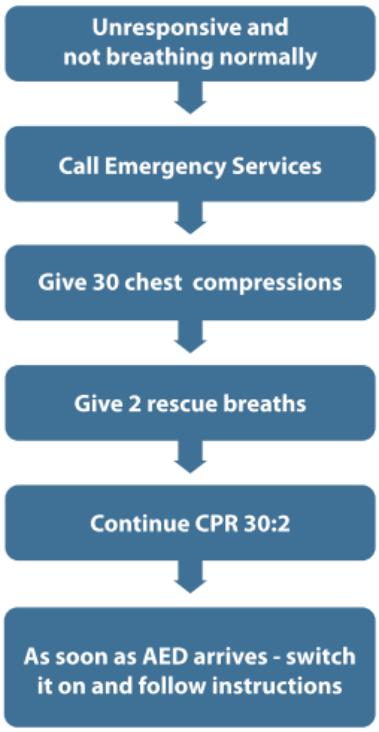

Figure 2.2. Basic Life Support and automated defibrillation algorithm [1]

2.2 Cardiopulmonary Resuscitation

CPR consists in a sequence of chest compressions and ventilations, intended to maximize survival in case of SCA [7], that must be repeated until victim recovery, by waking up, moving, opening eyes and breathing normally [1], EMS arrival, or exhaustion of the rescuer (Figure 2.3). Chest compressions aim to keep blood circulating, partially restoring coronary and cerebral blood flow, which increases the probability of the heart resuming its electrical activity with an effective rhythm, and the return of spontaneous circulation [7]. Ventilations, on the other hand, assure blood partial oxygenation [7]. Continuous chest compressions are most beneficial in early phases of OHCA, having priority in CPR in comparison to ventilation [7]. In fact, right after a cardiac arrest, the arterial blood remains highly oxygenated, and the victim's characteristic agonal breathing facilitates gas exchanges [7], ventilation becoming more important only in later phases.

CPR is most easily delivered by a provider kneeling by the side of the victim, as this facilitates movement between compressions and ventilations with minimal interruptions [7]. To deliver effective and high-quality chest compressions to an adult victim, CPR providers must take into consideration four maneuver components [1]: hand position, compression rate, compression depth and chest recoil (Figure 2.3).

With straight arms making a 90° angle with the victim's chest, chest compressions must be delivered on the lower half of the sternum, for an improved hemodynamic response [1]. Hands must be on top of each other, with fingers interlocked to ensure that pressure is not applied in the victim's ribs [7]. The recommended compression rate, which has been proven to increase survival among patients, is between 100 and 120 compressions per minute, without taking into consideration any interruptions [1]. While a low compression rate shows to be hemodynamically ineffective, a very high rate is associated with a decrease in compression depth [7]. The recommended compression depth for effective CPR ranges between 5 and 6 cm [1]. This is a difficult parameter to estimate in a practical context, since it is often influenced by factors such as fatigue, the provider's limited muscle strength and fear of

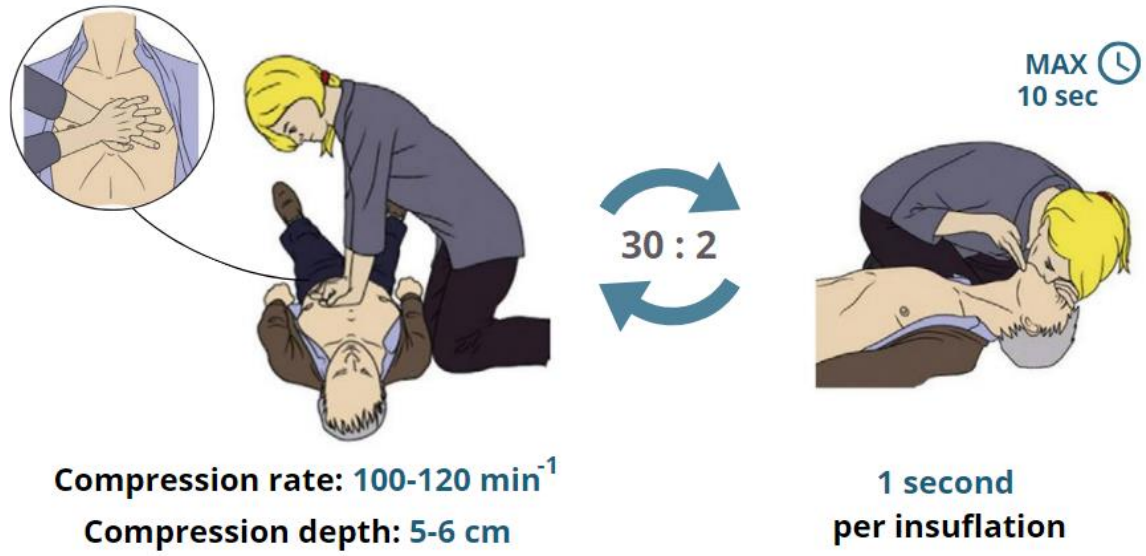

Figure 2.3. Adult Basic Life Support simplified algorithm. CPR performance: chest compressions and rescue breaths. Adapted from [7].

causing harm [7], which results, typically, in ineffective shallow compressions [7]. In contrast, compressions with more than 6 cm of depth are associated with an increased injury rate [7], and must be avoided. Lastly, permitting a full chest recoil between compressions allows a superior intrathoracic negative pressure, aiding the venous return to the heart, which improves cardiac output and, consequently, coronary and cerebral perfusion [11]. Thus, providers should avoid leaning on the victim's chest between compressions, allowing full chest recoil [1].

Effective ventilations follow specific guidelines to potentiate blood oxygenation. Trained providers must deliver the volume necessary to cause a visible victim's chest rise (about 500 to 600 ml), using 1 second duration inflations [7]. The recommended compression-ventilation ratio is 30:2 [1] (Figure 2.3). This ratio provides a good compromise between blood flow and oxygen delivery: once the blood flow during CPR is reduced, lower respiratory rates and tidal volumes can maintain an effective oxygenation [7]. Interruptions in chest compressions to provide ventilation should not exceed the 10 seconds in any circumstances [1]. Any pauses in chest compressions mean pauses in organ perfusion, and consequently need to be minimized to prevent ischemic injury [1]. In fact, it has been proven that survival is higher when chest compression fraction, (proportion of time of chest compressions during CPR) exceeds 60%, being this value considered the minimum to maintain CPR quality [1], [7].

To be noticed that, according to BLS guidelines [1], ventilations are not recommended for untrained bystanders to perform, being endorsed compression-only CPR (continuous compressions meeting the stipulated quality parameters). Only bystanders who are trained, able, and willing to give rescue breaths and chest compressions should do so for all adult patients in cardiac arrest [1], since complete CPR seems to slightly improve patient outcomes, in comparison with compression-only CPR [7].

Despite of the well-established medical science regarding BLS, and CPR proven impact on OHCA victim survival, this maneuver is still shortly attempted in OHCA cases, mainly due to general lack of knowledge of the community in BLS [12]. An effective community response that draws Chain of Survival and BLS elements together is the key to improving survival from OHCA. Raising the community awareness to CPR education by highlighting the value of bystander CPR, and by including training that prioritizes effective chest compressions could improve the adherence to the maneuver, the overall quality of bystander CPR and, hence, victim survival. On the other hand, even when resuscitation is attempted, OHCA survival rates remain suboptimal, revealing that educational activities are not sufficient or consistently achieving their intended outcomes [13].

2.3 Educational Strategies in CPR Training

Initially, CPR was taught to health care professionals and to first aiders. Subsequently, evidence emerged about the importance of community intervention to foster early resuscitation attempts as a key to increasing survival after cardiac arrest [3], as pointed in previous sections. This has led to the expansion of CPR education to other population groups [3].

Educating and training laypeople has a considerable impact on their willingness to undertake BLS in a real situation [14]. According to ERC guidelines, the primary goals of resuscitation training for laypeople are the reinforcement of the Chain of Survival and BLS algorithm performance (including the use of an AED), emphasizing high quality chest compressions [3], [14]. This content should be presented in a simplified and consistent manner, in order to facilitate the acquisition and retention of skills [13], [14]. Enhancing willingness to perform CPR as part of the CPR training program in this population may have a direct impact on survival rates for OHCA [3]. According to the educational needs of the community and the required competency level, there is a variety of teaching programs with different CPR training interval, frequency, duration, and need for retraining, along with the required teaching equipment for the level of training and assessment [3]. Depending on this training format, recertification is needed within 1 to 5 years [15].

Regarding CPR training, several studies have been made to refine training strategies with the view of improving skill acquisition and retention. Repetitive hands-on performance of skills in a manikin coupled with informative feedback and assessment promotes trainees' deliberate practice in key skills and their development toward mastery [13], [14]. The use of devices that provide directive feedback on compression rate, depth, chest recoil, and hand position can improve the quality of chest compressions during training [3], being considered an educational key feature to improve CPR performance [13], [14]. Additionally, spaced learning (training or retraining distributed over time) seems to be more effective than mass learning (education provided close together in time) [3], [16]. In fact, evidence suggests that more frequent (re)training improves not only CPR skills, but responder confidence and willingness to perform CPR [3], [16]. Recommended educational key points and core concepts in resuscitation education for bystanders are summarized in Figure 2.4.

Traditionally, instructor-led training courses remain the most frequently used method for BLS training [14], [17]. These courses, based in a theoretical and practical training on a manikin, are typically organized in a single period of training (mass practice), lasting 3 to 4 hours, with small groups (recommended 6 trainees per instructor) [14], [18]. CPR training sessions include a training manikin torso, which allows training to be targeted to the need of the trainee, with multiple practice attempts in order to achieve competence [19]. A standardized assessment of performance during and at the end of the training with feedback provided by the instructor is given [14], being commonly the only source of performance assessment for trainees' practical skills [2].

Some of the key problems with this training model are time, logistics and money [18]. In fact, evidence shows that several trainees report scheduling difficulties, underlying incompatibility to accommodate long CPR training courses [18]. Moreover, considering the number of certified

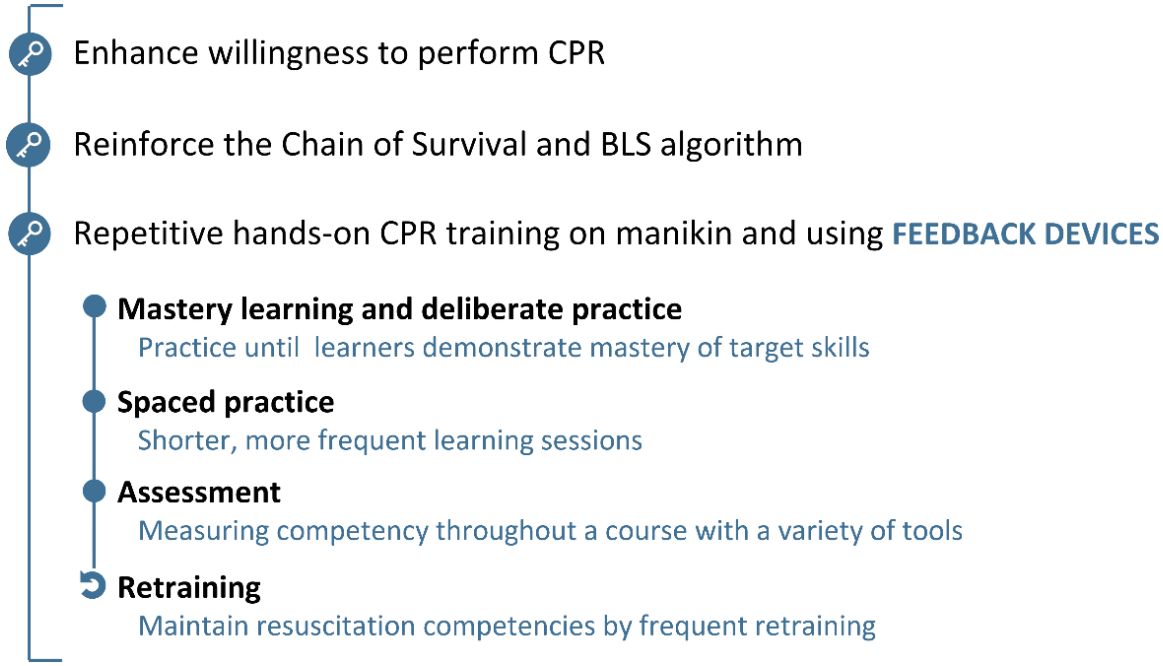

Figure 2.4. Key points and core educational concepts recommended for bystanders BLS courses. Adapted from [3], [13].

instructors and manikins required, traditional CPR courses can pose significant logistical and financial barriers [18].

Regarding content and methodology, this training model is usually rich in didactics, with too much time spent on cognitive material and overall time for skills practice being often compromised [18], resulting in insufficient and inadequate technical skills [12], and knowledge decay within 3 to 12 months [14]. Among other factors that may explain the poor retention of CPR skills, subjective instructor feedback, inadequate practice time, and low training frequency stand out [18], [2]. In particular, feedback on performance is strongly associated with improvement of skill acquisition and retention during BLS training, being a crucial component of the learning process [19], [2]. Instructors assess visually all iterations of trainees' skill performance to determine if, globally, it meets the required standards for high quality CPR [19], [2]. This is a complex task, which provides highly subjective feedback, potentially, assessment errors. In fact, there is strong evidence that instructors often provide poor feedback regarding correction of skills, especially on chest compressions performance [2], [19], [20]. Additionally, the interpersonal nature of sessions and the time constraints of training many trainees at once makes it difficult to equally distribute instructors' attention between trainees, compromising an adequate performance assessment [19].

To resume, traditional courses have often been considered lengthy, inefficient and labor-intensive [18], with poor feedback provided by the instructor. Recognizing these barriers to learning and performing CPR, other alternatives for CPR instruction have been proposed to make training shorter, more accessible, inexpensive, more focused on individuals practice, and requiring less resource utilization than traditional courses [18], without compromising skills performance and retention. With that in mind, the use of feedback devices can play an important role in making CPR training more adjusted to an ideal training process.

2.3.1 The use of Feedback Devices in CPR Training

Over the past few years, many new technologies have become available to teach CPR [3]. In particular, tools for self-guided CPR training, namely the use of feedback devices, with shortened instructor guidance, seems to be a useful tool for quality improvement regarding compression rate and depth, chest recoil, and hands position, being its use strongly recommended by ERC guidelines [3]. The implementation of these alternatives may not only provide better and complementary training and assessment through objective feedback [20], but also help to overcome cited traditional training limitations. On one hand, by providing real-time support with auditory and/or visual information on CPR quality, these devices allow a more objective evaluation of CPR performance [13], [19]. This rigorous and informative feedback during and after skills practice allows trainees to receive structured information on how to improve their performance [13], reinforcing their knowledge. On the other hand, feedback devices can promote more frequent (re)training, allowing short-duration trainings with increased practice time, and to a broader population, as they are easily accessible and logistically easy to set up, offering the opportunity of learning and continuous training outside the course context [18], [20]. Moreover, the possibility of frequent self-training allows skills development and maintenance over time adapted to each trainee's pace, increasing their confidence on the performance [20], which may enhance willingness to perform CPR.

To be noticed, however, that the use of these devices should ensure that training manikins respond and react accurately to CPR performance in accordance with guidelines [21]. The agreement between the performance feedback given by manikins and the guidelines still constitutes a challenge [21]. In fact, feedback devices are more prone to failure and inaccurate feedback provision, possibly giving an erroneous feeling of competence specially in non-supervised training settings. This means that, first, objective performance data from feedback devices should be systematically validated, and second, that the use of these devices do not exclude the contributions of a training instructor. Lastly, in is important to be noticed that feedback devices may be expensive and may not be available in all settings [21].

Nevertheless, feedback devices are assumed to be a key complement to improve resuscitation training as it allows an easier implementation of recommended educational objectives, promoting frequent training with a more objective, reliable and standardized feedback on skills' quality, which has proved to be effective for skills building and is expected to maintain competence over time [3]. Several studies have been made to study the actual impact of the use of feedback devices on CPR teaching and learning, including skills retention, although the results are not consensual. Relevant efforts are being made in order to overview these studies and clarify this impact [22].

Chapter Conclusions

The lifestyle of developed countries led to a high incidence of cardiovascular diseases, leading to an increasing tendency of SCA occurrences, which constitute one of the leading causes of death. OHCA cases are of worrying importance due to the extremely low survival rate of only 8%. Along the years, the importance of the community response to these cases have been emphasized, being reflected in a growing number of different BLS training approaches targeted at laypeople, with a wide variety of contents, formats, and tools. Although there is no clear consensus on the optimal training format, instructor-led short sessions with hands-on feedback-device-supported practice seems to be a superior alternative for high-quality CPR skills acquisition. To enhance skill retention, frequent re-training shows a clear advantage, although it is not the regularly observed approach for BLS education and CPR training. The use of feedback devices can not only improve CPR skills acquisition (and possibly their maintenance over time) due to the provision of objective feedback, but also help to achieve a more efficient training methodology, overcoming logistical and monetary limitations of traditional education. Thus, its use is strongly recommended by the ERC.

3

FEEDBACK DEVICES FOR CPR TRAINING AND QUALITY ASSESSMENT – STATE-OF-THE-ART

Several devices and technologies have been developed to provide correct and objective feedback during CPR training. Beyond the accurate real-time measurement of CPR performance, the way feedback is provided and the quality assessment of the overall performance, which includes the assessment of each CPR component, has great influence in training outcomes and effectivity. Taking that into consideration, this chapter overviews available feedback devices for CPR training, through an extensive market search, and explores the technologies described in literature used to assess CPR maneuver quality. CPR quality parameters are then reviewed and discussed. This chapter ends with the presentation of a feedback training prototype developed at the *Centro de Simulação Biomédica* of *Faculdade de Medicina da Universidade do Porto* (CSB-FMUP), representing the local state-of-the-art, which forms the basis for the development of this project.

3.1 On-the-market Feedback Devices

Along the years, several devices, with different measurement methods, design, usability and complexity, have been developed in order to provide guidance and objective feedback during CPR training [23]. Objective feedback is based on quality data measurements of several CPR performance variables, which are processed and often displayed as visual information or voice messages [23]. In particular, real-time feedback reacts to changes immediately, informing the trainee and the instructor whether current CPR is effective and, if not, how to improve it [23]. These devices must align with the latest guidelines for high-quality CPR, measuring the correct compression rate, depth and full chest recoil, and provide corrective feedback on performance by presenting the data in real-time [24]. Hand position, despite of not being considered as a requirement in feedback devices, is considered a relevant parameter for high quality chest compressions, and is often included.

Feedback devices range from a simple metronome or a clicker, which guide compression rate and compression depth, respectively, to more complex devices that monitor training and provide audiovisual feedback about actual CPR performance [25]. These include stand-alone devices, which

are typically small and portable devices to be placed between the chest and trainee's hands, and only provide feedback on chest compression quality [23]; AEDs with integrated CPR feedback that contain all the components for effective basic management of cardiac arrest (guidance and feedback for effective CPR and defibrillation) [23]; and manikins with integrated CPR feedback, which can provide feedback on chest compressions and ventilations, to assess about high-quality CPR during training [25]. Both stand-alone devices and AEDs with integrated CPR feedback are typically designed to be used in a real cardiac arrest situation, but can also take part in training settings, by being applied on the manikin. Stand-alone devices are reported as cost-effective and easy to use, but are also frequently reported as uncomfortable during CPR maneuver or training, promoting trainee's fatigue and risk of injury [23]. On the contrary, AEDs with integrated CPR feedback are rather expensive, heavy and can be difficult to handle for laypeople [23]. More recently, smartphone apps have been used to provide guidance and feedback during CPR, initially, through audio-prompts training instructions or metronomes [23], and later by exploiting the built-in accelerometer and providing real-time audiovisual feedback to the trainee [1]. As technology has evolved, the same concept has been applied to smartwatches thanks to their small size and their wearability [1]. Despite the premise that these smart devices could help to improve the quality of CPR due to their wide availability nowadays, the results on the effectiveness and utility of these devices for improving the quality of CPR have been conflicting [26].

Using the training manikin to provide feedback on CPR maneuver quality, by instrumenting it with adequate sensory technology, is a practical, user-friendly, comfortable and, nowadays, cost-effective alternative to contribute for good BLS education and high-quality CPR skills acquisition and retention. Thus, that was the alternative chosen to develop the present work. Considering this, a market search on adult manikin torsos with integrated CPR feedback, used exclusively for BLS education and CPR training was carried out. Table 3.1 summarizes the findings of this research, detailing the chest compressions feedback type. More complex instrumented manikins, with broader simulation features, were considered to be out of the scope of the present work, since they are not specifically designed for CPR training, implying that the accuracy of CPR quality measurements can be compromised in order to fit other simulation features. Feedback on ventilation parameters, present in most of the considered devices, were not included in this review as the focus of the present work lays on chest compression quality. Regarding sensory technology, all commercialized feedback devices reviewed do not disclose the technology/system used, even after extended search, which included patent databases. For that reason, this information was not included in Table 3.1. A review of main sensory technologies for chest compression quality assessment is presented in section 3.2.

The first step to provide high-quality CPR training is to use realistic CPR manikins that mimic performing CPR on a real person, with realistic anatomical features and high-fidelity chest compliance, essential for correct hand placement and correct compression execution, respectively. All the reported manikins consider human anatomical features, although chest compliance can differ significantly between models.

Regarding feedback features, the data collected by manikin instrumentation needs to be presented in some form of an interface in order to provide CPR guidance during training. Feedback can be visual, audible, or audiovisual, and its type and frequency have great impact on CPR quality [23].

Table 3.1. CPR training feedback devices currently available on market: extracted CPR quality parameters and feedback visualization (December 2020).

Device	**Description**	**Feedback**		
		Real-time CPR Parameters	**Real-time Feedback Type**	**Overall Training Report**
Simulaids® Visual Training Assistant Manikin with CPR feedback (Econo and Adult Brad manikins) [27], [28]	Instrumented manikin torso with cable connected external visual feedback system	Compression rate Compression depth	Visual feedback (all): external 2 LED system (binary feedback)	Nonexistent
Prestan® Ultralite Manikin [29]	Instrumented manikin with torso incorporated visual feedback system	Compression rate Compression depth	Visual feedback (rate): manikin-incorporated single LED system; Audio feedback (depth): manikin incorporated clicker.	Nonexistent
Prestan® Professional Adult Manikins [30]	Instrumented manikin with torso incorporated visual feedback system	Compression rate Compression depth	Visual feedback (all): manikin-incorporated 4 LED system; Audio feedback (depth): manikin incorporated clicker.	Nonexistent
Prestan® Professional 2000 Series Manikins [31]	Instrumented manikin torso with incorporated visual feedback system. Data communication via Bluetooth to an app, for additional feedback.	Compression rate Compression depth Chest recoil	Visual feedback: - Manikin-incorporated 4 LED system (rate, depth); - Prestan® Feedback CPR App (all); Audio feedback (depth): manikin incorporated clicker.	Available (if connected to Prestan® Feedback CPR App): CPR duration, mean CPR parameters value/quality, compression score and chest compression fraction.
3B Scientific® BasicBilly+ with Heartisense® CPR Add-on Kit [32]	Instrumented manikin torso. Real-time feedback provided by a cable connected external device or an app (data communication via Bluetooth).	Compression rate Compression depth Chest recoil	Visual feedback (all): Heartisense® CPR Add-on Kit App Audio feedback (rate): metronome available in the app	Available: CPR duration, mean CPR parameters value/quality, compression score and chest compression fraction.

Table 3.1 (Continued).

Laerdal® Little Anne QCPR [33], [34]	Instrumented manikin torso. Real-time feedback provided by a cable connected external device or an app (data communication via Bluetooth).	Compression rate; Compression depth; Chest recoil.	Visual feedback (all): Laerdal® SkillGuide or Laerdal® QCPR App. Optional audio corrective feedback; Audio feedback (depth): manikin incorporated clicker.	Available: CPR duration, mean CPR parameters value/quality, compression score, most severe errors on compressions and chest compression fraction.
BT® SMART CPR Training Model Sherpa X [35]	Instrumented manikin torso with incorporated visual feedback system and an external feedback software (data communication via Bluetooth).	Compression rate Compression depth Chest recoil Hands position	Visual feedback: - Manikin-incorporated LED, graphical, and quantitative values display system (all); - Sherpa X Software (all). Audio feedback (rate): metronome available in the app (optional)	Available (Sherpa X Software): CPR duration, number of correct compressions, mean CPR parameters value/quality and chest compression fraction.
Aero Healthcare® Brayden Pro [36]	Instrumented manikin torso. Real-time feedback provided by an app (data communication via Bluetooth).	Compression rate Compression depth Chest recoil Hand position Compression depth vs Compression rate plot	Visual feedback (all): Aero Healthcare® Brayden Pro App Audio feedback (depth): manikin incorporated clicker (optional).	Available: mean CPR parameters value/quality, compression score, and chest compression fraction.
Heartisense® CPR Feedback Kit [37]	Sensory kit to be attached to manikin chest without CPR feedback function. Real-time feedback provided by an app (data communication via Bluetooth).	Compression rate Compression depth Chest recoil Hands position	Audio-visual feedback (not specified): Heartisense® App	Available: mean CPR parameters value/quality, compression score, and chest compression fraction.

Visual feedback can assume a wide range of forms which can be displayed in the manikin structure, in an external visualization monitor, in a device with specific software, or through a smartphone app. Most commonly, it is qualitative, as simple light signals and/or real-time moving symbols or graphics, but it can also be quantitative, by displaying exact measurable values of compression parameters. Qualitative visual feedback, however, seems to provide a more intuitive way of correcting CPR performance [38]. LED systems are a cost-effective and easy to read solution for feedback [38], being widely used in less complex feedback systems. The information can be displayed as binary feedback (correct/incorrect) or by providing guidance towards compression parameter correction (below-correct/correct/above-correct), the last being more informative than the first approach. The use of more complex visualization tools, which display feedback through real-time updated symbols or graphics, are a more sophisticated and highly informative way to provide feedback, although it requires the development of a graphical user interface, which results in an additional cost. Most available training manikins use this type of visualization by developing a smartphone app or specific software, with easy-to-read symbols, as a vertically moving bar for compression depth and chest recoil guidance and a moving gauge for compression rate monitoring. The combination of different feedback visualization systems is also commonly used. Prestan's more advanced manikins [31] combine the LED system with a monitorization app for additional feedback. BT manikin, besides the manikin-incorporated display with an LED system, real-time moving symbols, and compression parameters quantitative values, is associated with an external software with additional feedback features [35]. However, additional input set by feedback systems add additional complexity to the training and may overstrain the trainee and impede optimal skill performance [23]. The form and intensity of feedback play an important role in directing the trainee's limited attention capacity, and a large variety of feedback may be bothersome rather than helpful [23].

Audio feedback can support training trough guidance sounds or by providing corrective verbal prompts, in case of inadequate performance [23]. Regarding the guidance sounds, some devices include a clicker and/or a metronome, for correct depth and rate guidance, respectively, which seems to improve compression quality [25]. Most of the available training manikins combine these audio tools with visual feedback display. Verbal corrective prompts, contrarily, inform the trainee to correct certain maneuver parameters through succinct recommendations, as an instructor would. In the presence of other feedback forms, these corrective prompts tend to interfere with trainee's attention or be ignored by trainees, especially if prompted excessively, being commonly an optional feature [23].

Devices that invested in additional training software development, including CPR training apps, allow a more complete and informative training that goes beyond accurate real-time feedback. Feedback devices that include a data report on overall performance are of great value for CPR training, as they allow a general overview of the performance, facilitating the training assessment. These reports provide trainees and instructors quantitative data on the performance, which can include percentages of the correct and incorrect parameters and other relevant training metrics, general training scores and detailed timelines of the maneuvers recorded through a training session. Detailed information about the most common training metrics and quality scores are included in section 3.3. Other highlight of this software development is the availability of distinct interfaces for trainees and instructors, adapted to their roles and needs during training. As the trainee interface focus on correction of individual performance, the

instructor interface allows the real-time monitorization of multiple trainees' performances and the further assessment of their respective quantitative data. This feature allows overcoming the difficult monitoring due to the high trainee-instructor ratio and ensures to do it accurately. Lastly, the presence of high-quality software permits adapting to changes in the CPR guidelines through software updates, although it could be associated to an additional maintenance cost [38]. Some devices overcome this expense by allowing manual configurations to quality assessment parameters, making adaptation to new guidelines easier [38]. However, the possibility to change freely assessment parameters may lead to non-standardized training. Many other available features of software development for CPR training, as gamified training modes, are not discussed since they are out of the scope of the present work.

Depending on the manikin quality and reliability, the sensory technology used and the sophistication of feedback provision, feedback devices are in a price range between €200 and €500. Since most organizations own manikins without feedback incorporated, CPR training representants, as Prestan and Laerdal, developed feedback add-on kits for their training manikins without CPR feedback function, to manage the high cost of full manikin replacement for training institutions. With that in mind, Heartisense developed an attachment feedback system that can upgrade any conventional CPR manikin to be fully interactive [37], which constitutes an interesting technological benefit for improved CPR training as it allows a broader access to feedback technology.

Regardless of their complexity, all these commercially available feedback devices are assumed to be validated and to provide accurate measurements for improved CPR training. Since sensory technologies behind the presented feedback devices are not open access, is, thus, missing which systems could possibly be behind such accurate measurements.

3.2 Technologies for Chest Compression Quality Assessment: a Literature Review

Chest compression parameters and quality can be measured with a variety of systems. Methods based on pressure sensors and/or accelerometers are the most commonly described systems in literature and in commercially available feedback devices, although other sensory technologies have been emerging. These systems usually focus on the extraction of compression depth signal and determine compression rate through simple signal processing techniques. Depending on the sensors used, feedback on hand position may or may not be possible. Table 3.2 summarizes the different technologies reviewed, focusing on the feedback provided, their general advantages, their limitations, and technological related improvements to overcome those same limitations.

Pressure sensors were the first technological approach to provide compression feedback [39]. Described pressure sensors are included in the electrical tactile sensors group, which detect tactile information through physical touch [40] and produces readable electrical signal through a transducer. Common electrical transduction techniques for pressure sensing are based on capacitive, piezoresistive and piezoelectric methods, which usually show good performance and usefulness [40]. In fact, they are widely used due to their simple sensor fabrication methods and easy of data acquisition and processing, allowing the development of simple, cost-effective and accurate devices for force detection [40]. Regarding their application to chest compression quality monitorization, pressure sensors measure the force applied in the sensor active area and set it in relation to compression depth, providing direct feedback on three of the four compression parameters: hands position, compressions depth and chest release [39]. Despite of this clear usability advantage, pressure sensors usually require protection from direct application of force, not only protecting it from damage but also to avoid bending the sensor, that can induce measurement errors [41]. This may require additional application of force during compressions, promoting provider's fatigue and misleading the required compression force, with concomitant ineffective training [23]. Additionally, variations in chest wall compliance, provided by different manikin chest stiffness [39], as well as compressions delivered on compliant surfaces, as mattresses [42], can hamper an accurate estimation of compression depth from compression force. Regardless of these limitations, some commercially available stand-alone feedback devices, as CPREzy, still use this technology [23]. Several approaches have been developed using pressure sensors, although introducing some innovation factor to overcome the discussed limitations. Sainio *et al.* [42] proposed a system with two pressure sensors (type non-specified), one placed in the manikin's chest and the other aligned at its back, to correct the error introduce by compliant surfaces effect. Similarly, Nicolau [43] developed a fully functioning CPR training prototype, using two off-the-shelf piezoresistive sensors, with feedback on all the compression quality parameters, although some repeatability issues were detected. The details of Nicolau's work are further detailed in section 3.4, since it integrates the local state-of-the-art, which is the foundation of the present work. Kokubo *et al.* [44] developed a capacitive flexible pressure sensor capable of measuring not only chest compression depth accurately, including on compliant surfaces, but also of evaluating pressure distribution on chest during compressions, providing precise hand position information. Although, in theory, these new technologies overcome some common problems of pressure sensors, they have not been produced as commercially available devices.

Table 3.2. Sensory technologies for chest compression parameters assessment available on literature, including their general advantages, limitations, and technologically related improvements (D – compression depth; Re – chest recoil; R – compression rate; H – hand position).

Sensory Technology	Feedback				Advantages	Limitations
	D	**Re**	**R**	**H**		
PRESSURE SENSOR (general)	x	x	x	x	Cost-effective; Simple signal processing; Direct information on compression depth, chest recoil and hand position.	Require protection from direct application of force, requiring additional force application; Errors introduced by chest wall compliance variations; Errors introduced by sensor bending; Overestimation of compression depth due to compliant surface effect;
Pressure sensor improvements						
[42] Two pressure sensors (type non-specified)	x	x	x	x	Cost-effective; Overcomes overestimation of compression depth due to compliant surfaces effect.	NA
[43] Two piezoresistive pressure sensors	x	x	x	x	Cost-effective off-the-shelf sensors; Simple electronics; Overcomes overestimation of compression depth due to compliant surfaces effect.	Low repeatability.
[44] Flexible capacitive pressure sensor	x	x	x	x	Resistant to sensor bending errors; Overcomes overestimation of compression depth due to compliant surfaces effect.	Custom production (probably expensive).
ACCELEROMETER (general, with double integration as signal processing)	x		x		Cost-effective; Reliable technology;	Need of acceleration signal processing to obtain any feedback; Cumulative integration errors; Errors introduced by sensor tilt; Overestimation of compression depth due to compliant surface effect; Lack of feedback on hand position and chest recoil;

Table 3.2 (Continued).

Accelerometer improvements							
[45]	Improved linear filtering signal (processing technique)	x		x		Cost-effective; Low algorithmic complexity.	Small reduction on integration error; Lack of feedback on chest recoil.
[45]	Detection of the zero-crossing instants in the velocity signal (processing technique)	x		x		Cost-effective; Large reduction on integration error.	Medium algorithmic complexity; Small integration error; Lack of feedback on chest recoil.
[45]	Spectral Analysis of the acceleration signal (processing technique)	x		x		Cost-effective; Immune to integration errors.	High algorithmic complexity; Lack of feedback on chest recoil.
[46]	Kalman Filtering (processing technique)	x	x	x		Cost-effective; Very accurate measurements; Provides feedback on chest recoil.	Very high algorithmic complexity.
[47]	Two accelerometers + spectral Analysis of the acceleration signal	x		x		Cost-effective; Overcomes integration errors; Overcomes overestimation of compression depth due to compliant surfaces effect.	High algorithmic complexity; Lack of feedback on chest recoil.
SENSOR COMBINATION (general)						Overcome common limitation of the use of a single sensor type;	Increased processing complexity.
[38]	Accelerometer + piezoresistive pressure sensor	x	x	x	x	More accurate compression depth measurements; Feedback on all compression parameters.	Increased processing complexity.
[48]	Two accelerometers + potentiometer	x	x	x		More accurate compression depth measurements; Overcomes overestimation of compression depth due to compliant surfaces effect.	Increased processing complexity.
[49]	Two accelerometers + piezoresistive pressure sensor	x	x	x	x	More accurate compression depth measurements; Feedback on all compression parameters; Overcomes overestimation of compression depth due to compliant surfaces effect.	Increased processing complexity.

Table 3.2 (Continued).

[50]	Accelerometer + two magnetic coils	x	x	x		Accurate compression depth measurements.	Increased processing complexity. Complex electronics; Low repeatability.
[51]	Inertial Measurement Unit (accelerometer + gyroscope + magnetometer)	x	x			Cost-effective; Overcomes errors introduced by accelerometer inclination.	Increased processing complexity. Lack of feedback on chest recoil.
NEW TECHNOLOGIES (general)							
[52]	CMOS image sensor with infrared illumination sources	x	x	x	x	Highly accurate measurements; Directly measures compression depth.	Complex processing; Computationally laborious; Dependent on the reflectance of the surroundings (due to the use of infrared light).
[53]	RGB-D sensor (computer vision-based tracking system)	x	x	x		Directly measures compression depth; Correct measurements even on compliant surfaces.	Complex image processing; Computationally laborious; Need precautions to avoid optical interference which compromises tracking algorithm efficiency; Dependent on the reflectance of the surroundings (due to the use of infrared light).
[54], [55]	Impulse-radio ultra-wide band time-difference-of-arrival sensor	x	x			Highly accurate measurements; Correct measurements even on compliant surfaces.	Expensive technology; Complex processing; Need of initial manufacture calibration.

Alternatively to pressure sensors, accelerometer-based systems were later developed [39]. These devices measure acceleration of the manikin's chest during chest compressions, and use in-built processors to calculate compressions depth in real-time, leading to simple and cheap devices [39], as Zoll PocketCPR [23], a commercially available accelerometer-based stand-alone feedback device. Thus, it is not possible to obtain direct feedback on compression parameters from raw acceleration signal, meaning that signal processing is always required. The most straightforward approach to obtain chest displacement from acceleration is by applying double integration. However, since all accelerometers are sensible to movement-associated noise, double-integrating the acceleration signal is prone to cumulative errors which cause a significant drift in displacement signal, impeding an accurate estimation of compression depth [39]. Considering the small distance intended to be measured, these cumulative errors have a very relevant impact in compression depth calculations. Other errors are introduced in compression depth calculation by the use of accelerometers, with origin on the compliant surface effect [39], and on sensor tilting during compressions, since gravitational acceleration component is dependent of sensor orientation [39]. Some developments have been made to surpass the integration cumulative errors by using signal processing techniques over the extracted acceleration signal. Resetting initial conditions of velocity and displacement after each compression is the most common and simple approach to overcome this limitation, with the cost of chest recoil information being lost, meaning that the actual compression depth value is unknown [45]. De Gauna *et. al* [45] proposed three methods, with different algorithmic complexities: an improved linear filtering, that computes compression depth signal from acceleration signal by using a designed band-pass filter that performs double-integration; the detection of the zero-crossing instants in the velocity signal, which computes velocity signal from acceleration signal by performing single-integration and calculates compression depth and rate from the analysis of zero crossing instants; and the spectral analysis of the acceleration signal, which computes compression depth and rate directly from the acceleration signal by using the fast Fourier transform. Among the discussed alternatives, the algorithm based on the spectral analysis of the acceleration signal provided the most accurate results, since it computes compression depth and rate directly from the acceleration signal, avoiding integration errors, although it has the highest algorithmic complexity. Both remaining methods are algorithmically less complex and reduce the cumulative integration error, the second method with greater reduction than the first, since it performs integration only once. All of these methods lack on chest recoil detection, which is a major drawback of these processing techniques. Boussen *et al.* [46] developed an original method using an accelerometer and an algorithm derived from the inertial navigation theory with Kalman filter for retrieving chest compression depth, rate and chest recoil, with great accuracy. This predictive filter is based in a set of mathematical equations that provides efficient recursive computational means to predict the current state and update it according to sensor readings, in order to obtain a more accurate estimation of the next state, minimizing the associated error. Despite of their complexity, all the described methods are vulnerable to error in compression depth caused by sensor tilting during compressions [39] and to error due to the compliant surface effect [23], [39]. The use of two accelerometers, one placed on manikin's chest and other on manikin's back, was proved to overcome this last limitation [47], [48] since the accelerometer placed on manikin's back measure compliant surface acceleration separately, and allows the correction of manikin's chest displacement values.

Bringing together different sensors is a common solution to overcome reported limitations of single sensor use, in particular, accelerometer limitations. The conjunction of an accelerometer with a reference sensor for integration error compensation is the most widely used alternative. Caleb *et al*. [38] added a reference piezoresistive pressure sensor to an accelerometer to increase the accuracy of the compression depth calculation and to obtain feedback on hand position and chest recoil. Song *et* al. [48] used a potentiometer as a reference sensor for two accelerometers, surpassing errors in compression depth calculation and errors introduced by compliant surfaces. Gohier *et al*. [49] used two accelerometers associated with a piezoresistive pressure sensor to obtain more accurate compression depth values, including on compliant surfaces, and feedback on chest recoil. The addition of a reference sensor brings clear benefit to overall system performance, with the drawback of leading to complex devices, with increased processing complexity, as the algorithms for calculating differential distances with these reference sensors might not be trivial [39]. Due to its benefit, this kind of technology is commonly used by commercially available feedback devices, as the Laerdal CPRmeter [23]. Kandori *et al*. [50] proposes a chest compression depth gauge using two magnetic coils and an accelerometer. The waveform obtained from the use of magnetic coils, which are proportional to compression force, instead of being used as a reference signal for the accelerometer calibration, is combined with the acceleration signal to obtain a chest compression depth waveform, with small error associated. However, since these sensors use an alternating current in the primary coil, they require more complex electronics, as the alternating signal amplitude must be demodulated in order to be used [40]. Additionally, magnetic coils, due to their mechanical nature, have low repeatability as coils may not maintain the same position between readings [40], compromising training's feasibility. Lee *et al.* [51] used an inertial measurement unit (IMU), which combines a three-axis accelerometer with a three-axis gyroscope and a magnetometer to provide depth information during CPR. This alternative uses a novel displacement estimation algorithm that considers the orientation of the device, avoiding errors introduced by the sensor tilt during compressions. The algorithm removes gravitational acceleration from the raw acceleration signal by calculating Euler angles through IMU data, processing only movement acceleration signal using double integration associated with designed filters to remove other noise sources, in order to calculate chest compression depth.

Other sensor types and new sensory technologies have been studied over time, giving rise to more complex devices. Centen [52] proposed an external system using a CMOS image sensor with infrared illumination sources, capable of three-dimensional imaging based on the time-of-flight principle, to monitor compression depth throughout CPR training. The infrared emitter illuminates the training scenario (training manikin and surroundings), with the emitted infrared light being reflected and returning to the image sensor where its time-of-flight is calculated for every pixel in the image sensor. The time-of-flight distance data is used to construct a compression gradient of the surfaces being imaged, which is used to extract the depth information of each chest compression. The compressed area appears cyclically deeper in the gradient than the stationary portions of the image. The processing of this gradient allows the extraction of an accurate measurement of chest displacement and recoil, compression rate and hand position. This optical compression depth measurement technique is described as highly accurate, overcoming most of the general errors of accelerometer-based and pressure sensor-based systems, since it directly measures chest displacement, instead of setting it from other measurement type. Another emerging technology for CPR training systems is computer

vision-based tracking, which can track position of the hands while performing chest compressions. Loconsole *et al.* [53] proposed a vision-based markerless solution using a commercial RGB-D sensor, i.e., a standard VGA color camera integrated with an infrared range sensor combining image color with per-pixel depth information. The associated tracking algorithm identifies the manikin as the object to be compressed and tracks trainee's knuckles during chest compressions, measuring the compression depth and chest release through image processing. This solution, despite of handy, require complex image processing algorithms that can be corrupted by interferences that affect the region of interest, jeopardizing the tracking algorithm efficiency. Both these optical solutions have de drawback of being dependent on the reflectance of the surrounding medium since they use infrared light for displacement measurements. On a different note, Kim *et al.* proposed a time-difference-of-arrival sensor, which measures the signal transmission time between two antennas using impulse-radio ultra-wideband, and convert it into distance in order to accurately measure the chest compression depth during CPR training [54]. This solution presented very high accuracy on compression depth measurements, independently of the support surface [55]. Provision of compression rate information was not studied. This sensor requires transmitter and receiver synchronization during use, which requires initial manufacture calibration, leading to an increased cost [54].

The research of sensory technologies that can accurately measure compression parameters to provide feedback on CPR training quality is not recent and have been gaining relevance in latest years, as community awareness for BLS education and effective skills acquisition is increasing. Several technologies have been implemented and perfected with novel approaches, giving still space for the emergence of new technologies. Of notice, however, up to date, there is no gold standard to evaluate the accuracy needed for chest compression measurements in such devices despite of the growing interest around their applicability [46], which represents an important limitation in technological validation and research standardization. As important as accurately measuring compression parameters, is setting them as useful information about their quality, giving the trainee the opening to identify improvement opportunities.

3.3 Assessment of Chest Compression Quality: a Review of Quality Parameters

After presenting CPR feedback devices available on the market and described technologies in literature for measuring chest compression's parameters, it is now important to review the main variables of the CPR maneuver that dictate the quality of chest compressions in real-time, and the most relevant training metrics for the overall performance (Table 3.3). Despite these well stablished parameters and metrics, clearly described in the current BLS guidelines, there is yet a need to develop a universal score to define and determine the overall quality of chest compressions [56].

Table 3.3. Chest compression parameters and recommended metrics for training feedback, in real-time and for overall training, respectively, according to the last ERC guidelines [1], [7].

	CPR Parameter/ Metrics	**Ideal Value (ERC Guidelines 2020)**	**Description**
Real-time training	Hand Position	Center of the chest	Hand placement during CPR maneuver.
	Compression Depth	5 to 6 cm	Recommended depth for each compression.
	Chest Recoil	Complete (0 cm)	Allow chest full decompression between compressions.
	Compression Rate	100 to 120 compressions per minute	Number of compressions per minute, not considering any interruptions.
Post-training metrics	Adequate Hand Position	100 %	Quality of correct hand placement during training.
	Compression Depth: Adequate depth Mean depth	 100 % 5 to 6 cm	Quality indicators of correct compression depth during training.
	Chest Recoil: Adequate recoil Mean recoil	 100 % 0 cm	Quality indicators of correct chest recoil during training.
	Compression Rate: Adequate rate Mean rate	 100 % 100 to 120 compressions per minute	Quality indicators of correct compression rate during training.
	Chest Compression Fraction	Compression-only CPR: 100% Full CPR: > 60%	Ratio of the time passed applying chest compressions to the complete training time.
	Compression Pause Time	< 10 seconds between compression cycles	Time between compression cycles (pauses).
	Average Duty Cycle	30 to 50 %	Ratio of the time the chest is actively compressed in the total time of a compression-decompression cycle.

Currently, the measurement and reporting of chest compressions overall quality is not standardized, significantly limiting the potential scope of benefit. Besides being an important element to identify pitfalls on trainee's performance during training, a reliable quality score also allows the comparison of skills between successive CPR attempts, different groups of people or different training programs [57].

The first overall chest compression quality parameters were based on simple scoring systems, which constructed a final score by adding penalization points of different significances, depending on the failed CPR parameter [57], [58]. With the improvement of the computational capacity of feedback devices, more complex overall training evaluation systems emerged, based on the calculation of different chest compression quality metrics mentioned at Table 3.3. Table 3.4 reviews the most relevant quality scores available in literature, based on Klosiewicz *et al*. systematic review on the theme [56].

Table 3.4. Quality scores for overall CPR training available in literature (R – compression rate; D – compression depth; Re – chest recoil; H – hand position; DC – duty cycle; CCF – chest compression fraction; No.C – number of compressions per cycle). Adapted from [56].

Ref.	Quality Score	Considered Parameters							Underlying Conditions
		R	D	Re	H	DC	CCF	No.C	
[59], [60]	Excellent CPR (%)	x	x	x				x	% of chest compressions with > 90% of correct Rate, Depth and Recoil
[61]	Efficient Chest Compressions (%)	x	x	x				x	% of chest compressions with 100% correct Rate, Depth and Recoil
[62]	Chest Compression Quality (%)	x	x	x				x	(% of correct Rate + % of correct Depth + % of correct recoil) / 3
[63]	Chest Compression Quality (yes or no)	x	x	x	x			x	Yes if > 70% of chest compressions with correct Rate, Depth, Recoil and Hand position
[64]	Adequate Chest Compressions (%)	x	x	x	x	x		x	% of chest compressions with 100% correct Rate, Depth, Recoil, Hand Position and Duty Cycle
[65]	Overall CPR quality score (%)	x	x	x		x		x	% of chest compressions with 100% correct Rate, Depth, Recoil and Duty Cycle
[66]	Excellent CPR (%)	x	x	x			x	x	% of chest compressions with 100% correct Rate and Depth and > 80% correct Recoil and Chest Compression Fraction > 80%
[56], [67]	Laerdal® Chest Compression Score (%)	x	x	x	x			x	NA
[68]	CPR.PT Quality Score (%)	x	x	x	x			x	% of chest compressions with 100% correct Recoil and Hand position x stepwise function for compression Rate x stepwise function for compression Depth

NA – Not Available.

There is no doubt that overall quality of chest compressions is determined by several factors. Chest compressions of adequate quality should be featured by appropriate compression rate and depth, full chest recoil after each compression and correct position of the hands, combined with a low rate of interruptions, as specified in section 2.2. However, it has not been indicated that any of the above-mentioned parameters prevail over another [56]. Although they affect blood flow through different mechanisms, they are of equal importance [56]. For that reason, any article in Klosiewicz *et al*. review [56] that excluded compression rate, depth or recoil from the overall quality formula, was not considered for Table 3.4. In fact, a compression that do not fulfill correctly one of these parameters, cannot be considered as properly delivered. Regarding hand position, an incorrect hand-positioned compression inevitably has a major negative influence on the other registered compression parameters, especially on compression depth [57]. This may justify its omission from some formulas. For that reason, CPR quality formulas which did not include this parameter were still considered for Table 3.4 as its influence may be implicit in the remaining parameters. Many articles reviewed in [56] resorted to Laerdal CPR score for training analysis. Although their quality formula is unknown, it was also included, since Laerdal technology is considered to be validated.

Concerning the discriminated overall quality formulas, most propose that CPR quality should be defined as the percentage of compressions that meet simultaneously all criteria defined by the authors [56]. In all formulas, single compressions are treated in a dichotomous way, as correct or incorrect, regardless of how many quality parameters need to be improved [56]. This is a reasonable approach if considering whether a compression is correct in terms of the CPR guidelines [56]. Regarding chest compression parameters, the presence of compression depth, rate and chest recoil in a final quality score is unquestionable. Hand position, on the contrary, can give rise to doubts. Although Klosiewicz *et al*. considered in their systematic review [56] that this parameter should be considered separately, it is also true that a compression with incorrect hand position cannot be considered effective, even if the remaining parameters are read as correct by the feedback system. Duty cycle, despite of being an interesting training parameter, is not considered to bring a relevant meaning for overall quality. The chest compression fraction, on the other hand, indicates not the quality of the compressions but the efficiency of the training [56]. Thus, this parameter must be discussed separately, and not be integrated in an overall chest compression quality formula. It could be interesting, however, to consider it for a full CPR quality training score.

Although many proposals have been developed, no single, universal indicator of chest compression quality has been designed and subsequently applied in order to standardize training feedback and assessment. While this can be a limitation of CPR feedback systems, the review of these proposals clarifies the highlights of an adequate approach on overall chest compression quality, which is a parameter to be included in the present work.

3.4 CPR Personal Trainer – A CPR Feedback Training Prototype from CSB-FMUP

CPR Personal Trainer is a CPR training prototype recently developed at CSB-FMUP, consisting of a standard CPR training manikin instrumented with off-the-shelf piezoresistive pressure sensors connected to an open-source electronic processing unit and an information system (Figure 3.1). The instrumentation arrangement has the ability to accurately measure the quality parameters of chest compressions and ventilations. Similarly to previous sections, ventilation setup is not discussed since it is out of the scope of the present work.

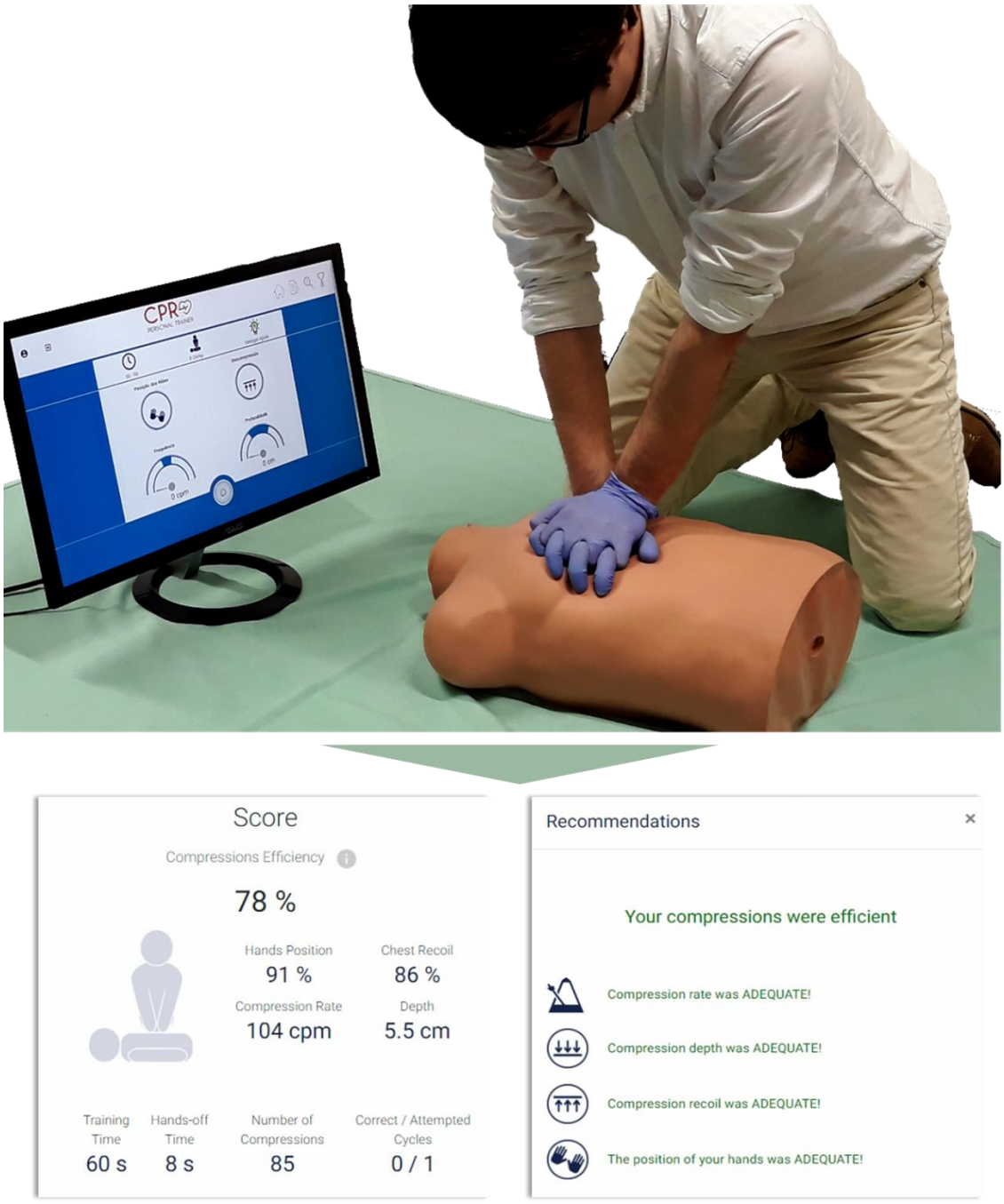

Figure 3.1. CPR Personal Trainer prototype and interface. Adapted from [69].

The proposed solution was designed to be a non-invasive and cost-effective add-on, envisioning its application to different manikins in order to allow a broader access to the technology [43], [68]. With that in mind, quality on compression depth and rate, chest recoil and hand position for each compression are assessed by the combination of two piezoresistive pressure sensors, one placed on manikin's chest and other on its back, locations which maximized the amount of useful data collected while taking into account sensor stability during compressions, and sensor deterioration with repetitive use [43]. These sensors do not require a complex implementation and were easily assembled with an Arduino Nano for data collection and processing. To assess about compression depth, a relationship between pressure sensors' conductance and chest displacement was set using an analog infrared distance sensor in a calibration process. The data collected is then processed based on peaks analysis in order to find the remaining compression parameters. Considering the results, this system successfully differentiated each chest compression parameter, with great measurement accuracy, and a reduced cost of only €150 per add-on, excluding the manikin cost [43], [68]. Nevertheless, continuous and prolonged training lead to inaccurate results relative to the expected conductance for a given force, a repeatability issue already reported in literature for piezoresistive sensors. Additionally, to be noticed that the calibration process needs to be customized depending on the manikin used due to the chest compliance variability.

The obtained signal is analyzed by extracting relevant data of chest compressions performance to provide feedback on training quality. The described measurement system is connected to a user-friendly online Graphical User Interface, which manages training workflow, providing visual and audio feedback. CPR Personal Trainer also provides reports for each training session, a performance analysis with suggestions to improve the procedure, the overall progression along the sessions and the performance evolution of the trainee regarding each CPR maneuver component [20], [43], [68] (Figure 3.1).

Despite of the repeatability and reproducibility limitations, a study proved that CPR Personal Trainer allowed the achievement of a similar level of knowledge when compared with the traditional instructor-based training method, with improvements regarding skill acquisition, validating that low-cost tools with feedback for CPR self-training can provide an alternative or a complementary extension to traditional methods for CPR skills acquisition and maintenance [20], [43], [68].

Chapter Conclusions

Tools for self-guided CPR training are an alternative to traditional training. In particular, their feedback feature provides objective, reliable and standardized assessment of skills acquisition, being a step towards a more effective training, as feedback allows trainees to be aware of their real-time performance and monitor their own actions accordingly. Along the years, several proposals of different feedback devices emerged, with different complexities and measurement technologies. The latter ranged from simple sensory units, as pressure sensors and accelerometers, to more complex approaches with sensors combination or the development of novel technologies. Despite the emergence of these feedback devices, advances and improvements in this technology are still possible, and further development is still needed. In fact, there are still several limitations regarding the development of feedback devices for CPR training. To the date, there is no gold-standard to evaluate the accuracy of such devices and technologies, as there are no recommendations for the accuracy needed for chest compression measurements. Furthermore, validation tools for such measurements are also needed. Concerning quality assessment, despite of the standardized quality parameters recommended in CPR guidelines, there is no overall quality score to regulate overall training assessment.

4

SCREENING AND ANALYSIS OF OFF-THE-SHELF SENSORS FOR CHEST COMPRESSIONS DETECTION

Being established the benefit of educating the community in BLS by using technological devices for CPR training, and being overviewed the existing feedback devices and the available technologies for chest compression quality assessment during training, there is now an opening for novel approaches and improvements. The aim of this project is the development of a feedback system to support CPR training, focusing on chest compressions. With that in mind, a standard commercialized CPR manikin was instrumented with off-the-shelf sensors, in an operational approach, and connected to an open-source electronic platform for compressions data acquisition. The goal of this implementation is to achieve quantifiable accurate measurements for the selected chest compression parameters: hands position, compression depth, compression rate, and chest recoil. This chapter presents the first steps of this development process, consisting in sensor screening through the selection of commercially available sensors, the study of their response to compressions and the consequent effectiveness in detecting different compression parameters. The most appropriate sensory approach is selected from the analysis of each sensor output, considering the established requirements for this application.

4.1 Requirements for Sensor Selection

Similarly to previous developed work in CSB-FMUP [43], the developed solution should envision a set of technical and operational requirements for sensor selection, considering the intended application. From a technical point of view, the selected sensor must allow accurate chest displacement measurements, either in a direct manner through raw sensor output, or by indirect means, with sensor output calibration for displacement measurements. Furthermore, sensor resolution must be sufficient to guarantee trustworthy and reliable data, by providing a resolution in the order of the millimeter, given the working range of this application. From an operational point of view, the selected sensor should allow simple implementation, including a low computational load regarding both signal acquisition and processing. In fact, since this application implies real-time sensor readings at a high sampling rate, sensors that require complex data processing might not allow real-time sensor implementation as the provided sensor readings might exceed the time for an appropriate sampling for this application.

Additionally, the selected solution should envision an easy assembly and generic implementation to different training manikin models. Moreover, it should include a contained development cost, making this solution accessible to low resources training sites. Lastly, the selected solution should overcome the different limitations presented by existing solutions available in literature (see section 3.2).

The established requirements envision a sensor capable of quantitative and accurate measurements of the chest compression parameters, with easy and generic implementation on training manikins at a reduced cost, conditions that would lead to broader access to technology.

4.2 Market Search for Sensor Selection

Based on the established technical and operational requirements, an extensive search was made for different sensors available on the market. Sensors of different natures were selected to be tested in the manikin, ranging from ultrasonic and infrared sensors to accelerometers and IMUs (Figure 4.1). The working principle, general technical characteristics and cost of each selected sensor can be found in Table 4.1. Pressure sensors and similar sensor types that comply with the determined requirements were not considered in this market search since they present several limitations already described in the literature and were previously tested in CSB-FMUP [43] (see section 3.4). These limitations include sensor deterioration due to excessive and cyclical force exerted during compressions, with consequent loss of reproducibility and validity for displacement measurements.

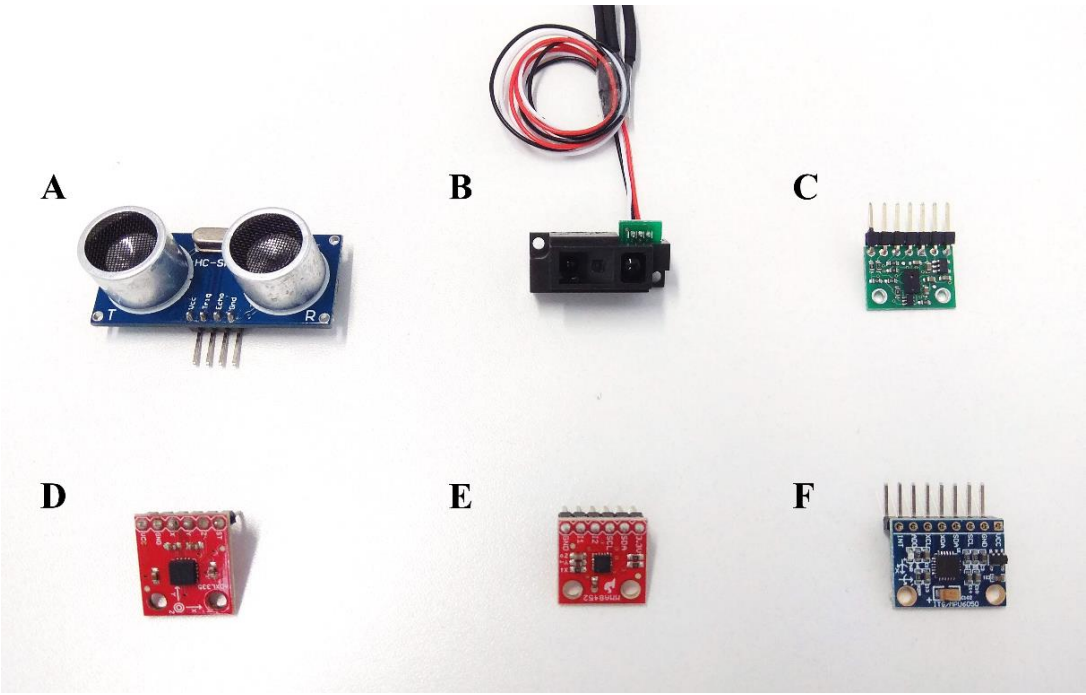

Figure 4.1. Sensor selection for chest compression detection: Ultrasonic sensor HC-SR04 (A), infrared optical analog sensor GP2Y0A51SK0F (B), infrared optical digital sensor VL6180X (C), analog accelerometer ADXL335 (D), digital accelerometer MMA8452 (E) and digital IMU MPU-6050 (F).

Table 4.1. Selected sensors for chest compression parameters detection, considering general characteristics according to available information on local stores (prices collected in May 2021).

Sensor	Sensor Type	Measurement Range	Output Type	Other Characteristics	Price
HC-SR04 [70]	Ultrasonic Sensor	2 to 400 cm	Pulse Width Modulation	Resolution: 3 mm.	€ 3,69
GP2Y0A51SK0F [71]	Infrared Optical Sensor	2 to 15 cm	Analog Voltage	High resolution (NA) for smaller ranges.	€ 16,24
VL6180X [72]	Infrared Optical Sensor	0 to 10 cm	Digital 8-bit distance reading (in mm)	Accurate measurements; Resolution: 1 mm; High immunity to noise.	€ 13,22
ADLX335 [73]	Accelerometer	±3 g	Analog Voltage	Low susceptibility to noise.	€ 17,71
MMA8452 [74]	Accelerometer	±2g, ±4g, ±8g	Digital	Provides both unfiltered data and high-pass filtered data; Very low susceptibility to noise.	€ 12,79
MPU-6050 [75]	IMU (Accelerometer + Gyroscope)	Acc: ±2g, ±4g, ±8g, ±16g Gyro: ±250 dps, ±500 dps, ±2000 dps	Digital	NA	€ 6,09

NA – Not Available

Concerning the chosen sensor types, ultrasonic sensors directly assess the distance of a target object by emitting an ultrasonic pulse and measuring the time it takes for its echo to return. Ultrasonic sensor HC-SR04, which is the most commonly used sensor of its type, was considered adequate for the application intended, and will be evaluated in the following sensor testing phase. Infrared optical sensors usually use the intensity of reflected light to directly measure the distance of target objects. That is the working principle of analog sensor GP2Y0A51SK0F, a sensor selected due to its adequate measurement range in comparison with other available infrared sensors. Differently, digital infrared sensor VL6180X, instead of using light intensity, uses a precise clock to measure the time that light takes to bounce back from a surface, providing more accurate measurements, with higher immunity to noise, a feature considered relevant for the proposed application. Both ultrasonic and infrared sensors require an open-medium for sound and light to propagate for signal acquisition, which is a relevant requirement to be considered on their implementation in the manikin, as some manikins are filled inside with an elastic foam to provide structural integrity. Accelerometers and IMUs measure inertial variables, requiring more complex processing techniques to assess displacement. Analog accelerometer ADLX335 and digital IMU MPU-6050 are the most commonly used sensors of their type, with no other commercially available sensors of their type showing clear benefit in comparison. Digital accelerometer MMA8452 was selected as the resulting high-pass filtered data was considered interesting for the intended application. Since these sensor types do not directly provide displacement measurements, its use would require the development of algorithms to be implemented in real-time to extract displacement

data from the sensed inertial measurements. Besides simple integration techniques, Kalman filter was aimed to be applied on both these sensor types for displacement signal extraction. However, these solutions with higher processing load must still allow real-time data extraction, in order to fulfill the established requirements. Due to the algorithmic complexity of its implementation, time constraints did not allow the further development of these approaches. The use of accelerometers and IMUs may still be considered possible approaches for future developments on the topic, although their use does not bring any innovative feature since many efforts have been made to extract compression parameters from inertial measurements (see section 3.2).

Thus, from the selected sensors through market search, only ultrasonic and infrared sensor groups were selected for testing in order to assess the reliability of their performance for chest compression detection and assessment.

4.3 Selected Sensors Implementation and Testing

Having selected the sensors to be tested, the next phase consisted of sensors preparation and assembling, which included programming scripts and circuits planning for extracting relevant measurements.

For sensor implementation, an Arduino Nano was used due to its reduced size, easy assembly on a breadboard, and accessible prototyping programing tools. Simple Arduino scripts were designed for each sensor in Arduino Integrated Development Environment (IDE) in order to obtain displacement data during chest compressions.

Ultrasonic sensor HC-SR04 uses Arduino's *pulseIn* function to measure the time the emitted ultrasonic pulse echo takes to return to its origin. This time-of-flight period is then converted to distance using sound propagation velocity on air at room temperature (considered 20 ºC), approximately 343 ms^{-1}. **Infrared sensor GP2Y0A51SK0F** provides analog readings, which are converted to voltage by mapping them to values between 0 and 5 V, using Arduino's *map* function. To assess distance readings, the graphically available sensor calibration data presented in manufacturer's datasheet [76] was manually sampled and a curve fitting method was applied to assess the relationship between sensor analog voltage readings and the corresponding distance. Although the presented data in sensor's datasheet comprised measurement distances up to 20 cm, the curve fitting was designed considering only data points between 2 and 15 cm since it was an adequate measurement range for the intended application with the most linear behavior. This provided a nicely fitted third-order polynomial equation, with a correlation coefficient of 0.9973, which was applied in the script in order to obtain distance measurement from measured analog voltage. **Digital infrared sensor VL6180X** used a pre-prepared library by sensor's manufacturer, which directly provided distance measurements in millimeters.

All scripts included an initial baseline set, by averaging 20 distance measurements before data acquisition run. Since the acquired signal by the sensors is inverted relatively to the signal intended to be extracted (chest displacement), chest displacement measurements were thus set by subtracting to the established baseline value the read value by the sensor. Depending on the computational load of

different functions used for each sensor, data sampling rate was different for all scripts. However, it was taken into consideration that sampling rate should never be inferior to 40 samples per second, in order to obtain a correctly sampled signal, without aliasing errors, even when performing high frequency compressions.

All selected sensors were directly assembled to Arduino analog or digital pins, with no need of additional electronic components. To ease data acquisition, a pushbutton was added to all circuits providing a better control on acquisition start and end. Sensor assembly on breadboard and connection to Arduino Nano can be found in Figure A.1, Figure A.2 and Figure A.3 of Appendix A. Finally, the acquired data was sent to a standard computer through an USB connection, with a selected baud rate of 9600 bits per second, and was loaded in real-time for Microsoft Office Excel worksheets, by means of PLX-DAQ software.

After completion of script preparation and circuit integration of each sensor, testing protocols were established to assess sensor performance: in a first stage sensor response to compressions was tested considering different assemblies on the manikin to select the most reliable arrangement; in a second stage sensor response to the variation of compression parameters was assessed.

4.3.1 Sensors Functional Testing

To assess the best way for sensor application on the manikin in order to obtain the most reliable signal possible, several configurations were tested by implementing a simple test protocol to assess sensors response to compressions, consisting in 10 to 15 correct compressions after signal stabilization (see "Test Protocol I" in Appendix B). With this test protocol, signal characteristics such as baseline stability, responsiveness to compressions and decompressions, and baseline re-establishment after a set of compressions were considered to assess sensors' adequate response.

To preserve the concordance with previous work, the same standard commercialized CPR manikin used in [43] was instrumented: a Simulaids Adult Brad CPR Manikin with a customized hollow compartment in the foam filling of manikin's chest for ultrasonic and infrared sensor assembly. However, sensor stability in this hollow compartment was low, with sensors positioning changing during compressions, implying a very unstable signal (Figure 4.2). Moreover, the change in manikin's

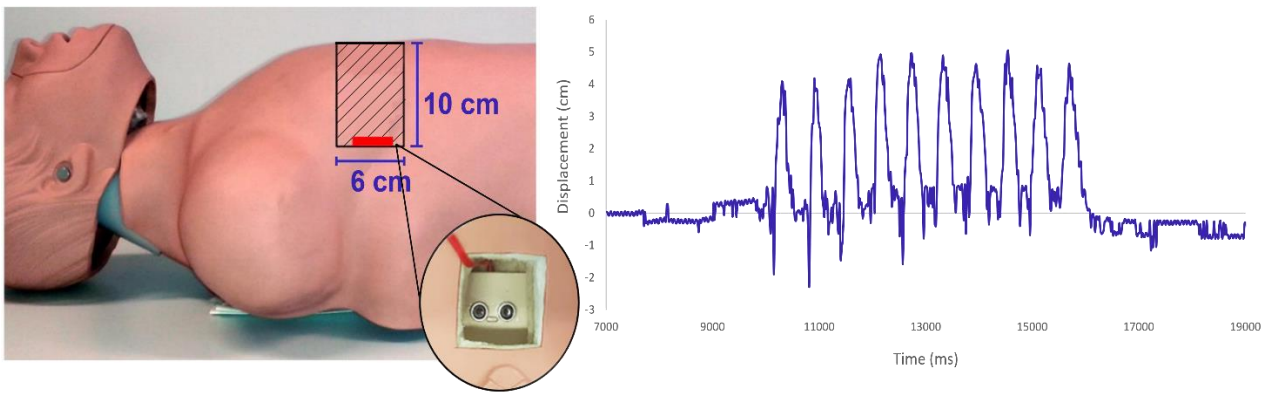

Figure 4.2. Instrumentation of customized Simulaids Adult Brad CPR Manikin with ultrasonic sensor HC-SR04 (adapted from [43]), with corresponding unstable displacement signal during compressions performance.

structure to fit these sensors was not a practical solution to implement, and modifies manikin's chest compliance, which is not convenient. For those reasons, a Laerdal Little Anne was used instead. This manikin is completely hollow, facilitating ultrasonic and infrared sensor implementation, with chest compliance given by a large metal spring. Two different arrangements were tested, by positioning each sensor on the interior of manikin's thoracic structure or on the interior side of manikins' back (Figure 4.3). To improve acquired signal homogenization, a customized surface was strategically added to the manikin, removing manikin structure irregularities.

The results obtained for ultrasonic sensor HC-SR04, digital infrared sensor VL6180X and analog infrared sensor GP2Y0A51SK0F, with a simple qualitative analysis considering the targeted signal characteristics, are available in Figure 4.5, Figure 4.4, Figure 4.6, respectively.

Ultrasonic sensor HC-SR04 assembly on manikin's back shows clear advantage in comparison with its assembly on manikin's chest (Figure 4.5). Despite good response to compressions, with both approaches being clearly adequate for chest compressions detection, some differences exist regarding baseline stability. Sensor assembly on manikin chest is less reliable during compressions, resulting on additional erratic deviations up to 4 mm and a slight baseline drift of 3 mm after chest compressions.

Digital infrared sensor VL6180X provided a baseline with good stability, with an associated constant variability of 1 to 3 mm, with good response to chest compressions and no significative baseline drift after compressions for both arrangements tested (Figure 4.4).

For both assemblies, the infrared analog sensor GP2Y0A51SK0F presents a noisy response to compressions and poor baseline stability, (Figure 4.6 A1, B1) with a constant variability of 2 to 3 mm

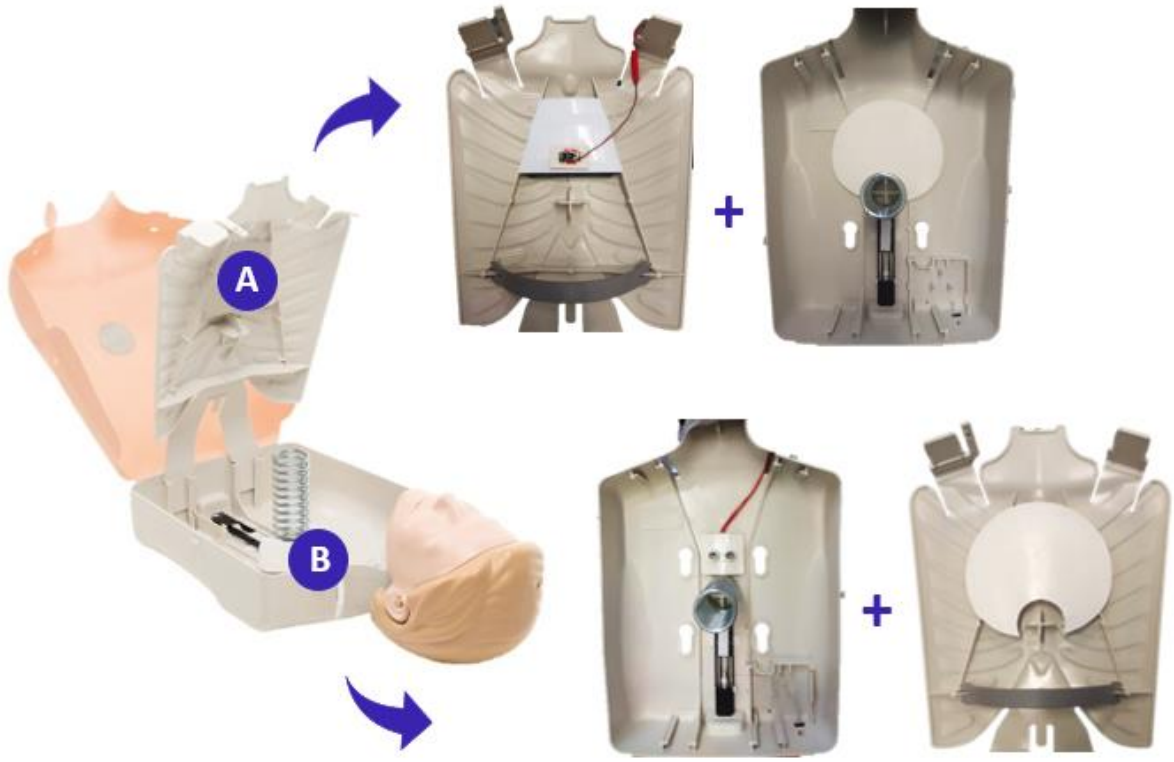

Figure 4.3. Sensor arrangements tested in Laerdal Little Anne: sensor placed in manikin's chest, with reflector surface on its back, exemplified with infrared sensor GP2Y0A51SK0F (A) and sensor placed on manikin's back, with reflector surface on its chest, exemplified with ultrasonic sensor HC-SR04 (B).

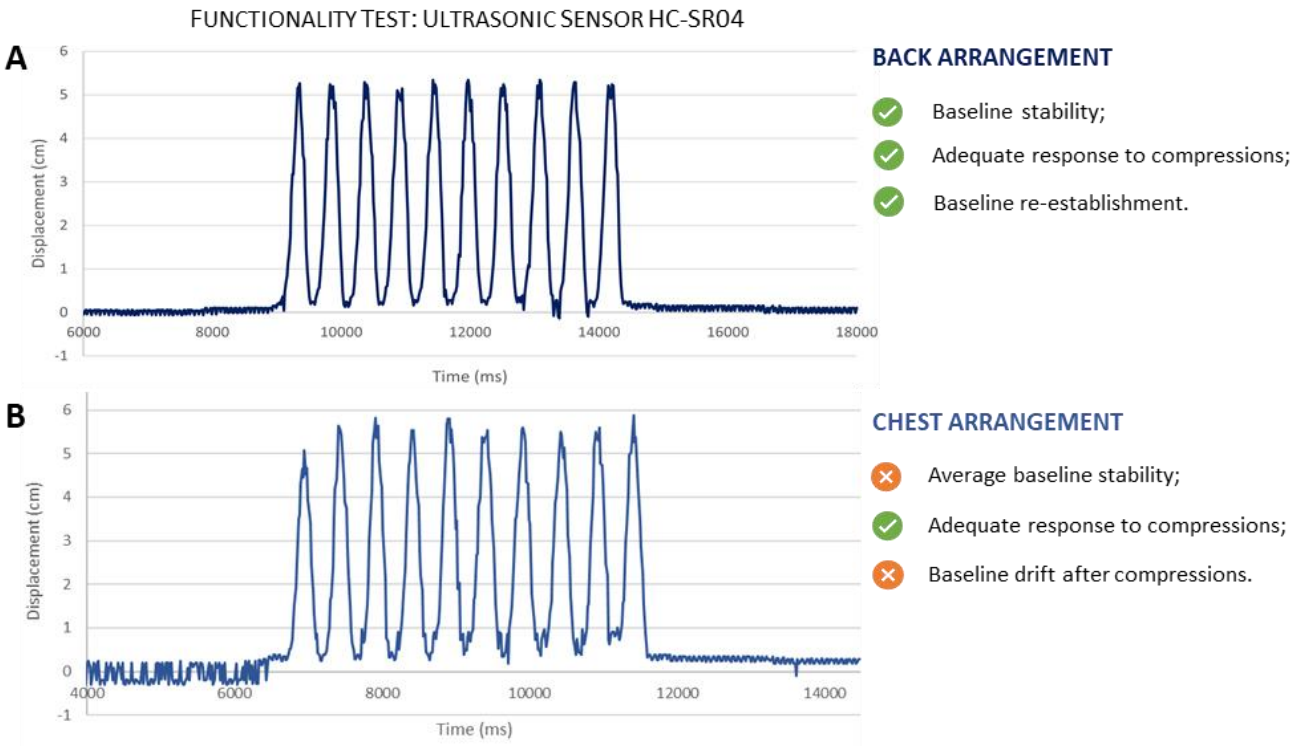

Figure 4.5. Obtained results for "Test Protocol I - Sensor Response to Compressions" for ultrasonic sensor HC-SR04 in the different arrangements tested: (A) on manikin's back and (B) on manikin's chest.

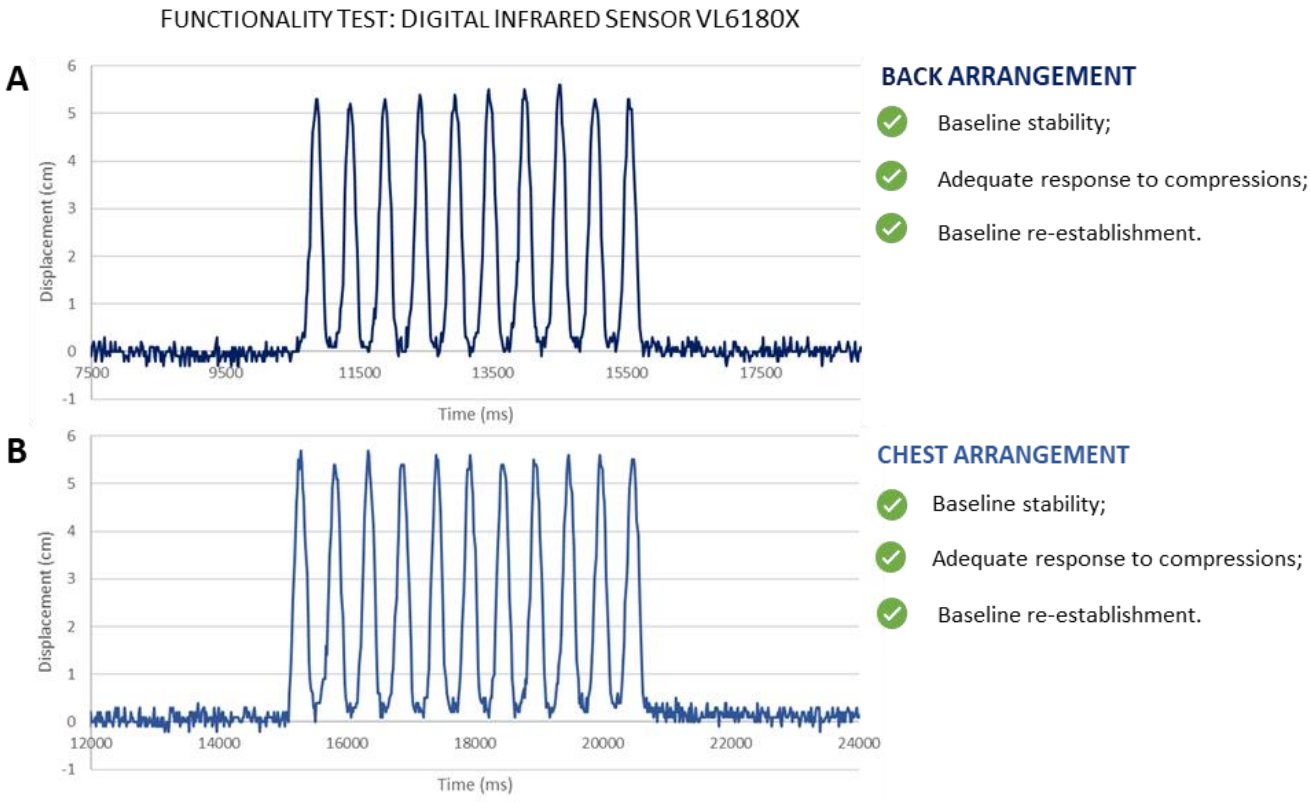

Figure 4.4. Obtained results for "Test Protocol I - Sensor Response to Compressions" for digital infrared sensor VL6180X in the different arrangements tested: on manikin's back (A) and on manikin's chest (B).

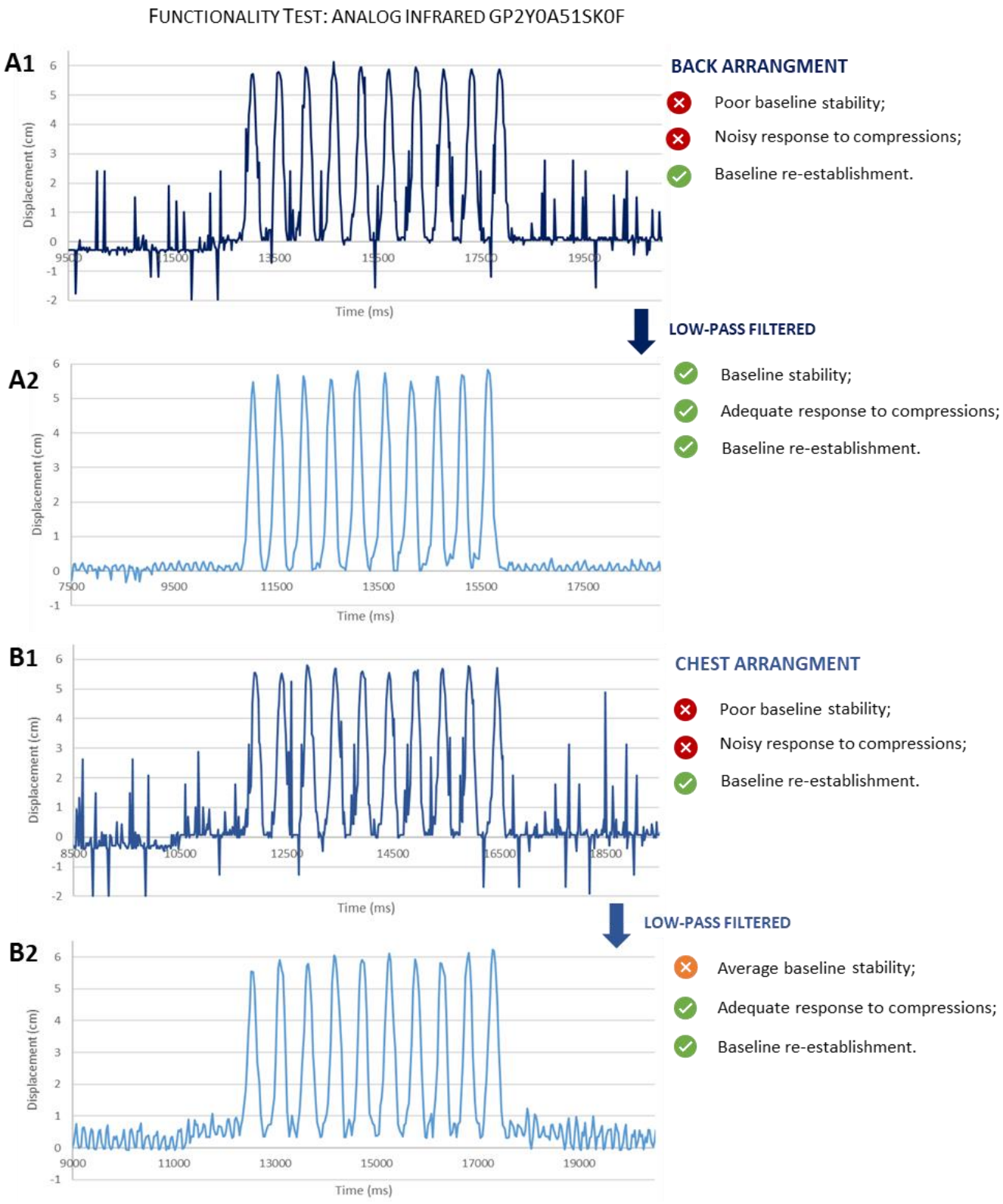

Figure 4.6. Obtained results for "Test Protocol I - Sensor Response to Compressions" for analog infrared sensor GP2Y0A51SK0F in the different arrangements tested: (A) on manikin's back and (B) on manikin's chest back, raw (A1, B1) and real-time low-pass filtered (A2, B2).

and sporadic values between 2 to 5 cm, which are very relevant errors taking into consideration the intended measurement range. This noise was attempted to be reduced with sensor cleaning, infrared dispersion controlling techniques and, ultimately, with sensor substitution, but without improved

results. No justification was found for this phenomenon, but it was considered to provide low confidence on the measured values. Using a real-time low-pass filter, this noise is diminished, with no critical processing load introduced (Figure 4.6 A2, B2). Using this real-time processing tool, the sensor positioning on manikin's chest resulted in a less noisy signal, with a constant variability of 2 to 6 mm, in comparison with its assembly on manikin's back, which has a constant variability of 1 to 3 mm, both with baseline re-establishment after compressions.

Overviewing the obtained results, and concerning sensor arrangement on the manikin, independently of their working principle, sensor positioning in manikin's back seemed to be more robust to chest compressions rough movements, providing a more reliable and stable signal.

Regarding sensors response, and concerning the two tested infrared sensors, analog sensor GP2Y0A51SK0F with real-time data processing and digital sensor VL6180X present similar results. In fact, analog sensor GP2Y0A51SK0F was considered to provided low confidence on the measured values due to its highly noise baseline, which impede the use of this sensor raw displacement data. Despite of the improved results after the real-time low-pass filtering process, the fact that the use of this sensor requires a manual sampled calibration inserts an unavoidable and subjective uncertainty factor, which is expected to introduce measurement errors. Thus, VL6180X's data was considered more trustworthy since it did not require a manually sampled calibration process, contrarily to GP2Y0A51SK0F sensor. For the presented reasons, analog infrared sensor GP2Y0A51SK0F was excluded, and no further testing was made.

Concerning ultrasonic sensor, in comparison with digital infrared sensor VL6180X, it shows an equally adequate response to compressions, although with an apparently less variable baseline and higher reliability. This apparent improved stability is, in fact, a signal artifact, due to the lack of resolution of ultrasonic sensor for values bellow 3 mm, having the baseline stability associated with this sensor no real significance. The response provided by both ultrasonic sensor HC-SR04 and infrared sensor VL6180X can be thus considered equivalent regarding response to chest compressions and baseline behavior.

Thus, ultrasonic sensor HC-SR04 and infrared sensor VL6180X, placed on manikin's back, were selected as the preferred arrangements regarding sensor response to compressions, since both sensor types were considered adequate for compression detection.

4.3.2 Sensors Performance Testing

Being selected the sensors and the arrangements with better sensory response, the next testing stage included the assessment of their performance in the detection of the different chest compression parameters and their respective variations. For that purpose, a new test protocol was designed, consisting of four different settings, in which a single chest compression parameter varied, while maintaining the remaining parameters in their (correct) operating-point (see "Test Protocol II" in Appendix B). Independent tools were used to standardize chest compressions execution: for frequency, a metronome mobile app; for chest displacement, Little Anne's clicker mechanism; and for both

frequency and depth, the Practi-CRdM Compression Depth and Rate Monitor, a wrist-wearable device that provides real-time feedback on compression quality of these two parameters through visual LED signals and audible “beeps”.

The obtained results are represented in Figure 4.7. As expected, both sensors have a stable baseline that is re-established after every compression set, which is a good indicator of systems robustness to compressions. Regarding compression parameters, both ultrasonic and infrared selected sensors are capable of accurately detecting variations on compression depth, rate and chest recoil (Figure 4.7. C to J), with clear differentiation among shallow, correct, and deep compression depth, low, correct, and high compression frequency and full or non-full chest decompression. Regarding hand position, both systems fail to distinguish between correct and incorrect hand position, with high amplitude peaks being detected even with incorrect hand position during compressions (Figure 4.7. A, B).

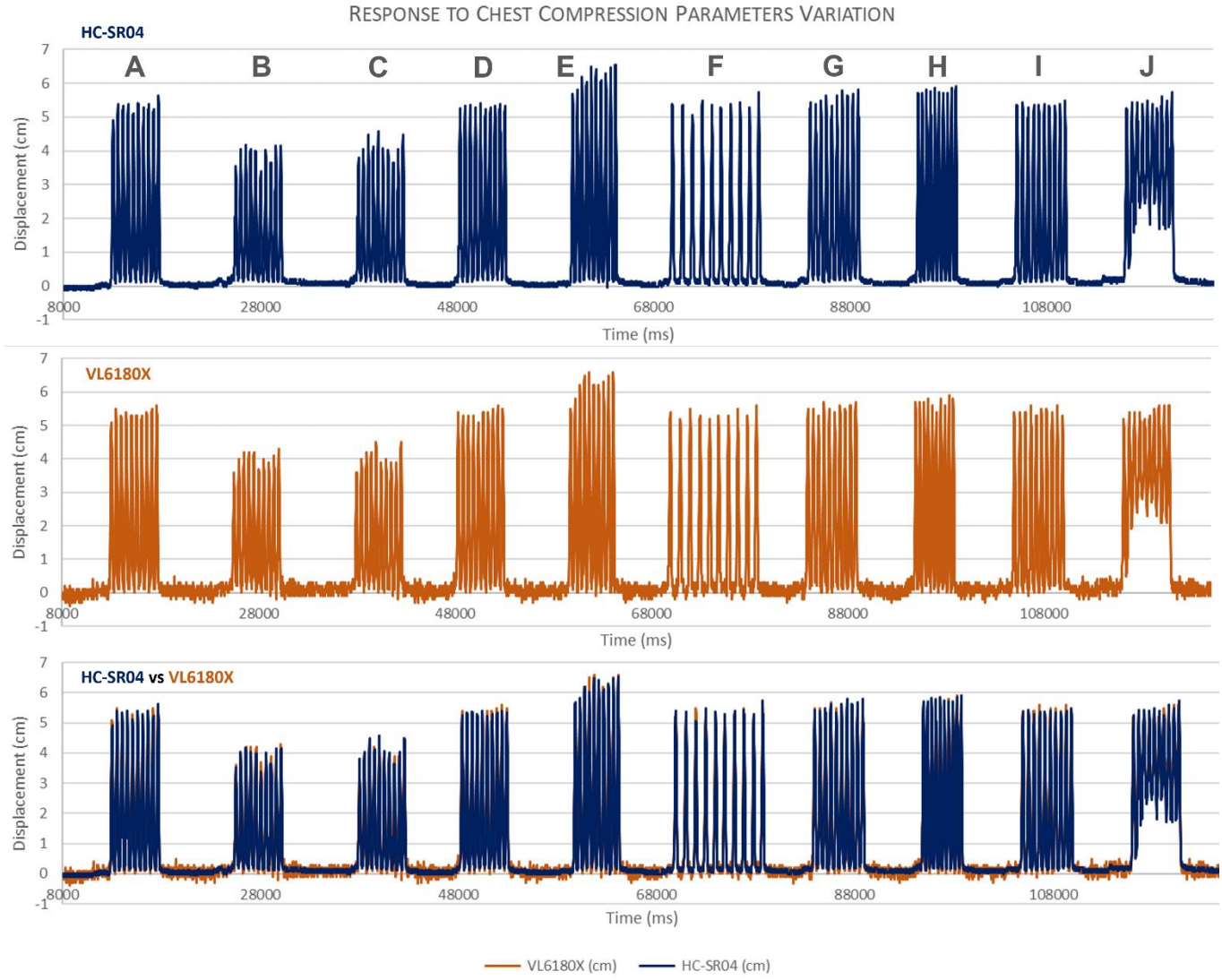

Figure 4.7. Obtained results for “Test Protocol II - Sensor’s Response to Variations in Compressions Components” for ultrasonic sensor HC-SR04 (on top) and digital infrared sensor VL6180X (in the middle), condensed in a single acquisition. The graphic on the bottom represents both sensor signals superposed. Ten chest compression parameter variations were considered: (A) correct hand position, (B) incorrect hand position, (C) shallow compression depth (< 5 cm), (D) correct compression depth (5 to 6 cm), (E) extreme compression depth (> 6 cm), (F) low compression rate (< 100 cpm), (G) correct compression rate (100 to 120 cpm), (H) high compression rate (>120 cpm), (I) correct recoil, (J) incorrect recoil.

Signal superposition shows that measured peaks, either for compressions depth and chest recoil, are slightly different for ultrasonic and infrared tested sensors, a difference justified be sensors' intrinsic measurement variability. Thus, both measurements were considered equivalent and equally valid. Concerning the sensors inability of hand position detection, it is an expected result as both sensors directly measure displacement, independently of where the force is applied. Even with incorrect hand position, manikin's thoracic structure presents relevant displacement, invalidating the single use of any of these sensors to correctly assess this parameter.

The performance tests indicated that both ultrasonic sensor HC-SR04 and infrared sensor VL6180X, are adequate to detect variations in compression depth, rate and recoil. However, their isolated use for complete chest compression assessment quality is not feasible since they lack on the detection of the quality of hand position, a compression parameter that must be guaranteed by an additional sensor, with a different sensory principle, explored in the next section.

4.4 Sensor Selection for Hand Position Assessment

In order to overcome ultrasonic and infrared sensors reported limitation, the most straightforward approach to about hand positioning was to use pressure sensors, an attempt inspired in Nicolau's work [43] (see section 3.4). Since the use of pressure sensors is intended to provide an on/off parameter regarding hand position, reported repeatability issues due to sensors wear were considered a minor issue for this application. For the same reason, the technical requirements established in section 4.1 do not apply in pressure sensors selection. Nevertheless, the established operational requirements maintain, namely: selected sensors must allow reduced development cost and simple implementation, including easy assembly and generic implementation to different training manikin models, and a low computational and processing load regarding signal acquisition. A similar approach was used: sensor selection including sensor screening through different commercially available pressure sensors, and the performance testing to assess their response to hand positioning during chest compressions.

4.4.1 Market Search for Pressure Sensor Selection

An extensive search was made to select the most appropriate pressure sensors for the intended application. More complex pressure sensors, with other measurements comprised (as barometric pressure, vibration, *etc.*) were not included. Most on-the-market available pressure sensors presented similar characteristics, differing essentially on active area dimension and lifespan. The selected sensors to be tested are presented in Table 4.2. These sensors were selected due to their high estimated lifespan and low price, varying only in active area dimension and format, in order to test which format would be most adequate for correct hand position detection. Both are piezoresistive pressure sensors, typically consisting of a pressure sensitive element which changes its resistance upon application of force [40].

These sensors generally require simple implementation and are hardly susceptible to noise, although they may suffer from hysteresis associated problems [40].

Table 4.2. Selected pressure sensors general characteristics according to available information on local stores (prices collected on May, 2021).

Pressure Sensor	Working Principle	Dimension	Output Type	Other Characteristics	Price
Interlink FSR 402 [77]	Piezoresistive	1,8 mm diameter (round)	Analog Voltage	Stand-Off Resistance: 10 MΩ Force range: 0,1 to 100 N; Lifespan: 10 million times tested; Hysteresis: +10%; Drift: <5%; Repeatability: ± 2%.	€ 11,01
Interlink FSR 406 [78]	Piezoresistive	4,4 x 4,4 cm (squared)	Analog Voltage	Stand-Off Resistance: 10 MΩ Force range: 0,1 to 100 N; Lifespan: 10 million times tested; Hysteresis: +10%; Drift: <5%; Repeatability: ± 2%.	€ 16,73

4.4.2 Sensors Testing

Having selected the sensors to be tested, the next phase consisted of sensors preparation and assembling, which included programing scripts and circuit planning for extracting relevant measurements.

Regarding sensor assembling, both sensors were placed in the target compression area of manikin thoracic structure, on a protective foam structure. The placement of the sensors considered the stability of both sensors' active area and connections, considering the sudden compression movements. Additionally, sensors were covered with a layer of a protective foam, not only to protect against sensor deterioration due to the intensity of the applied force, but also to promote homogeneous force distribution and sensor stability (Figure 4.8). Both sensors were integrated in a voltage divider circuit with a pull-down resistor, as recommended by manufacturer datasheets [79], [80], and were integrated in the previously used breadboard arrangement (see Figure A.4 and Figure A.5 of Appendix A).

Concerning sensor implementation software, a simple Arduino script was designed to implement these pressure sensors in order to assess hand positioning. The read analog values between

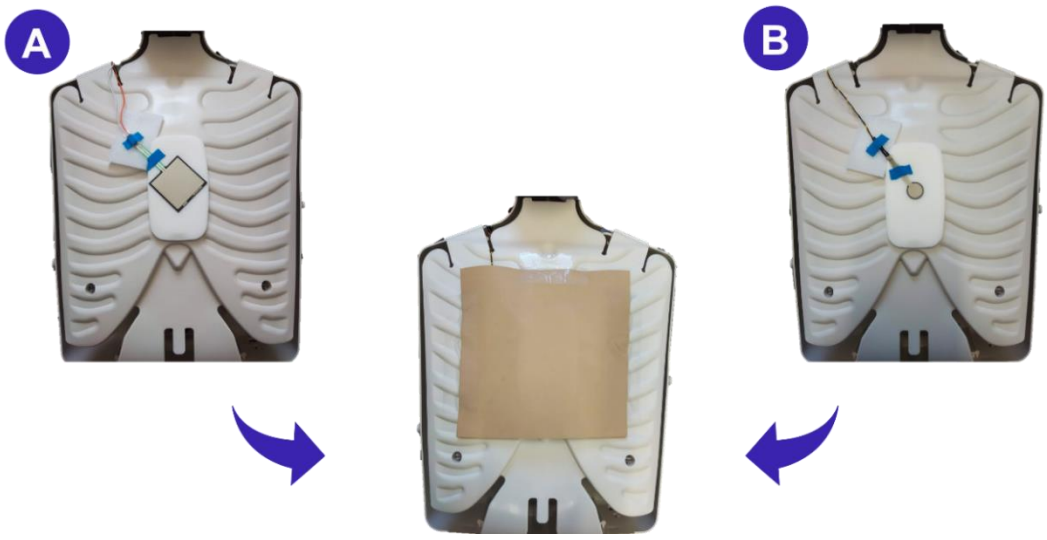

Figure 4.8. Pressure sensors arrangements on the manikin: (A) Interlink FSR 406 and (B) Interlink FSR 402.

0 and 1023 were mapped to voltage values between 0 and 5 V using Arduino's *map* function. According to the designed circuit, the sensors resistance is given by Equation (1),

$$R_{sensor}(t) = R_{PD} \times \left(\frac{V^+}{V_{out}(t)} - 1\right) \quad (1)$$

with $R_{sensor}(t)$ as the variable resistance of the pressure sensors, R_{PD} as the measuring pull-down resistor, V^+ as the operating voltage provided by the Arduino (+5 V) and $V_{out}(t)$ as the resulting sensor's variable voltage. The selected pull-down resistor was of 0.2 kΩ for Interlink FSR 406 squared sensor and 2.2 kΩ for Interlink FSR 402 round sensor, which were the resistance values that provided a better sensitivity response to the applied force. Higher resistance values, usually used with these sensors and recommended in the respective datasheets led to easy signal saturation. In order to linearize Equation (1), the inverse of the resulting resistance (conductance) was used and scaled by a factor of 10^6 to facilitate signal representation and analysis.

To assess sensors response to hand positioning, a simple test protocol directed to this parameter was implemented, consisting in a set of compressions performed with correct hand position and four sets of compressions, each with a different incorrect hand position (see "Test Protocol III" in Appendix B). To assure reproducibility of the variation of hand position, the manikin torso was divided into five different compression areas (Figure 4.9).

The obtained results are available in Figure 4.9. Round pressure sensor Interlink FSR 402 showed advantage by being insensitive to all incorrect hand positions tested, providing measurable signal only when compressions were applied in the correct compression area. Contrarily, squared pressure sensor Interlink FSR 406, possibly due to its bigger dimension, detected measurable signal with incorrect hand position, when applying compressions on manikin's ribs, even though with lower amplitudes. Thus, round sensor Interlink FSR 402 aimed to be the perfect fit for hand position assessment. To clarify that, even with its reduced size, the chosen round sensor was capable of

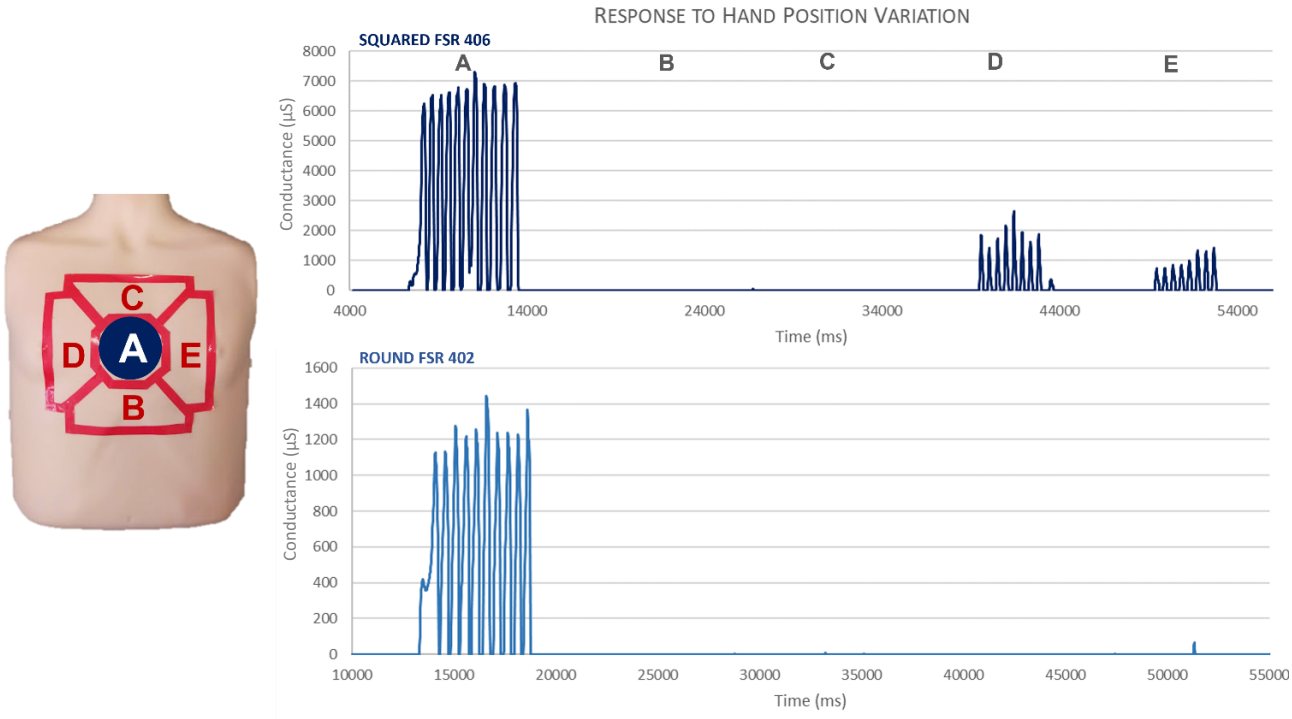

Figure 4.9. Obtained results for "Test Protocol III - Pressure Sensors' Response to Hand Position" for both pressure sensors tested, Interlink FSR 406 (on top) and Interlink FSR 402 (on bottom), considering five test positions: (A) middle of the chest (correct hand position), (B) stomach (bellow correct hand position), (C) middle of the sternum (above correct hand position), (D) right ribs (on the right of correct hand position) and (E) left ribs (on the left of correct hand position).

measuring hand position in all the chest area considered for correct hand position, an additional acquisition with hand position variation inside the correct chest compression area was made, confirming that the sensor was sensible to applied pressure in all the correct chest compression area.

4.5 Critical Analysis of the Obtained Results

Both ultrasonic sensor HC-SR04 and infrared sensor VL6180X, were considered to adequately and accurately detect variations in compression depth, rate and recoil, with equivalent responses regarding chest compression detection and baseline behavior. As both of these sensors lack on hand position assessment, an additional round piezoresistive pressure sensor, Interlink FSR 402, was integrated in the measurement system, which effectively differentiated correct from incorrect hand position during chest compressions, in all the positions tested. The accurate detection of the four established compression parameters is then guaranteed with this sensory system.

Concerning the previously established requirements, all the three sensors allow an accessible development cost and a simple implementation, with easy circuit integration, low computational load for data acquisition, and a generic and highly reproducible implementation in different manikin models, with the restriction that these must present a hollow structure. In such conditions, the selected distance sensors are expected to have great reproducibility and reliability. As piezoresistive pressure sensor is

intended to provide an on/off signal regarding correct/incorrect hand position, no issues regarding sensors' repeatability and reproducibility previously documented were considered relevant.

The combination of either ultrasonic or infrared selected sensors with the chosen pressure sensor, based on the qualitative analysis performed, seems to provide an accurate, affordable, and reproducible solution to the detection of the four quality parameters of chest compression during CPR training, and justify further developments in order to be integrated in a training prototype and tested during CPR training.

Chapter Conclusions

The research for development of a feedback system to support CPR training, focusing on chest compression parameters assessment, was introduced with an operational approach by instrumenting with off-the-shelf sensors a standard training manikin. A methodic approach was applied, including a market search and sensor selection, circuits design, script programing and application of different test protocols to select the most adequate sensors for the intended application. Ultrasonic and infrared optical sensors were tested with encouraging results regarding the response to different chest compression depth, rate and recoil, as both directly measure chest displacement. The provided response by both ultrasonic and infrared was considered equivalent regarding baseline stability and re-establishment, and response to chest compressions. It was, however, not possible to privilege one over another, since both are considered to provide trustworthy measurements, and are often used as a validation tool to other sensory technologies for chest displacement measurements in the state-of-the-art [43]. Hand position, a parameter not assessable through the single use of these sensors, were measured through an additional piezoresistive pressure sensor, included to assess correct hand positioning during compressions. Based on the obtained results, the combination of an infrared or ultrasonic sensor with a piezoresistive pressure sensor provides accurate measurements of the compression parameters, with easy and generic implementation on hollow training manikins at a reduced cost.

5

AN INNOVATIVE EXPLORATORY APPROACH USING OPTICAL FIBER TECHNOLOGY FOR CHEST COMPRESSION DETECTION

Optical fibers have, for several years, been an important part of the communication industry development, with well-known applications in this field. In parallel with these developments, optical fiber sensing technology has been an important part of sensor applications, as they have been studied to sense physical-related parameters such as strain, stress, pressure, vibration, bending and, among others, displacement [81]. Its application as a sensing system to assess chest compression quality during CPR training, namely chest displacement, is worth to be explored, as no similar approach was found on the literature. This chapter offers a brief presentation of general introductory concepts in waveguide theory and overall optical fiber characteristics, exploring then in further detail the use of optical fibers as a sensing system, considering the measurement scale of interest. Finally, an experimental innovative approach for chest compression detection using optical fiber is presented, with a methodology similar to the work previously developed with off-the-shelf sensors (see Chapter 4).

5.1 The Optical Fiber as a Sensing System: Introductory Concepts and Applications

Along the years, a variety of optical fibers have been developed by manipulating their chemical and physical structure, expanding optical fiber's applications not only in communication field, but also as a sensing mechanism. Optical fibers work by confining and guiding the light waves within the fiber core by the principle of total internal reflection. They are typically formed by three concentric elements: the core, consisting in the light carrying portion of the fiber; the cladding, which surrounds the core, and a protective jacket, which protects the fiber from external damage. If the refractive indices of the core; and cladding are n_1 and n_2 respectively, with $n_1 > n_2$, then for a ray entering the fiber, if the angle of incidence θ_i at the core-cladding interface is greater than the critical angle θ_c, then the ray undergoes a total internal reflection at that interface and is guided along the fiber inside the core [82].

This phenomenon is mathematically represented by Snell's Law, in Equation (2). If the angle of incidence is below the critical angle, the light refracts and is only partially reflected at the interface.

$$\theta_c = \sin^{-1}\left(\frac{n_2}{n_1}\right) \tag{2}$$

Only light incident on the fiber within a range of angles will be incident on the core–cladding interface at an angle of incidence greater than the critical angle, allowing total light reflection [82]. This phenomenon is given by fiber's numerical aperture, an indicator of the light gathering efficiency that gives the range of angles over which the system can accept or emit light. Within the angles of incidence allowing total light reflection, only discrete angles result in constructive interference, each corresponding to a guided mode. Optical fibers that support only the fundamental mode, corresponding to the highest angle of incidence allowed, are called single-mode fibers whilst multi-mode fibers support several modes [82]. All these fiber properties directly depend on physical and chemical manufacture of the fiber, as core diameter and material refractive indices, and can be manipulated and designed according to the interest of fibers application.

Beyond the reviewed manufacture parameters of optical fibers, light losses are a crucial parameter that should be considered in optic fiber functioning. The loss mechanisms contributing to attenuation in an optical fiber include intrinsic sources inherent to the material, as light absorption, Rayleigh scattering, due to inhomogeneities in the core refractive index and scattering due to irregularities at the core-cladding interface, and extrinsic sources as bending losses and losses at joints and connectors. The overall attenuation is a relative measure of the output to input intensity that express all these contributions, given by Equation (3),

$$\alpha = -\frac{10}{z}\log\left(\frac{P(z)}{P(0)}\right) \tag{3}$$

where α is the attenuation coefficient, $P(z)$ is the optical power at fiber's length z, and $P(0)$ is the optical power at the fiber's origin. In communication applications one tries to minimize such effects so that signal transmission and reception is reliable. Thus, single-mode glass fibers are usually preferred as they provide low signal loss, high information capacity, or bandwidth, and low light dispersion due to their thinner fiber cores. However, in optical fiber sensing, the response to external influence is deliberately enhanced so that the resulting change in optical radiation can be used as a measure of the external perturbation [83], giving rise to a series of different sensing methods. Thus, is now pertinent to review the most common sensing systems applied to optical fibers and their most relevant in biomedical applications at the scale of interest for the scope of this project, since there are no reported developments regarding the use of optical fiber sensors for chest compression monitorization during resuscitation training.

Optical sensing systems have three basic components: the light source, the optical fiber as the sensor element, and the light detector [84]. In general terms, a physical quantity can change the physical properties of the sensing element, which, in turn, leads to a change in the light properties that are read

and analyzed in a light detector [84]. Since light properties can be considered in most circumstances independent parameters, they offer a wide range of solutions to sense several physical quantities [84]. The most common working principles applied to fiber optical sensors for biomedical applications are based on intensity, phase, and wavelength modulation [84]. Both intensity-modulated and wavelength-modulated working principles and applications of interest will be further explored. Phase-modulated techniques, done by interferometric-based sensors, will not be explored since they were considered to have a complex implementation to the intended application.

5.1.1 Intensity-modulated Optical Fiber Sensing Systems

Intensity modulated sensors' working principle is based on the variation of the light intensity provoked by the variation of a physical quantity [84]. The operationalization of these systems is very simple in structure and cheap in cost [85], requiring simple optical light sources and a receiver capable of converting light power changes into a voltage signal [85], additionally to the optical fiber itself, which is their main advantage comparing to other optical sensing systems. Along the years, several configurations employed on biomedical applications have been described, which inspired the use of optical fiber as a sensing mechanism for CPR quality assessment. The review of these approaches, their main advantages and limitations, and light source and fiber type used in operationalization are resumed in Table 5.1. Patil *et al.* [86] developed a displacement sensor based on two optical fibers facing each other at a known distance, to measure fingers joint angles. The measure will change the distance and alignment between the two fibers and, consequently, the light intensity transmitted. Yoo *et al.* [87] used the reflexive method by placing optical fibers in front of a movable reflecting mirror to assess respiratory rate. The chest displacement during respiratory cycle varies the original mirror distance to the fiber tip changing the intensity of the reflected light. Both these approaches could be easily adapted to the application in study. However, configurations that imply the light propagation outside the fiber are associated with greater noise and are easily unstable for measure dynamic movements, which directly affects the accuracy of the sensor. To overcome this limitation, it is possible to modulate the light transmission of an optical fiber due to the bending of the fiber [81], with optical power decreasing when the fiber is under bending deformation. In fact, fiber bending can cause light leakage as the angle of incidence is compromised and total internal reflection might fail, meaning that the light may be no longer confined and guided by the core of the fiber. This fiber bending can assume two forms: microbend, due to microscopic fiber deformations in the core-cladding interface that can be reinforced by non-uniform lateral stress or pressure, and macrobend, that is characterized by a radius of curvature, that compromises incidence angle and, thus, total internal reflection (Figure 5.1).The amount of light leakage through fiber bending depends on fiber physical and chemical properties. Kopola *et al.* [88] tried the microbending transmission loss technique to quantify biting force measurements, which can be assumed to be as high as force applied during compressions, but with low sensitivity to the high applied forces. Regarding macrobending losses, the fiber can be formed into a U-shape, round loops,

Table 5.1. Applications of interest for the scope of the development of a sensory solution for CPR training assessment, using intensity-modulated optical fiber sensors.

Ref.	Measurement Technique	Application	Reported Advantages	Reported Limitations	Operationalization	
					Light Source	**Optical Fiber**
[86]	Intensity loss: misalignment between two fibers	Joint angle monitoring (fingers)	NA	Difficult to maintain fiber's alignment;	820 nm GaAIAs emitter	Multi-mode glass fiber
[87]	Intensity loss: reflective method using a mirror	Respiration monitoring (rate)	High sensitivity	Bulky system	530 nm LED	Multi-mode polymeric fiber
[88]	Microbend loss	Biting force measurement	Good repeatability	Low measurement resolution	LED (NS)	NA
[89]	Macrobend loss: U-shape form	Respiratory monitoring (rate)	NA	Instable and noisy signal	1310 nm FP laser	Single-mode glass fiber
	Macrobend loss: sinusoidal form		High reliable response (extension range: 30 mm)	NA	1550 nm SLED source	
[90]	Macrobend loss: sinusoidal form	Respiratory monitoring (rate)	Simple and compact measurement system; High repeatability; High sensitivity.	Uneven light attenuation between each fiber curve	1310 nm LED	Glass fiber (mode NA)
[91]	Macrobend loss: sinusoidal form	Joint angle monitoring (elbow)	NA	Low resolution	1550 nm broadband source	NA
[92]	Macrobend loss: single loop	Respiratory monitoring (rate and tidal volume)	Linear response (measurement range of 6.5 mm); Sensitive to very low amplitudes and high oscillatory frequencies (15 Hz).	Fiber damage for small bend radius due to excessive force	780 nm GaAlAs laser diode	Single-mode glass fiber

Table 5.1 (Continued).

[93]	Macrobend loss: multiple loop	Respiratory monitoring (rate and depth)	NA	Difficult configuration to maintain; Low signal to noise ratio;	NA	NA
	Macrobend loss: figure-of-eight		Self-sustain position; Good repeatability; Wide linear response (extension range: 50 mm); Good sensitivity; Robust and reliable	Need for frequent calibration; Inaccurate for large displacements	950 nm LED	Multi-mode glass fiber
[94]	Macrobend loss: linear form, side polished	Joint angle monitoring (knee)	More sensitive than regular macrobend; Sensitive to the bending direction.	NA	660 nm LED	Polymeric fiber; Side polished fiber.
[95]	Macrobend loss: linear form, side-polished	Respiratory monitoring (rate)	Good linear relationship with curvature; Sensitive to the bending direction; Higher sensitivity than regular macrobend; Good response to high frequencies.	NA	660 nm LED	Multi-mode polymeric optical fiber; Side-polished fiber

NA – not available; NS – not specified

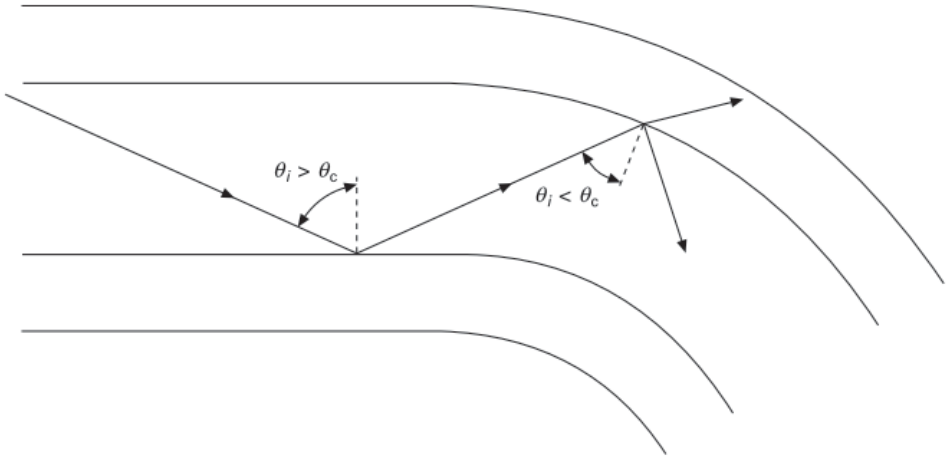

Figure 5.1. Effect of macrobend phenomenon on light propagation inside an optical fiber, with θi as the angle of incidence at the core-cladding interface and θc as the critical angle [82].

sinusoidal shape or other bending configurations to allow light intensity attenuation [81]. The variety of easily achievable transducer approaches is one of the main advantages of macrobending loss sensors, allowing the possibility to fit the best configuration for a certain application. Several configurations were tested for respiration monitoring and joint angles monitoring. U-shaped optical fiber resulted in a very noisy and unstable signal, that found improved reliability in sinusoidal shape approach [89], [90]. However, fiber bending loss using sinusoidal configurations showed some limitations as uneven force distribution among each individual curve [90] and low resolution for elevated deformations [91]. Loop configurations, despite of the good response to stimulus, were reported to be unstable configurations, with considerable noise associated and a non-proportional response between number of loops and bending losses [92], [93] . A different optical fiber geometry using a figure-of-eight shape to cope with the limitations of the previous technique was proposed. Augousti *et al*. [93] studied a figure-of-eight fiber optic sensor with a linear response over a large displacement range, good repeatability and good response to high frequencies. It was also described as more robust and reliable conformation with increased sensitivity, in comparison with other fiber conformations for similar applications. More recent application using intensity modulated techniques use side-polished fibers in linear configurations, that facilitate light leakage towards macrobending, providing higher sensitivities to bending [94], [95] . This requires, however, additional fiber treatment. Although there are some limitations compared to other modulation techniques, such as lower sensitivity, potential error sources including unpredictable light loss in the fiber due to absorption and scattering [81], and variable losses due to connectors, intensity modulated optical fiber sensors are widely used in different applications, particularly in cases where no fine measurement precision is requested. The reasons behind their extensive and diversified applications include their components and assembly simplicity [85], flexibility, easy measurement method [81], small sensor size and overall low cost.

Regarding operationalization choices, both glass and plastic, multi-mode and single-mode fibers were used, with the corresponding light sources at the working wavelength (infrared, for glass fibers and visible for polymeric fibers). As single-mode glass fibers presented great advantage for long distance applications, as in the communications field, multi-mode polymeric fibers might be more

beneficial for intensity modulated sensing systems. In fact, contrarily to traditional glass fibers, polymeric optical fibers provide higher flexibility, simple assembly and connections, easy handling and lower cost, although they present lower bandwidth and higher optical loss in shorter distances [81]. Similarly, multi-mode fibers, having larger fiber cores, suffer greater light attenuation and dispersion. However, since these applications use short lengths of optical fiber, these limitations are of little relevance. To be considered, however, that these losses still exist and, even with little relevance within the most beneficial operationalization choice, must be minimized in order to allow light loss origin being essentially on fiber bending. It is critical to consider the selection of the fiber, wavelength operating range, detector and other issues to make sure the designed sensor is capable to produce good measurement results [81].

5.1.2 Wavelength-modulated Optical Fiber Sensing Systems: Fiber Bragg Gratings

Wavelength modulation is typically achieved through use of fiber Bragg grating (FBG) sensors, which are characterized by a periodic perturbation of the refractive index of the fiber core, called the Bragg grating. Their working principle is based on the light reflection: when the light travels inside the grating structure, a light portion gets reflected from each grating plane, forming a beam of reflected light centered at the Bragg wavelength, given by Equation (4),

$$\lambda_B = 2\Lambda n_1 \tag{4}$$

where Λ is the grating period that forms the distance between two adjacent grating planes, n_1 is the effective core refractive index, and λ_B is the Bragg wavelength. Thus, the grating structure that follows this Bragg condition works as a mirror that reflects selected wavelength λ_B and transmits the remaining (Figure 5.2) [96]. When the fiber is stretched or compressed along its axis, the refractive index will change by photo-elastic effect, along with the spacing between the grating [84]. Because the Bragg wavelength is directly proportional to the grating period, a shift in the Bragg wavelength will be observed making possible to monitor the induced strain [84]. This mechanism can be used as a generic sensing element to quantify several physical quantities as force, pressure, vibration, among others [84] with extraordinary accuracy. Being one of the most studied topics recently in optical fiber sensor field, the same applications tested with intensity modulated sensors were adapted for FBG sensors for improved measurement techniques (Table 5.2). In general, the use of FBG sensors provides highly accurate measurements, with high sensitivity and linear response to axial strain, providing direct and absolute measurements [97]. Additionally, they are reported as having low fatigue and high durability than other optical technologies. The main drawback of the use of FBG is the relative high price of stable light sources and wavelength demodulation devices needed by grating based optical fiber sensors to detect wavelength shift (that can range up to 30 000 €), although these systems can obtain much higher accuracy than intensity modulated optical fiber sensors [85].

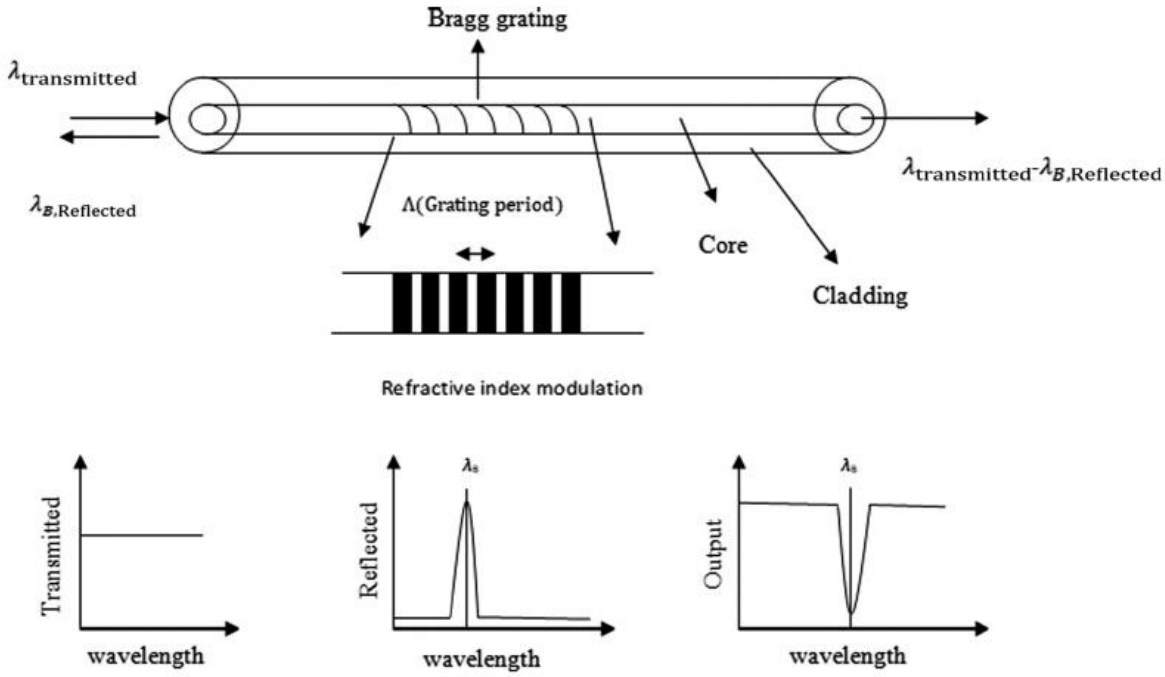

Figure 5.2. Structure of fiber Bragg grating along with the transmitted, reflected, and output spectra [96].

Table 5.2. Applications of interest for the scope of the development of a sensory solution for CPR training assessment, using FBG sensors.

Ref.	Application	Reported Advantages	Reported Limitations
[98]	Respiratory movements monitoring	Good frequency response (up to 10 Hz); Good signal-to-noise ratio.	Difficult to guarantee long-term stability; Periodic calibration needed for accurate measurements; Expensive interrogation method.
[99]	Knee Kinematic Monitoring	Good response to detailed gait movements	Expensive interrogation method
[100]	Bite Force measurement	Large force measurement range (up to 900 N); Good resolution.	Expensive interrogation method
[101]	Vertical pressure assessment	Cost effective sensor production; Extended pressure range (up to 800 kPa); Good sensitivity.	Expensive interrogation method

5.1.3 Technology Analysis: Macrobending vs FBG

Some of the ideas just presented seem to be appellative to experimentally test an approach using optical fiber technology as a sensing mechanism for CPR training assessment. In fact, there are many inherent advantages of optical fiber sensors in comparison to mechanical and electrical sensors, including their ability to be lightweight but still mechanically robust, of very small size and simple structure, low power, all dielectric and thus resistant to electromagnetic interference [81]. Additionally, it provides a fast response speed, with high sensitivity [84]. Depending on the detection method, optical fibers are also affordable to use for many applications [81]. For any sensing technology to be viable in the long-term, it is important to consider the cost-effectiveness of the sensory system and the reliability of measurements over other existing techniques [85].

Intensity-based optical fiber sensors, despite of their geometric versatility, have several limitations imposed by variable losses that are not related to measured quantities, which leads to the lower sensitivity and lower accuracy of the measurement system. However, compared with the other optical fiber sensor types, the tremendous advantages on price, turn intensity-based sensors a very relevant option in applications fields where no fine measurement precision is requested.

FBG sensors, on the other hand, are highly sensitive and accurate in comparison to intensity-modulated sensors. However, this high-performance system is at the expense of higher price, which limits their widespread usage for many applications.

Regarding the intended application for CPR training assessment, the accuracy needed for the working measurement scale might be possible to achieve using an intensity-modulated approach, corroborating the idea of the development of a portable and easily adaptable sensing system at an accessible development cost. On the other hand, as the accuracy and resolution of FBG sensors might be excessive for the measurement scale intended for CPR training quality assessment, not justifying such higher equipment cost, their use might potentially be a good validation tool, which is missing in this application filed.

Optical fiber sensing systems, however, remain unknown to many engineers and researchers, probably because most development and research solutions are focused on conventional sensors and non-optical technologies. In fact, an important drawback of some optical fiber sensors is the lack of scientific information reporting their use in practice, with the absence of detailed technical specifications, as repeatability, reproducibility, working range, accuracy, response time, among others, even with the associated use of commercial optical sensory solutions.

5.2 An Experimental Approach using a Polymeric Optical Fiber as Macrobending Sensor for Chest Compression Detection

The use of optical fiber sensors, namely intensity-based macrobend sensors, in the several applications seen in section 5.1, inspired its use for assessing chest compressions quality, namely as a low-cost displacement sensor to measure compression depth, as an alternative to previously tested optical and ultrasonic sensors. This is a completely innovative approach on the topic, with no previously reported use of this technology for chest compression detection. Similarly to the methodology used in Chapter 4, this chapter presents, as an exploratory approach, the application of different macrobend configurations in the detection of different chest compression parameters, to evaluate the viability of the use of this technology as a sensing mechanism for quality assessment. This experimental approach was only possible due to an established collaboration with the *Instituto de Telecomunicações* of *Universidade de Aveiro* (IT-UA), namely, with the researchers Maria de Fátima Rodrigues (PhD), Paulo Antunes (PhD) and Nélia Alberto (PhD).

5.2.1 Requirements for Macrobending Sensor Application

The first step for this experimental approach goes through the selection of the appropriate optical fiber, light source and photodetector. As the aim of the sensory system is to enhance light loss due to macrobending phenomenon, multi-mode polymeric optical fibers were the preferred choice for this application, considering their high flexibility, higher light attenuation, and low cost. Since a short fiber length was planned to be used, no relevant issues regarding complete loss of measurable signal over the fiber were expected. Regarding light source, the only mandatory characteristics was to function in a visible wavelength in order to be compatible with the selected polymeric fiber, and to provide the highest optical power possible. The photodetector should be compatible with the remaining system choices. Taking into consideration the established requirements and the limitations on component availability, IT-UA provided the necessary components for this experimental implementation, including a high optical power IF-E93 LED, a HFBR-EUS100Z multi-mode optical fiber and an IF-D91B photodetector, which relevant working characteristics are presented in Table 5.3.

Of notice, is that the resultant optical fiber macrobending sensor must be aligned with the previously established technical and operational sensor requirements detailed in section 4.1. This includes quantitative and accurate chest displacement measurements through sensor output, with a resolution in the order of mm, simple implementation, with low processing load that allow a real-time application, easy and generic assembly in different training manikins, and an accessible development cost. As an innovative approach, it should also envision overcome other solutions limitations reported in the literature.

Table 5.3. General working characteristics of the optical fiber measurement system components chosen (prices collected on May 2021).

Ref.	Component	Characteristics	Price
[102]	Source: IF-E93	Peak Wavelength: 522 nm (green) Output Power: 600 µW Forward Voltage: 3.1 V	€ 9,66
[103]	Optical Fibre: HFBR-EUS100Z	Type: Multi-mode Numerical Aperture: 0.47 Core Diameter: 1 mm Core Refractive Index: 1.492 Cladding Refractive Index: 1.417 Cable Attenuation (530 nm): NA [Cable Attenuation (660 nm): 0.22 dB/m]	€ 1,02 (per meter)
[104]	Photodetector: IF-D91	Spectral Bandwidth: 450 to 1050 nm Forward Voltage: 0.7 V	€ 4,14

5.2.2 Macrobending Sensor Testing

Similarly to the methodology adopted for electronic sensor, after having selected the components of the macrobending sensor to be tested, the next phase consisted of sensor preparation, including circuit planning and measurement script programming.

Circuit design for the light source and photodetector integration in the macrobending sensory system was developed in collaboration with IT-UA, envisioning the previously established requirements. LED light source was integrated in a simple voltage divider circuit with a pull-down resistor, while the selected photodetector was integrated in a transimpedance amplifier circuit, in order to amplify the current output of the photodiode to usable voltage values. Both circuits were impressed in a PCB board and then connected to Arduino in the previously used breadboard for signal acquisition. Both schematic designs and respective integration in the breadboard are available in Figure A.6 of Appendix A.

A simple Arduino script was design to read raw analog values to study optical fiber response to chest compressions. In this first experimental approach, no conversion to a physical quantity was made.

Completed script preparation and circuit integration of the macrobending sensor, similar sensor test protocols were applied to assess sensor performance. As in the methodology for electronic sensors, the first testing stage will assess sensor response to compressions considering different macrobending sensor arrangements, and, after the selection of the most reliable arrangement, a second testing stage will evaluate sensor response to the variation of compression parameters.

5.2.2.1 Macrobending Sensor Functional Testing

To assess the best macrobending sensor arrangement in order to obtain the most reliable signal possible, several fiber conformations were tested, inspired in the reviewed work with macrobending sensors. Compressions applied directly on optical fiber were not recommended due to the risk of material damage, limiting possible assembly configurations. Fiber assembly on Adult Brad CPR manikin, horizontally placed on manikin's chest, near the compression area, provided low amplitude signal variations, excluding the use of this manikin for further experimentation. Similarly, fiber assembly along Laerdal Little Anne inferior joints of the thoracic structure, which has considerable bending during compressions, also provided low amplitude signal. Little Anne's metallic spring, however, allowed the exploration of several reviewed macrobending geometries, represented in Figure 5.3. The previously designed protocol for sensor response testing (see "Test Protocol I " in Appendix B) was applied to all the conformations. Several arrangements for the same sensor conformation were tested, (different sized loops, wider or narrowed U-shapes, *etc.*), in order to obtain the most optimized amplitude response for each conformation, without making permanent fiber deformation due to bending. Higher fiber bending leads to higher signal amplitudes but induces permanent deformations in the fiber that are not recommended for correct fiber use.

The results for the selected arrangements are presented in Figure 5.4, with the corresponding qualitative analysis regarding compressions detection. For the best conformation selection, signal characteristics as stable baseline, high amplitude in order to potentiate further high-resolution calibration, and an adequate recoil response, were the considered main target parameters to assess about sensors adequate response. Loop (Figure 5.4 B) and figure-of-eight (Figure 5.4 E) conformations present a positive amplitude response towards chest compressions since the applied force on manikin's

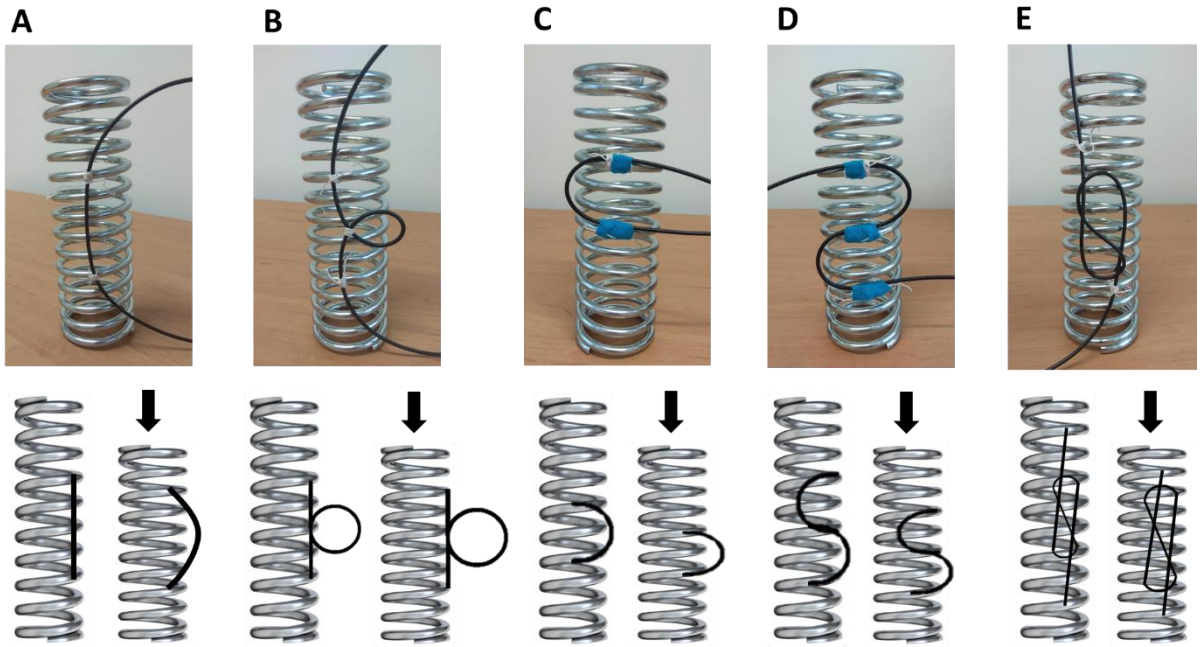

Figure 5.3. Selected optical fiber macrobending sensor arrangements (on top) and corresponding mechanical fiber response to spring compression (on the bottom): linear-shaped (A), loop-shaped, with a 1,5 cm diameter (B), 3,5 cm U-shaped (C), 7 cm period sinusoidal-shaped (D) and 3 cm wide figure-of-eight-shaped (E).

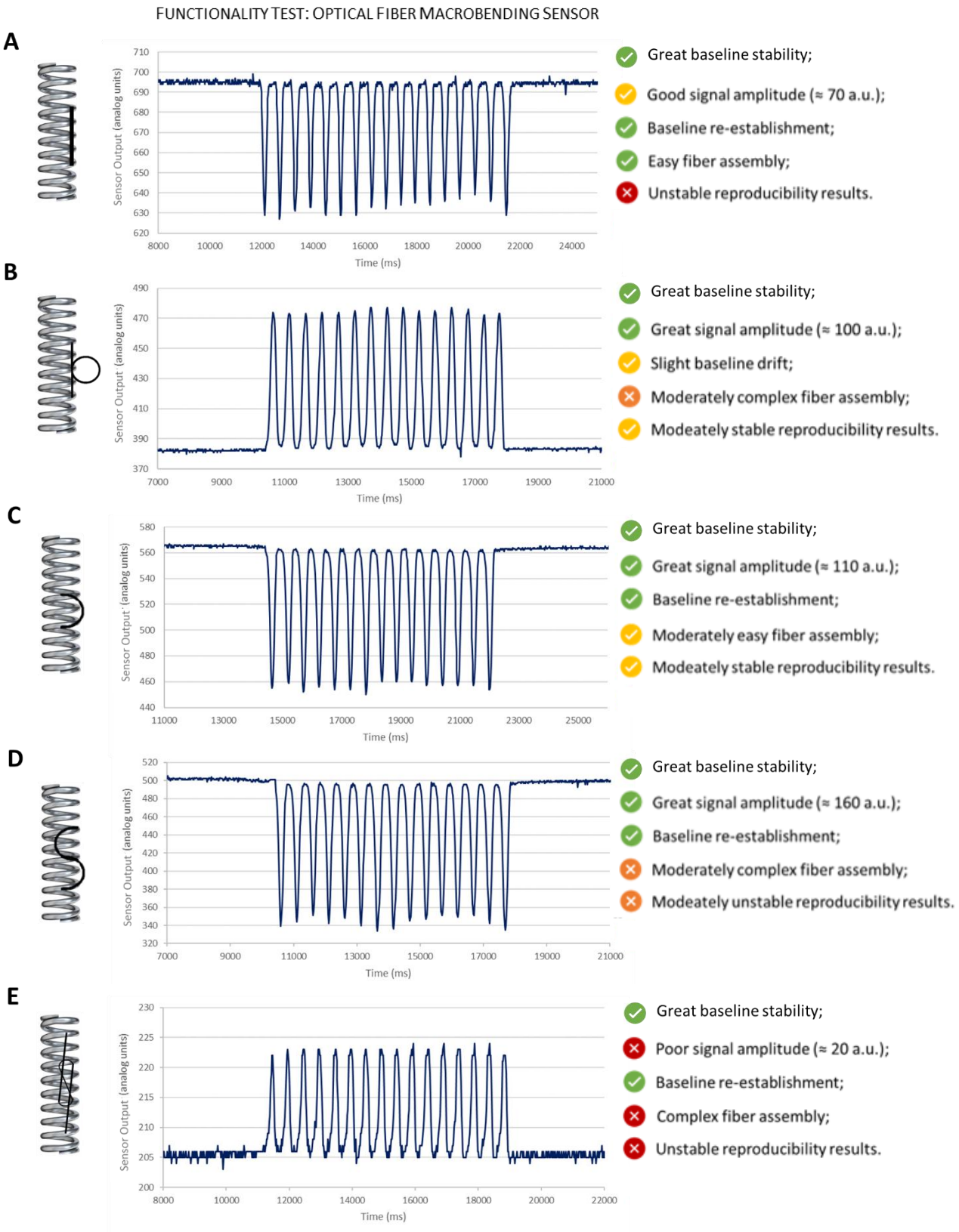

Figure 5.4. Obtained results for "Test Protocol I - Sensor's Response to Compressions" in the different optical fiber conformations tested, linear-shaped (A), loop-shaped, with a 1,5 cm diameter (B), 3,5 cm U-shaped (C), 7 cm period sinusoidal-shaped (D) and 3 cm wide figure-of-eight-shaped (E), and respective qualitative analysis.

spring looses the bended fiber, increasing optical power received by the photodetector. Contrarily, linear (Figure 5.4 A), U-shaped (Figure 5.4 C) and sinusoidal (Figure 5.4 D) conformations enhance fiber bending towards chest compressions, decreasing optical power received, with a negative amplitude response during chest compressions.

As a general note, the tested arrangements present a good response to compressions, with amplitudes considered adequate for posterior calibration for chest displacement. The only exception was the figure-of-eight conformation, which presented lower amplitudes towards compressions, with only 20 analog units (Figure 5.4. E). The provided baseline is extremely stable, before and after chest compression, with a small and constant variability of only 1 analog unit. This variability has no physical significance, since it is measured in analog units, and depending on the resolution achievable with the calibration, might or might not be neglectable. Only loop conformation presented a slight drift on baseline after compressions, probably due to some friction resistance created on loop crossing point, which was loosely tied for higher loop stability, and that could impede the reestablishment of the initial loop diameter (Figure 5.4. B). Finally, recoil values are recurrently aligned with the baseline, or very near this value.

An additional specification evaluated for this sensor was the assembly reproducibility and the reproducibility of the results after sensor reassemble. Linear-shaped conformation was considered the most easily reproducible assembly on manikin's spring due to its simplicity, followed by U-shaped, loop, sinusoidal, and figure-of-eight conformations, and was expected to provide the most reproducible signal. However considerable variability in the provided results regarding baseline value and, mainly, signal amplitude was detected for linear conformation. This may be due to the non-controlled fiber movement during compressions, since the fiber portion connected to the manikin's spring can bend freely. Additionally, in these conformations, the free fiber that is not connected to the spring tends to be aligned in the vertical direction, perpendicularly to manikin's thoracic and back structure, which implies an additional and non-controlled fiber bending due to these structures' presence. In particular, this additional fiber bending due to the thoracic structure is variable during chest compressions, contributing to higher variability of read values for these conformations. U-shaped and sinusoidal conformations, although having a more complex assembly on manikin's spring, have also a more controlled movement during compressions, with free optical fiber not interacting with other manikin structures as it tends to be aligned horizontally. Using a mold for fiber shaping and assembly on the spring, these conformations presented less variable reproducibility.

Based on the above analysis, U-shaped conformation was the selected approach to proceed the exploration of an optical fiber macrobending sensor, since it conciliates a great sensory response to chest compressions, presenting a stable baseline and response to compressions with reasonable amplitude, with a medium-complexity assembly, on which free fiber do not suffer any additional non-controlled bending deformations due to other interactions with manikin structure. Sinusoidal conformation presents higher amplitude signal, but at a cost of a more difficult and less reproducible assembly. For that reason, it constitutes the backup alternative to U-shaped arrangement, if this conformation show poor resolution or sensibility during further sensor testing.

5.2.2.2 Macrobending Performance Testing

Being selected the most adequate optical fiber arrangement, the next testing stage will focus on the detection of the different chest compression components and their respective variations. Similarly to off-shelf sensors testing, independent tools were used to standardize chest compressions execution (metronome mobile app, Little Anne's clicker mechanism, and Practi-CRdM Compression Depth and Rate Monitor). This macrobending performance testing was divided in four different steps, as follows.

Step 1 – Assessing Macrobending Sensor Sensibility to Compression Parameter Variations

In the first step, the same test protocol previously designed for off-the-self sensors was applied (see "Test Protocol II" in Appendix B) to assess if the chosen conformation provides the necessary sensitivity to differentiate the different compression parameter variations. The sensor was assembled in the manikin and connected to the Arduino, as previously done for functionality tests.

The obtained results are represented in Figure 5.5. Selected macrobending sensor successfully detects variations on chest compression depth and rate (Figure 5.5 C to H), with good response to compressions and an extremely stable baseline, even in extreme compression conditions as excessive depth and high compression frequencies. Regarding hand position, the macrobending measuring system fail to distinguish between correct and incorrect hand position, with measurable amplitude peaks being detected even with incorrect hand position during compressions (Figure 5.5 A, B). As experienced with the tested electronic sensors, this is an expected result due to optical fiber's assembly directly to manikin's spring, that invalidates the single use of this technology to assess about this parameter. No other alternatives using macrobending optical sensors for hand position were tested. Concerning chest recoil, an apparent lack of sensitivity is glaring (Figure 5.5 I, J), with recoil values being close to the baseline, for very poorly executed decompressions.

To be noticed, however, that this protocol is not intended to quantify chest compression parameters variations, but to assess if sensor responsivity to these same variations is distinguishable. In fact, it is not expected a linear calibration curve between optical power loss due to fiber bending and

Figure 5.5. Obtained results for "Test Protocol II - Sensor's Response to Variations in Compressions Components" for the chosen optical fiber macrobending sensor, condensed in a single acquisition. Ten chest compression parameter variations were considered: (A) correct hand position, (B) incorrect hand position, (C) shallow compression depth (< 5 cm), (D) correct compression depth (5 to 6 cm), (E) extreme compression depth (> 6 cm), (F) low compression rate (< 100 cpm), (G) correct compression rate (100 to 120 cpm), (H) high compression rate (>120 cpm), (I) correct recoil, (J) incorrect recoil.

chest displacement during compressions in the full measurement range. This calibration will be crucial to assess sensor functionality for compression detection and the corresponding parameter variations, namely in sensor sensitivity in the two interest areas: compression peaks and recoil points.

Step 2 - Macrobending Sensor Calibration

Step 1 was followed by a calibration process with previously used displacement sensors to convert macrobending sensor output to quantifiable displacement measurements. This process included circuit rearrangement, new scripts programing and the design of the calibration protocol.

Firstly, since the chosen conformation implies the loss of optical power with chest compressions, the photodetector circuit potentiometer value was optimized with a small and linear piece of optical fiber so that the potentiometer provided the highest read value possible, with a margin for values saturation. Since both ultrasonic and infrared sensor showed similar performance, two calibrations were made, one with HC-SR04 ultrasonic sensor data, and other using VL1680X infrared sensor readings. The three sensors were assembled in the manikin and connected to the Arduino, as suggested in Figure A.6 of Appendix A.

An additional Arduino script was design to acquire simultaneously readings of HC-SR04 ultrasonic sensor, VL6180X infrared sensor and optical fiber macrobending sensor, including the previously used techniques to obtain chest displacement from electronic sensor readings. As before, it was assured a sampling rate higher to 40 samples per second to avoid aliasing errors in all training conditions.

A new protocol was designed to determine the relationship between loss in optical power and chest displacement, which included three acquisitions of 30 correct compressions, two acquisitions of 30 shallow compressions, two acquisitions of 30 strong compressions and two acquisition of 30 compressions with incorrect recoil (see “Calibration Protocol for Optical Fiber Macrobending Sensor” in Appendix B). A curve fitting method was used to determine the relationship between optical power loss and chest displacement for both calibrations (Figure 5.6). This curve was determined forcing origin interception, making a zero variation in optical power reading to correspond to a zero variation on chest displacement measurement. The resultant relationships for HC-SR04 ultrasonic sensor and VL6180X infrared sensor calibrations are given by Equation (5) and Equation (6), respectively,

$$d_{HC-SR04_{cal}}(t) = 1 \times 10^{-6} p(t)^3 - 4 \times 10^{-4} p(t)^2 + 0{,}0699 p(t) \quad (5)$$

$$d_{VL6180X_{cal}}(t) = 2 \times 10^{-6} p(t)^3 - 5 \times 10^{-4} p(t)^2 + 0{,}0815 p(t) \quad (6)$$

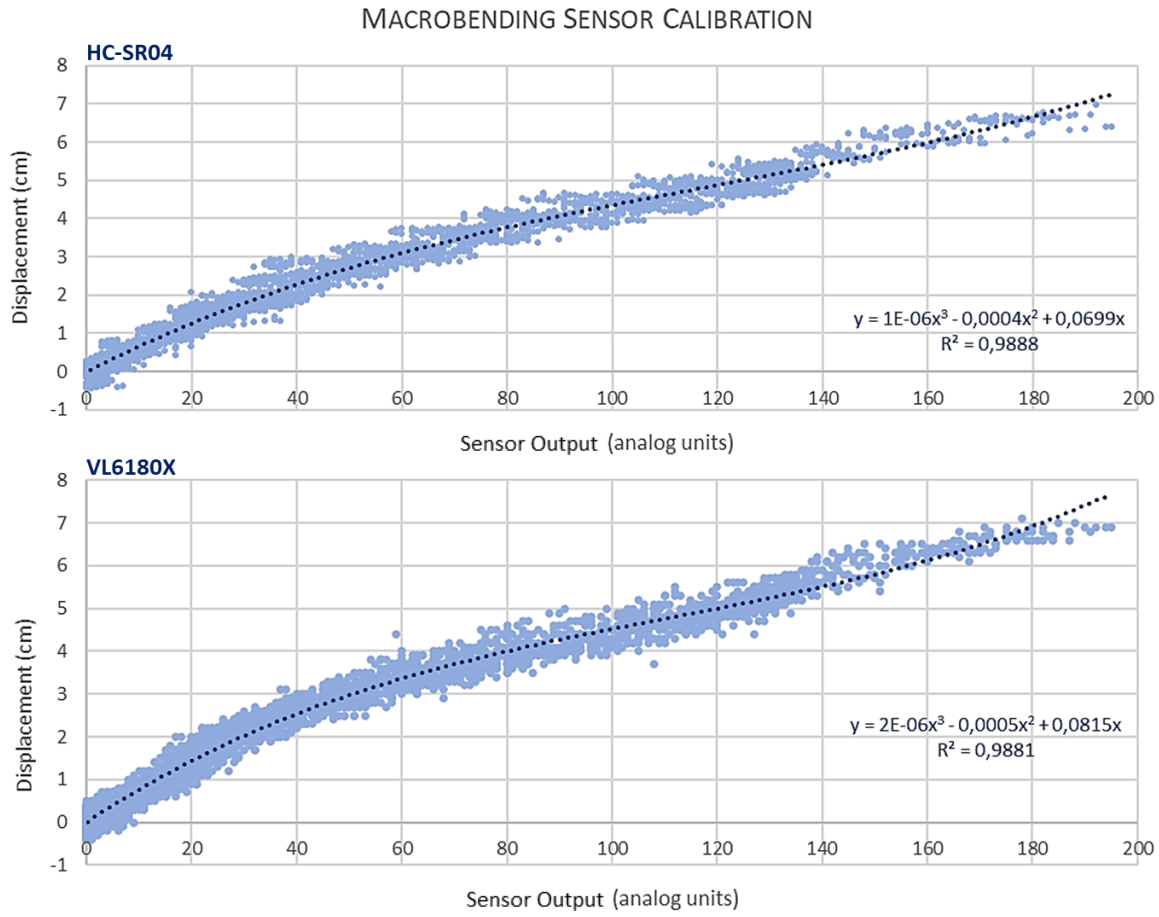

Figure 5.6. Optical fiber macrobending sensor calibration with HC-SR04 ultrasonic sensor (top) and with VL6180X digital infrared sensor (bottom).

with $d_{HC-SR04_{cal}}(t)$ and $d_{VL6180X_{cal}}(t)$ representing the displacement obtained with HC-SR04 ultrasonic sensor and VL6180X infrared sensor, respectively, and $p(t)$ representing measured optical fiber sensor output, measured in analog units. These calibrations presented higher correlation coefficient of 0.9888 and 0.9881 respectively.

Step 3 – Assessing Macrobending Sensor Viability as a Displacement Sensor during Chest Compressions

Being set the relationship between optical sensor output and chest displacement, Test Protocol II was repeated to assess more objectively the functionality of optical fiber macrobending sensor as a displacement sensor for the detection of chest compression parameters variation.

The sensor arrangement described in Step 2, with ultrasonic and infrared sensors on manikin's back and U-shaped optical fiber macrobending sensor on manikin's spring, was used, as well as the same Arduino script, with displacement measurements acquired simultaneously for both electronic sensors and the novel displacement measurements of the calibrated macrobending sensor.

Hand position test was not included since all the assembled sensors fail on the detection of incorrect hand position, as no different behavior was expected after macrobending sensor calibration either with HC-SR04 ultrasonic sensor nor VL6180X infrared sensor.

Figure 5.7 presents the obtained results. Both macrobending sensor calibrations accurately detect variations on compression depth, rate and chest recoil, with small differences regarding displacement measurements using ultrasonic and infrared sensors for optical fiber calibration, as expected. An objective and quantitative analysis of the error associated with these calibrations is presented in the next testing step.

Step 4 – Assessing Macrobending Sensor Error

A quantitative analysis of optical fiber macrobending sensor calibration error is essential to qualify sensors reliability as a possible CPR quality assessment system. Measurement difference between the two electronic sensors (ultrasonic HC-SR04 and infrared VL6180X) is merely indicative of its intrinsic measurement variability. Measurement differences between macrobending sensor and

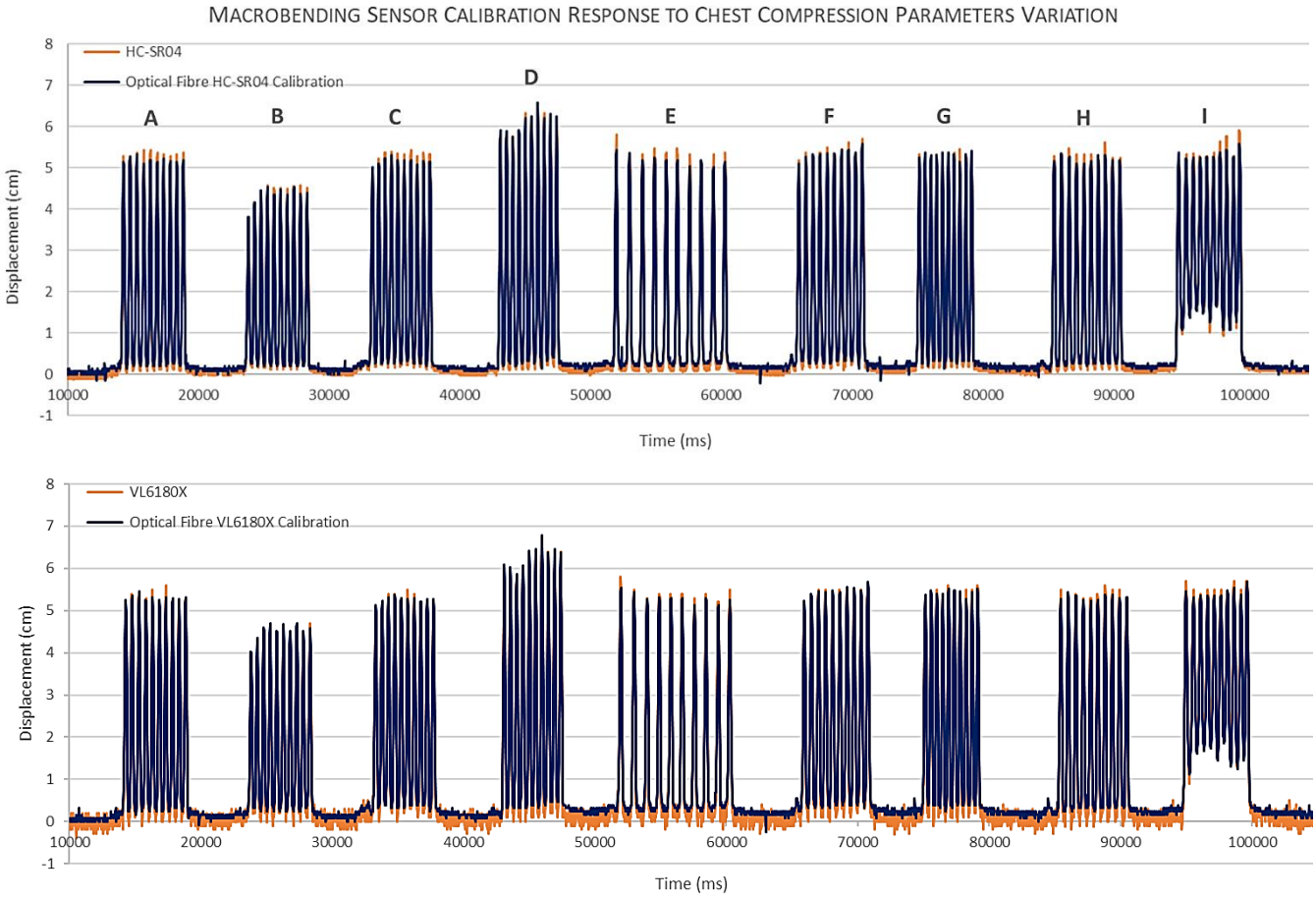

Figure 5.7. Obtained results for "Test Protocol II - Sensor's Response to Variations in Compressions Components" for the chosen optical fiber macrobending sensor, after calibration, condensed in a single acquisition. Nine chest compression parameter variations were considered: (A) correct compressions (control), (B) shallow compression depth (< 5 cm), (C) correct compression depth (5 to 6 cm), (D) extreme compression depth (> 6 cm), (E) low compression rate (< 100 cpm), (F) correct compression rate (100 to 120 cpm), (G) high compression rate (>120 cpm), (H) correct recoil, (I) incorrect recoil.

the two electronic sensors used for its calibration offer an indication of calibration quality and macrobending sensor system accuracy, considering the electronic sensors as the real displacement values. Since there are no recommendations for the accuracy needed for chest compression measurement technologies, a measurement error of 0,5 was considered acceptable.

For that purpose, a new testing protocol was designed. In two different days it was acquired two sets of 30 compressions for each compression variation assay (correct compressions, depth variation, rate variation, recoil variation and hand position variation), with 20 to 30 minutes of rest between each assay to avoid the influence of physical fatigue (see "Test Protocol IV" in Appendix B). The previously described sensor arrangement and Arduino scripts used in Step 3 was used for simultaneous data acquisition of the three instrumented sensors.

Root Mean Square Error (RMSE) is a standard way to measure the error of a model in predicting quantitative data, which is calculated by Equation (7),

$$RMSE = \sqrt{\frac{\sum_{n=1}^{N}(x_{OF}(n) - x_E(n))^2}{N}} \tag{7}$$

with $x_{OF}(n)$ as the data obtained with optical fiber macrobending sensor, $x_E(n)$ as the data obtained with the electronic sensor used for optical fiber sensor calibration, and *N* as the number of considered datapoints.

RMSE was applied to each compression variation assay data, in order to calculate the error between ultrasonic sensor HC-SR04 and optical fiber macrobending sensor calibration with ultrasonic sensor HC-SR04, and infrared sensor VL6180X and optical fiber macrobending sensor calibration with infrared sensor VL6180X. This detailed analysis was considered relevant to confirm and quantify sensors sensibility and responsivity to the different parameter variations tested.

The analysis of the obtained RMSE shows that the obtained calibrations can be considered equivalent. Both calibrations present an RMSE of 0,2 cm for correct compression, depth variations (for both shallow and deep compressions) and rate variations (for low and high frequency compressions). Incorrect recoil variation presented a RMSE of 0,3 cm. These RMSE values are acceptable considering the stipulated requirements and are within the expected values for sensor measurement variations. Regarding hands positioning variation, both macrobending sensor calibrations, with the corresponding electronic sensor present RMSE values that are worth to explore. For incorrect hands positioning, both macrobending sensor calibrations present considerable differences in comparison to the corresponding electronic sensors, with a RMSE of 0,8 cm. This phenomenon is easily justified due to the distinguished assembly between electronic sensors, on manikin's back, and macrobending sensor, on manikin's metal spring. It is thus expected that, in incorrect hands positioning, chest displacement and spring displacement are not equal, with spring displacement being bigger that chest movement on electronic sensors reading area. This considerable difference between electronic and optical measurement systems for incorrect hands positioning will have direct impact on provided individual depth feedback, which is a limitation to be considered for quality assessment (see Chapter 6).

5.2.2.3 Critical Analysis of the Obtained Results

After sensor calibration, optical fiber macrobending sensor shows good resolution (0,07 cm and 0,08 cm for calibration with ultrasonic sensor HC-SR04 and with infrared sensor VL6180X, respectively) and sensitivity to compressions in all the tests executed, contradicting the previously concerns raised in the first testing stage, about sensor lack of resolution or sensibility, especially regarding chest recoil detection. Moreover, the small differences regarding displacement measurements between used electronic sensors and optical fiber calibration provides good confidence on both obtained calibrations. This difference was quantified through the calculation of RMSE, with the residual value of 0,2 cm for correctly performed compression and for all the chest compressions variations, except for incorrect hands positioning. This is an expected result given the properly fitted calibration curves. Furthermore, these error values fit the established requirements for sensor accuracy. Incorrect hand position presented a RMSE of 0,8 cm for both calibrations, which is an important error with further implications for chest compression depth quality assessment, and a limitation to be considered.

Considering functionality, this sensory approach seems to maintain ultrasonic and infrared strengths as a sensory mechanism, as it provides a highly stable baseline and an equally adequate response to compressions. To be reminded, however, that, in comparison to the tested electronic sensors, this sensory technology could be less reproductible, as previously reported, with its use being exclusively adapted to the selected training manikin.

Concerning the previously established requirements for sensor selection according to this application needs, the selected macrobending sensor, beside accurate and quantitative measurements of chest displacement, allows an accessible development cost and a simple implementation, with easy circuit integration and low computational load for data acquisition. Regarding sensor assembly on the manikin, this macrobending sensor implementation is fitted to the used training manikin, and assembled in a conformation that, comparing to the previously electronic sensors, has higher complexity concerning system's reproducibility.

Considering this system strengths and limitations, the obtain results with calibrated macrobending sensor justifies further developments, with its integration in a CPR training prototype in order to be tested during CPR training.

5.3 Preliminary Tests using Fiber Bragg Grating Sensors for Chest Compression Detection

The established collaboration with IT-UA, beside allowing a fully experimental and exploratory approach using polymeric optical fibers as a macrobending sensor to detect chest compressions, also provided the possibility of performing preliminary tests using FBG sensors for the same purpose. These tests were carried in IT-UA facilities, with the local equipment and FBG sensors previously designed

for other IT-UA research applications. Thus, it is important to emphasize that the tested sensors were neither designed nor optimized for chest compressions detection.

Two different FBG sensor designs were tested: a strain FBG sensor embedded in kinesio tape, previously used for gait monitoring [99], and a pressure FBG sensor embedded in a rigid epoxy resin structure. As strain is applied in kinesio tape or pressure is applied in the resin structure, the deformations sensed in these structures are shared with the FBG sensor, inducing variations in the measured Bragg wavelength. Both sensors were assembled and tested in a Simulaids Adult Brad CPR Manikin. The operationalization was finished using a I-MON USB 512 Ibsen interrogator, with an incorporated broadband light source. Data acquisition was made using the evaluation software provided by the interrogation system. The different configurations tested are presented in Figure 5.8. Due to the glass composition of the fiber, sensor positioning in direct compression areas were not tested to avoid sensor damage. Concerning the strain FBG sensor, both second and third conformations tested (Figure 5.8 B, C) presented similar results, with chest compressions inducing kinesio tape distension, with a positive strain read in the FBG sensor. Third conformation, however, presented higher wavelength shift, meaning higher amplitude signal, since this sensor positioning experiences an additional distension due to thoracic structure side dilation during chest compressions, besides the distension due to regular compression effect (Figure 5.9). In the first and forth sensor conformation tested (Figure 5.8 A, D), the obtained response was against the expected strain application on the kinesio tape, giving a negative wavelength variation and with very low amplitudes. Regarding pressure FBG sensor, a single conformation was tested, with sensor positioning on manikin's back (Figure 5.8 E). The obtained response presents an unstable behavior between compressions, that might be due to hysteresis issues associated with sensors resin volume.

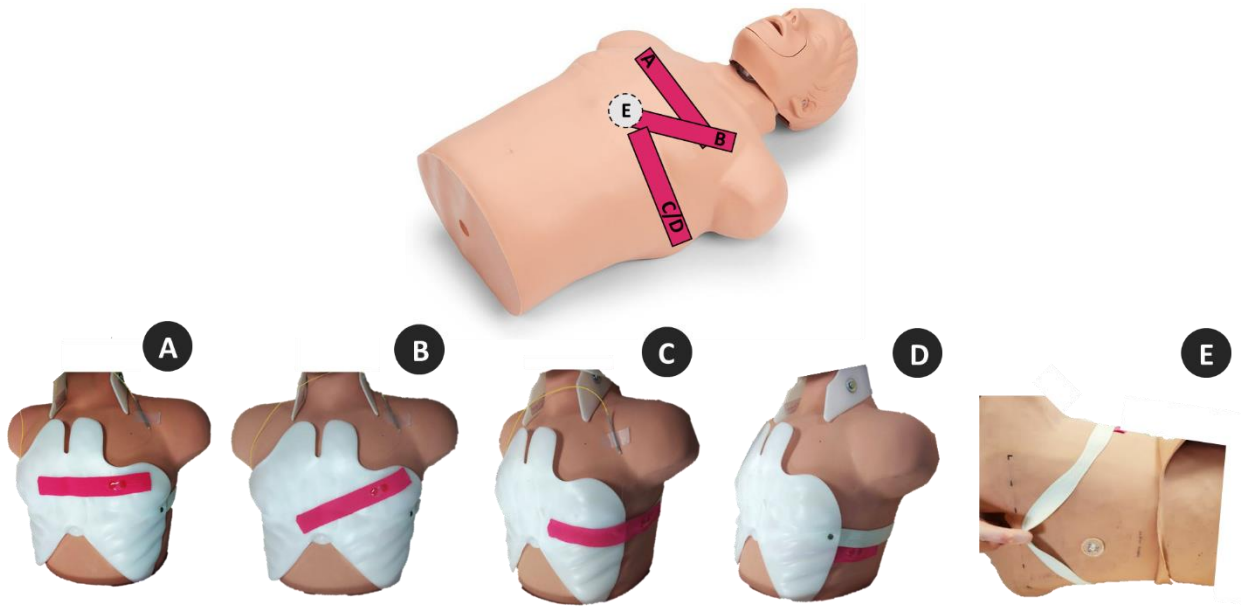

Figure 5.8. Different configurations tested using FBG sensors, with a graphical representation of sensor positioning, on top, and the different arrangements tested, on the bottom: sensor positioned horizontally above the mammary line, with kinesio tape not crossing compression area (A); strain sensor positioned obliquely in the direction of the compression area, with kinesio tape crossing compression area (B); strain sensor positioned horizontally on the ribs, above the thoracic structure, with kinesio tape not crossing compression area (C); strain sensor positioned horizontally on the ribs, under the thoracic structure, with kinesio tape not crossing compression area (D); pressure sensor position on manikin's back, aligned with the compression vertical line (E).

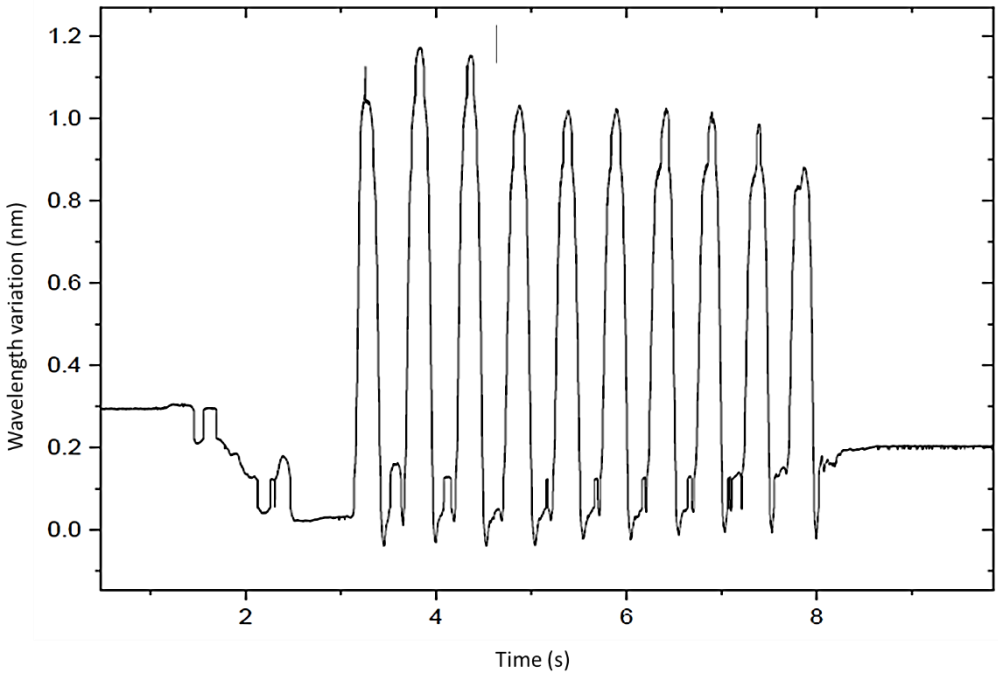

Figure 5.9. Strain FBG sensor response to chest compressions, using strain sensor positioned horizontally on the ribs, above the thoracic structure, with kinesio tape not crossing compression area.

With these preliminary tests carried out using FBG sensors, it is possible to confirm the high resolution and sensibility of this technology theoretically discussed in section 5.1. Furthermore, it was possible to assure the feasibility of its use for chest compression detection, with promising results, even with sensors that were not designed nor optimized for this application. Strain FBG sensor, embedded in kinesio tape showed to be the most viable solution among the tested conformations with this sensor. Pressure FBG sensor, embedded in an epoxy resin structure, despite of the corrupted results by hysteresis, could lead to an interesting approach for compression detection, if other dimensions and resin volume were considered, without compromising sensor's resistance.

The use of FBG technology seems to be an approach worth to consider for chest compression detection, not for the intended low-cost feedback training device, due to the expensive devices needed for wavelength shift detection, but as a validation tool for existing measurement technologies, which is an important limitation regarding CPR training devices. Further developments using this technology are proposed as future work, including adequate sensor design and characterization and further functional tests for chest compressions detection.

Chapter Conclusions

An innovative approach for the development of a system to provide feedback in CPR training, focusing on chest compression parameters assessment, was explored using optical fibers as sensing mechanism and consequent instrumentation of this technology in a CPR training manikin. Both intensity-modulated macrobending sensors and wavelength-modulated FBG sensor were taken into consideration for experimentation.

Regarding macrobending sensory system, after a theoretical and operational insight on optical fiber sensors, a similar approach to the methodology used for electronic sensors screening was employed, including circuit planning, scripts programing and testing protocol planning in order to define the best macrobending sensor arrangement. Several bending arrangements already documented in literature for other applications at the same working scale were tested, with obtained results not always corresponding to the already documented behavior regarding tested fiber arrangements, showing that this sensory technology is highly dependent on the application it is designed for. In the case of chest compression detection, U-shaped was considered the best approach, providing a compromise between output reliability and arrangement reproducibility.

Sensor output calibration for displacement measurements trough the already used electronic displacement sensors were applied and the performance tests were carried out. Encouraging results regarding the response to chest compression depth, rate and recoil were obtained, with clear and accurate distinction between the tested parameter variations, with highly trustworthy RMSE values, supporting selected measurement systems reliability. Moreover, this new sensory technology maintains electronic sensors baseline reliability and stability and sharped response to compressions. Hand position, was not assessed with this technology, invalidating the single use of a macrobending sensor for complete chest compression quality analysis.

This solution, despite of the lower reproducibility comparing to the tested electronic sensors, aligns with other development requirements envisioned for this application, by providing accurate measurements with adequate resolution and sensibility, easy implementation and accessible development cost.

Regarding FBG tested sensors, preliminary tests taken at IT-UA provided encouraging results regarding chest compression detection, with great sensibility and resolution. Although FBG sensors do not align with the established requirements for this application, namely due to high costs associated with used interrogation systems, this technology can be eventually used as a validation tool for existing measurement technologies, with further developments considered for future work.

6

FEATURE EXTRACTION AND COMPRESSIONS MECTRICS FOR ASSESSING TRAINING QUALITY

The selected sensory approaches for chest compression detection enter now in the last development stage, with their application in training manikins and the development of metrics for compression quality assessment. This chapter presents the final manikin assembly and circuit implementation, the developed feature extraction algorithm used for identification of compressions related parameters, and the calculation of a set of metrics for compression quality assessment. The developed system, including ultrasonic sensor HC-SR04, infrared sensor VL6180X and optical fiber macrobending sensor, combined with pressure sensor FSR 402, for hand position detection, along with the developed software, will be exposed to a training-like situation to test its usability.

6.1 Manikin Assembly and Circuit Implementation

Being established the operational conditions of manikin instrumentation, including the selection of the best sensory alternatives, the manikin was assembled with the four selected sensors for chest compression assessment, in the previously defined arrangements, and connected to a circuit, as presented in Figure 6.2 and Figure 6.1, respectively. Thus, the final assembly includes ultrasonic sensor HC-SR04 and infrared sensor VL6180X placed on manikin's back, optical fiber macrobending sensor attached on manikin's metal spring, in a U-shaped conformation, and pressure sensor FSR 402 on center of the manikin's chest. Values for specific circuit components (resistances) are described in Figure 6.1 caption.

An Arduino script was design to acquire simultaneously readings of all sensors. This script included the previously applied tools for each sensor implementation, described in previous chapters (see Chapter 4 and section 5.2). It was assured a sampling rate superior to 40 samples per second to avoid aliasing errors in all training conditions.

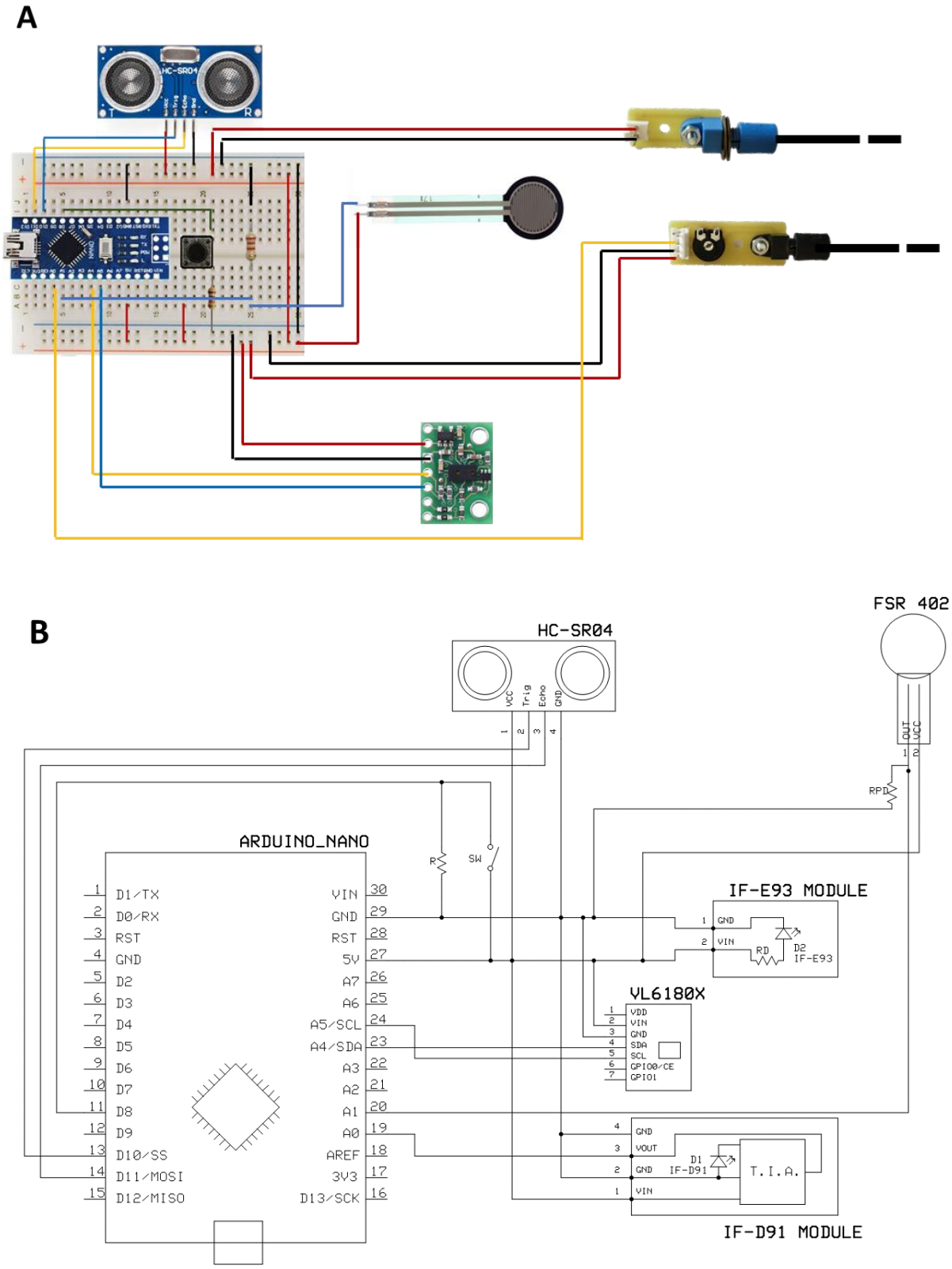

Figure 6.1. Ultrasonic sensor HC-SR04, digital infrared sensor VL6180X, optical fiber macrobending sensor with LED source IF-E93 and photodetector IF-D91, and pressure sensor FSR 402 circuit assembly on the breadboard (A) and respective circuit schematic (B), with R = 1 kΩ, RD = 75 Ω and RPD = 2.2 kΩ.

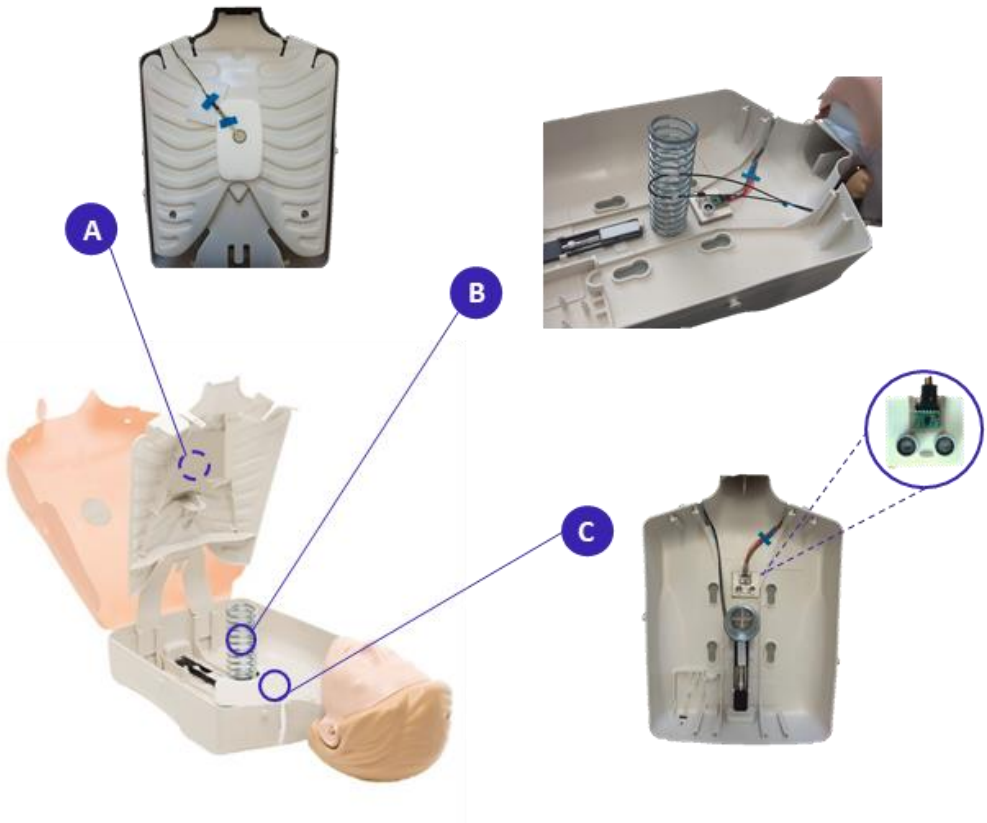

Figure 6.2. Selected sensors arrangement in training manikin for usability tests. (A) Pressure sensor FSR 402, on manikin's chest, in the compression area, (B) U-shaped optical fiber macrobending sensor, on manikin's spring, and (C) ultrasonic sensor HC-SR04 and infrared sensor VL6180X, on manikin's back.

6.2 Feature Extraction Algorithm

Taking into consideration the particularities of the intended application, a feature extraction algorithm was developed. This algorithm should allow real-time CPR training feedback, which implies a low computational load. Furthermore, it should be robust to previously tested variations in compression parameters (correct and incorrect). Thus, for each compression, it is required the detection of three essential points: compression start, compression maximum peak, and compression minimum peak (recoil). The correct detection of these compression points will not only allow real-time feedback on compression depth, rate, chest recoil and hand position, but also permit further analysis of the metrics described for compression quality assessment (see section 6.3).

Given the characteristics of the obtained signal with the selected sensors, feedback on compression depth, rate and recoil is extracted from ultrasonic, infrared or optical fiber macrobending sensors, while hand position is extracted from pressure sensor data. Thus, accordingly to the established requirements, compression start, peak and recoil points are extracted from ultrasonic, infrared and optical fiber macrobending sensor signal, with pressure sensor data being consulted upon peaks detection to assess hand position. As the signal is acquired, the values read are analyzed according to

the developed algorithm, which is explained below. Used thresholds and timeouts were defined empirically, taking into consideration the nature of the acquired data and their adequacy for real-time implementation.

The first algorithm section focusses on the detection of the compression start. This point is defined as the first signal data point *n* above a defined compression threshold of 0,7 cm, in order to avoid erroneous starting points along the baseline, especially in sensors with high baseline variability.

Found the compression start point, the next section consists in the detection of the compression maximum peak, corresponding to chest compression depth. A certain data point *n* is considered a possible peak point if the corresponding depth is higher than the depth of the two previous consecutive data points. If this displacement value is higher than the last considered peak, the peak value is updated as the new compression peak. This approach, *per se*, would detect not only the absolute maximum peak of the compression, but also other relative maxima along the compression signal. To overcome this limitation, a peak confirmation timeout of 200 ms was added. This implies that after a peak detection, there is a time window to confirm if that is the maximum displacement peak for that compression, either by ignoring following peaks with lower displacement values, or by updating maximum peak value for peak data points with higher displacement values. Exceeded that timeout, the detected peak is confirmed as the compression maximum peak. This technique would guarantee a single maximum peak per detected compression, overcoming the detection of erroneous peaks either from common signal roughness or pre-compression events, i.e., small compression-like signal structures resulting from movement hesitations that can precede a compression. The selected timeout of 200 ms was considered adequate to be implemented in real-time, making an appropriate balance between the time needed for peak confirmation and the small delay needed for feedback provision after peak detection. Furthermore, this confirmation time was still adequate for appropriate peak detection with high compression frequencies. Upon the detection of compression peak, pressure sensor is assessed to evaluate hands positioning. Several other algorithms for peak detection were tested while studying the most adequate alternative for this application needs. This work can be found in Appendix C.

After compression maximum peak detection, the minimum peak (recoil value) is the following point to be detected. The approach used for recoil detection was similar to the one used for peak detection, by comparing the possible recoil point with the previous two consecutive points. If this recoil value is smaller than the last considered recoil for that compression, the recoil value is updated as the new compression recoil. For recoil detection no timeout was needed to implement. The search for the minimum recoil point ends with one of two situations: 1) the depth difference of the current data point *n* from the last recoil point exceeds the stipulated compression threshold of 0,7 cm, marking the beginning of a new compression, or, 2) the time difference of the current point *n* from the start of the last compression exceeds the compression timeout of 1500 ms, marking the end of a compression cycle. Either way, the end of the compression is recognized by the algorithm, allowing the search for a new compression, with the resumption of the presented algorithm

The presented algorithm was tested with previously acquired data, including compression parameters variations, for all the selected sensors. It showed robustness to different depths, rates, recoils and hand position, and is considered to be adaptable to different training performances. Obtained results with the application of the presented algorithm for detection of target compression points to previously

acquired data of infrared sensor VL6180X, with sets of correct and incorrect compressions, can be found in Figure 6.3, as an example of the algorithm functionality. The use of VL6180X for that purpose was strategically selected as it presents the noisiest baseline among the used sensors, potentiating possible algorithmic failure, which was not verified.

Of notice is that the developed algorithm was not tested during real-time trainings, due to time constraints. For that, the algorithm needs to be integrated in an information system, with a graphical user interface, being out of the scope of the present work, although, aimed for future development.

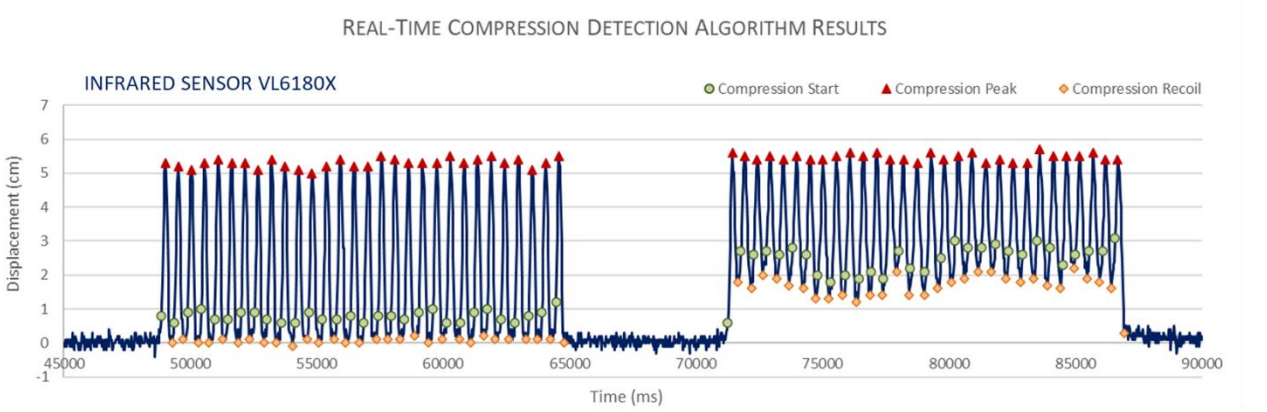

Figure 6.3. Real-time compression target points detection algorithm results, tested in infrared sensor VL6180X data. Highlight on compression start points (green), compression peak points (red) and compression recoil points (orange).

6.3 Compression Metrics Calculation

After acquired data is processed by the feature detection algorithm, with targeting compression points detection, these are used to provide metrics on the four compressions parameters: depth, rate, chest recoil and hand position. These metrics can be calculated for real-time feedback or for a post-training assessment, including an overall score for chest compression quality.

In the case of real-time feedback, the metrics are calculated as follows. Compression rate is calculated through the inverse of the time difference between the detected peak and the previously detected one for all the peaks of a compression set except for the first peak. In the later, the compression frequency is calculated through the inverse of the time difference between the start point of the next compression and its compression start point. Hand position is given by analyzing the corresponding value read by pressure sensor during compression peak detection, with correct hand position being considered for pressure values above 500 µS. Information on compression depth and recoil is directly measured from the three sensors data, with compression recoil being considered correct if recoil depth is inferior to 0.7 cm, a threshold chosen given the resolution of the selected sensors.

For the overall post-training feedback, other training metrics can be defined, including:

(i) General metrics:
- Number of compressions;
- Chest compression fraction (*i.e.* ratio of the time passed applying chest compressions to the complete training time);
- Training duration;
- Mean ventilation pause duration.

(ii) Compression Metrics:
- Mean and percentage of compressions with correct frequency;
- Mean and percentage of compressions with correct depth;
- Mean and percentage of compressions with correct recoil;
- Number and percentage of compressions with correct hand position (*i.e* valid compressions).

The designed overall compression score (OCS) was inspired in the research made on the theme (see section 3.3), considering the strengths and limitations of the reported compression scores. The designed score varies between 0% and 100%, and includes all the four compression parameters, with hand position as an eliminatory parameter. This means that only valid compressions, *i.e.*, compressions performed with correct hand position, are considered for overall compression score. Regarding the remaining compression parameters, as their relevance for compressions quality is equally weighted, the arithmetic average of the percentage of correct depth, correct rate and correct recoil of valid compressions is calculated. Thus, the overall compression score is calculated according to Equation (8),

$$OCS\ (\%) = \frac{CorrR + CorrD + CorrRe}{3} \times CorrH(\%) \quad (8)$$

with *OCS* as the overall compression score, *CorrR, CorrD* and *CorrRe* as the fraction of compressions with correct rate, depth and recoil, respectively, and *CorrH* as the percentage of compressions with correct hand position, *i.e.*, valid compressions.

The frequency and depth of compressions should not be evaluated in a dichotomous way since the effectiveness of a slight difference to the values recommended by the guidelines does not translate into a null impact of these compressions on the outcomes of the victim in cardiac arrest. Thus, for these parameters, branched functions were empirically developed that represented a greater approximation of the loss of effectiveness given a variation out of the values established by the guidelines. For the frequency of compressions, a score of 100% was considered when they were performed within the range of 100 to 120 compressions per minute, and a score linearly down to 75% when they were performed within the range of 90 to 100 compressions per minute or 120 to 130 compressions per minute. Regarding the depth of the compressions, a score of 100% was considered when they were

performed within the range of 5 to 6 cm, and a score linearly down to 75% when they were performed within the range of 4.5 to 5 cm or 5 to 5.5 cm. If any value read by the sensors is not in one of the aforementioned ranges, the score for this parameter corresponds to 0%. A representation of weight functions for each compression parameter for overall compression score calculation is available in Figure 6.4.

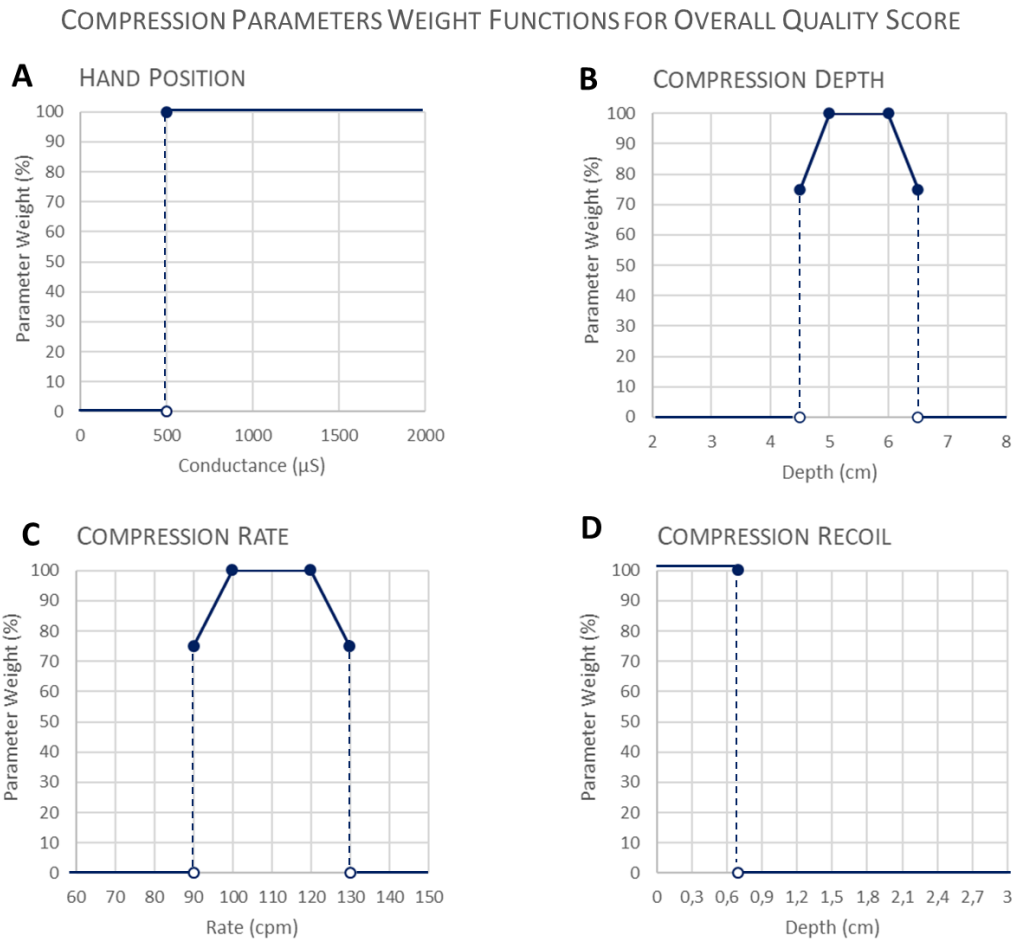

Figure 6.4. Compression parameters weight functions for overall compression score calculation, including hand position (A), compression depth (B), rate (C) and recoil (D).

6.4 Compression Quality Assessment During Training

A final test protocol was designed to mimic a real CPR training scenario, including compressions and ventilations, in the 30:2 ratio, as defined by the guidelines for adult resuscitation (see "Training Protocol" in Appendix B). The protocol was performed by two certified first aid providers, one being responsible for the circulation component of CPR training, through chest compressions, and the other securing ventilation, by correctly using a bag-valve-mask insufflator. No compression quality feedback tool or device was used during the training performance, so that no external factor influences training quality.

Obtained results for a training session are presented in Figure 6.5, with the corresponding training analysis by each of the instrumented systems available in Table 6.1. Since all the instrumented displacement sensors proved to have equivalent behavior to chest compressions, data measured by optical fiber macrobending sensor with infrared sensor VL6180X calibration was selected to show in more detail a segment of training data (Figure 6.6), as it provides one of the cleanest signals among all the sensors tested.

Concerning the obtained results for training analysis (Table 6.1), it is possible to confirm that all the sensors used for manikin instrumentation provide similar results regarding assessed quality metrics, with a similar overall compression score. The differences in the calculated mean of the different compression parameters between sensors are modest, in concordance with the results provided by the previously performed comparative study of sensors' measurement error. These slight differences between sensor measurements justify, however, the differences between the calculated percentage of correct parameters, influencing the overall compression quality score value. Additionally, slight time differences of target detected points, especially compression start and chest recoil points which vary more between different sensors data due to its proximity to the baseline, also influence the calculation of these metrics, especially metrics depending on time values. These deviations easily justify variations in metrics as compression rate and pause time.

By analyzing Figure 6.5 it is possible to confirm that all systems are capable of detecting ventilations. In fact, ventilations cause manikin's lung bag (which is placed between thoracic structure and manikin's skin) to inflate, provoking visible manikin chest rise, and a depression on the thoracic structure. This depression, of only few millimeters, is successfully measured by the 3 sensors, although they are not detected by the designed algorithm due to the used compression threshold values. Despite being out of the scope of this development work, the used sensors show potential benefit not only for compressions, but also for ventilation detection and assessment, which would provide complete training quality assessment. Thus, ventilation detection and its quality assessment using the implemented sensors must be taken into consideration for further exploration and future developments.

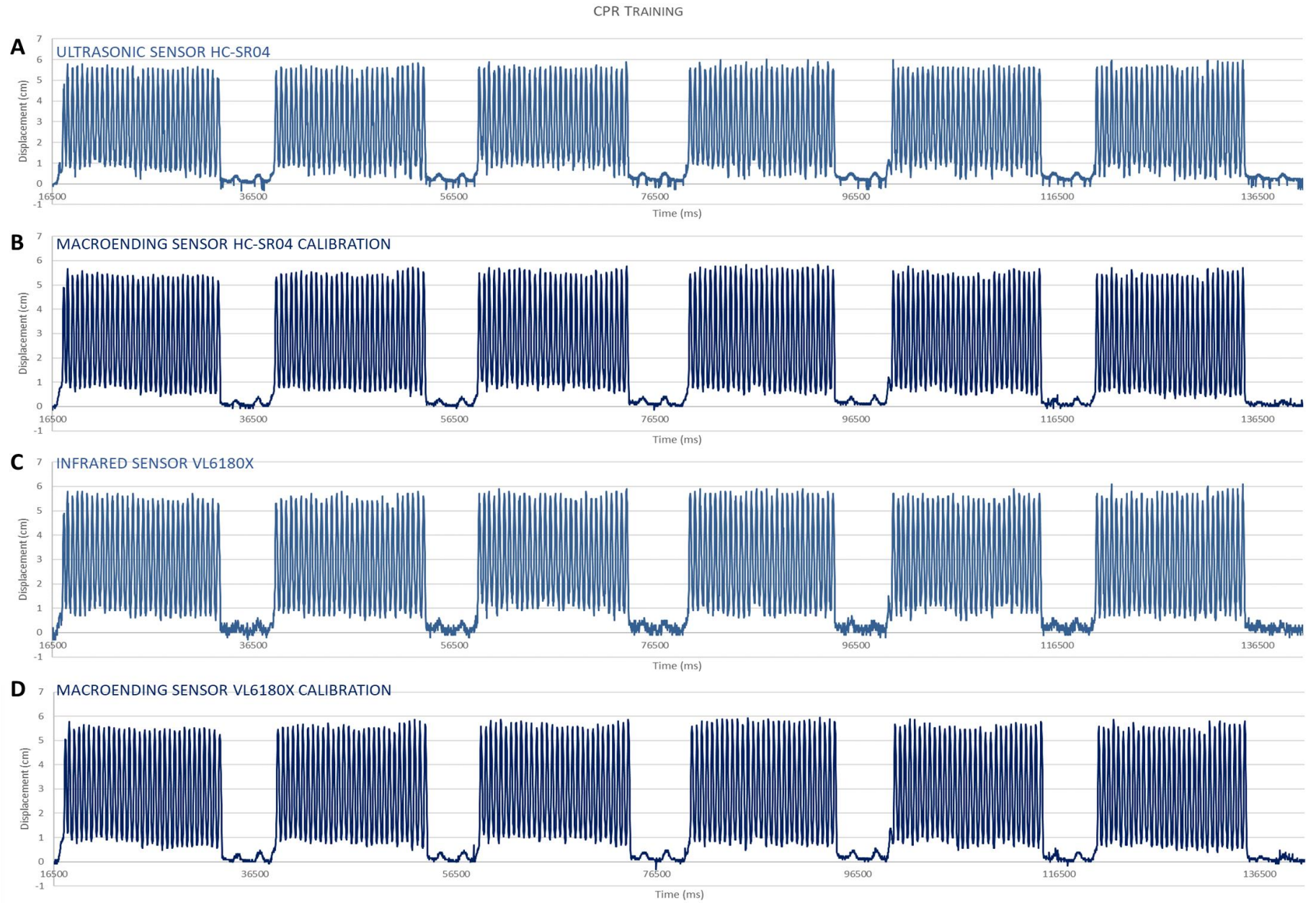

Figure 6.5. Results of "Training Protocol" implementation, with all the implemented measurement systems. (A) ultrasonic sensor HC-SR04, (B) optical fiber macrobending sensor with HC-SR04 calibration; (C) infrared sensor VL6180X; and optical fiber macrobending sensor with VL6180X calibration.

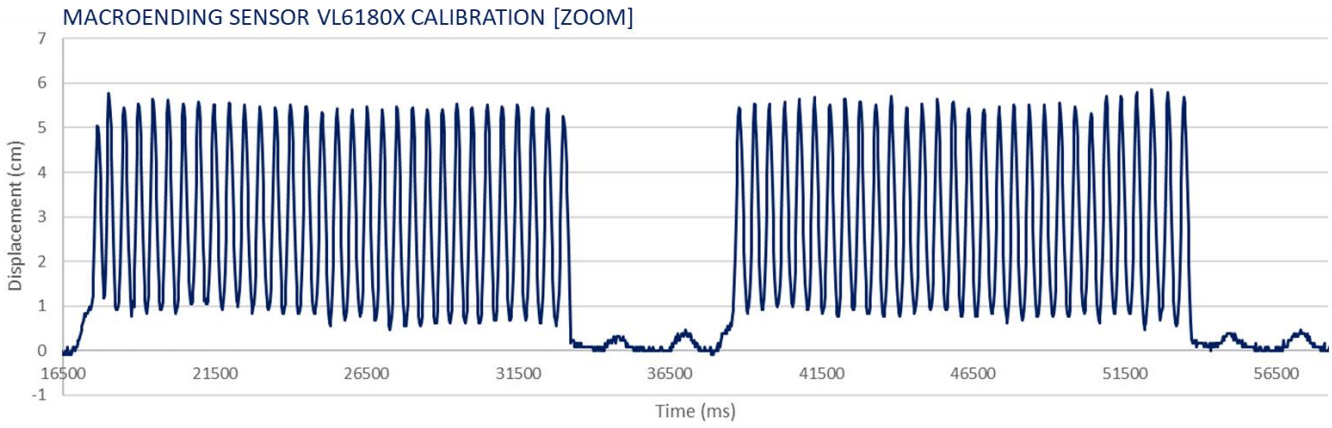

Figure 6.6. Zoom of the two first compression sets of results of macrobending sensor with VL6180X calibration.

Table 6.1. Training analysis, focused on chest compression quality, for the three implemented sensors, ultrasonic HC-SR04, infrared VL6180X and optical fiber macrobending sensor, with two calibrations using the previous electronic sensors (OF HC-SR04 Cal. and OF VL6180X Cal.). Assessment on hands positioning with pressure sensor FSR 402.

	HC-SR04	**OF HC-SR04 Cal.**	**VL6180X**	**OF VL6180X Cal.**
General Metrics				
No. Compressions	182	182	182	182
Chest Compression Fraction (%)	79 %	79 %	79 %	79 %
Training Duration (s)	118,4	118,3	118,7	118,0
Mean Ventilation Pause Time (s)	4,9	5,0	4,9	4,9
Compression Metrics				
Compression Rate				
Mean (cpm)	121	120	120	120
Correct (%)	79 %	82 %	84 %	78 %
Compression Depth				
Mean (cm)	5,6	5,5	5,6	5,6
Correct (%)	98 %	99 %	98 %	99 %
Chest Recoil				
Mean (cm)	0,6	0,6	0,8	0,7
Correct (%)	55 %	61 %	49 %	41 %
Hands Position				
No. Valid Compressions	182	182	182	182
Correct (%)	100 %	100 %	100 %	100 %
Overall Quality Score	**80 %**	**85 %**	**81 %**	**79 %**

Chapter Conclusions

The last development stage attained culminated in software design to attend to chest compression quality assessment requirements, allowing either real-time feedback and post-training compression quality analysis, and integration with the previously tested measurement sensory systems.

The developed algorithm was design to identify in real-time target compression data points, such as compression start, compression peak and chest recoil, in order to, on one hand, provide objective and immediate feedback on compression quality during training, and, on the other hand, to use the detected compression points to calculate compression metrics, useful to training quality analysis. These metrics included an empirically designed overall compression score, that intends to quantify compressions quality considering all four compression parameters. The design of this score took into consideration not only quality standards stipulated by the guidelines for each individual compression parameters, but also the resolution that the selected sensors were capable to achieve.

Usability studies for the implemented compression quality systems were executed, by exposing the instrumented manikin for complete CPR training sessions and analyzing performed compression quality. Equally encouraging results for all the instrumented measurement systems supporting their potential usability as an objective measurement system for quality assessment of chest compressions during CPR.

7

DISCUSSION AND RECOMENDATIONS

The low survival rate associated with OHCA, combined with the high propensity of cardiovascular diseases in developed countries, motivated the need to develop BLS knowledge, including the development of well-established guidelines to improve victim survival. Despite of that, CPR is still shortly attempted in OHCA cases or, if attempted, still presents suboptimal survival rates. This reveals not only the lack of community awareness for BLS and CPR education, but also that current educational activities are not successfully achieving their intended outcomes.

Tools for self-guided CPR training can make BLS education and CPR training more accessible to the community, and more adjusted to the individual educational needs. In particular, their feedback feature provides a more objective, reliable and standardized assessment on CPR skills performance, being a step towards a more effective training with strong skill acquisition and retention over time, among other advantages.

Several proposals of different feedback devices have emerged, with different complexities and measurement technologies, although there are still several limitations regarding their development for CPR training assessment. Beyond different measurement systems intrinsic limitations (see section 3.2), there is no gold-standard to evaluate the accuracy of such technologies nor recommendations for the accuracy needed for chest compression measurements. Furthermore, despite of the standardized quality parameters recommended in guidelines, there is no overall quality score to regulate and standardize overall training assessment. Thus, advances and improvements in this topic are possible, and further development is needed.

This project aimed the development of a feedback system to support CPR training, focusing on chest compressions, in order to achieve quantifiable and accurate measurements for the established chest compression parameters, namely, hands positioning, compression depth, compression rate, and chest recoil. Furthermore, the developed system is expected to overcome the different limitations presented by existing solutions (see section 3.2), envisioning an easy and generic implementation on training manikins at a reduced cost, leading to broader access to the technology.

With that in mind, a standard commercialized CPR manikin was instrumented with different sensors. Two different development approaches were taken into consideration: an operational approach, using off-the-shelf electronic sensors, and an exploratory and innovative approach, using optical fiber

as a sensing mechanism. For both approaches the same development methodology was used: (i) sensor selection according to the established requirements and (ii) functional and (iii) performance sensor testing, in order to select the most adequate sensory system. The systems selected as adequate were then integrated in a training prototype, and sensors acquired data was processed through a feature detection algorithm, in order to provide both real-time feedback on training performance and post-training analysis through performance metrics, including a designed overall compressions quality score.

Three different sensory systems were selected as adequate for the purpose of this project: an ultrasonic sensor HC-SR04, a digital infrared sensor VL6180X, and a polymeric optical fiber U-shaped macrobending sensor, capable of assessing compression depth, frequency, and chest recoil, all conciliated with a piezoresistive pressure sensor FSR 402, to assess hands positioning. The main characteristics of the three sensory systems, including their price (excluding the training manikin), advantages and limitations, are presented in Table 7.1.

Table 7.1. Main characteristics of the selected sensory systems, including their price, advantages and limitations.

Sensory System	Resolution	Price*	Advantages	Limitations
HC-SR04 + FSR 402	0,3 cm	€ 34,60	Adequate response to compressions; Identifies all compression parameter variations; Easy assembly; Low computational load; Highly reproducible.	Fitted only for hollow training manikins.
VL6180X + FSR 402	0,1 cm	€ 44,13	Adequate response to compressions; Identifies all compression parameter variations; Easy assembly; Low computational load; Highly reproducible.	Fitted only for hollow training manikins.
Macrobending sensor + FSR 402	0,08 cm	€ 45,73	Adequate response to compressions; Identifies all compression parameter variations; Low computational load.	Fitted only for hollow training manikins; More complex assembly and circuit integration; Low reproducibility; Overestimates compression depth with incorrect hand position.

*Includes all components of the sensory system and the electronic processing unit Arduino.

From a general point-of-view, the three selected sensory systems fulfill the project objectives and the established requirements, offering simple and affordable solutions to objectively measure relevant compression parameters and providing feedback during CPR training. The development cost of any of the systems, between €35 and €45, is considered very accessible, in the context of CPR training. Furthermore, system testing protocols, which included a range of possible variations in chest

compressions, proved robustness and reliability of all systems, with adequate analysis of compression parameters.

In a more detailed analysis of the obtain results, considering the selected electronic sensory systems, both ultrasonic and infrared sensors provided equivalent results regarding compression depth, rate and recoil, with slight measurement differences justified by intrinsic sensor measurement variability and their different resolutions. Thus, both systems can successfully detect and differentiate each chest compression parameter (excluding hands positioning), providing similar quality results. This equivalent behavior was useful to cross-check the electronic systems response to chest compressions.

In a more operational perspective, the location of these sensors, in the interior side of manikin's back, was optimized to promote an accurate extraction of displacement measurements, and can be applied in any hollow manikin, without the need of a pre-calibration. The need for a hollow structure was the main limitation presented for the use of these sensors. Both approaches include low computational load and easy circuit integration. The main difference between the two approaches lays on system development cost, with ultrasonic sensory system being slightly more affordable. However, the used infrared sensor presents a higher measurement resolution, which in terms of cost-benefit, is considered more relevant, leading to the recommendation of this sensor over the ultrasonic.

Regarding the experimental U-shaped optical fiber macrobending sensor, both calibrations performed with ultrasonic and infrared sensors were considered to provide equivalent results regarding compression depth, rate and recoil, as expected, with a very acceptable RMSE of only 0,2 cm. This new approach can successfully detect and differentiate each chest compression parameter (excluding hands positioning), providing similar quality results when compared to electronic sensors. In comparison with the recommended infrared sensor, the optical fiber macrobending sensory system presents an equally adequate response to compressions, but with a more stable and reliable baseline. The main limitation of this approach lays with compression depth overestimation with incorrect hands positioning, which has an associated error of 0,8 cm. This error is considered relevant, having implications in the calculation of individual compression depth score.

Operationally, macrobending sensor arrangement in an optimized U-shaped form, positioned on manikin's metal spring promote an adequate response among many other fiber conformations tested. This arrangement was fully adapted for the used manikin, although this arrangement was considered to be easily adapted to other training manikin models with similar structure. Similarly to the used electronic sensors, this sensor needs a manikin with an hollow structure, which is considered a limitation to its adaptability. Also noticeable, contrarily to electronic sensors, the use of a macrobending promotes difficulties in reproducibility and requires a pre-calibration customized to each type of manikin used. In a different note, macrobending sensory system showed great durability to compressions, with no measurable losses on optical fiber response due to fiber wear down, in more than 5 500 compressions, despite of its plastic composition. Furthermore, and similarly to electronic sensors, this system has low computational load and a relatively simple circuit integration.

As none of the described sensors were capable to provide information about hands positioning, a piezoresistive pressure sensor was integrated in the measurement system in order to assess exclusively this parameter, by being placed in the correct compression area on manikin's chest. As it is intended to provide a binary signal regarding correct/incorrect hand position, no issues regarding sensors' repeatability and reproducibility previously documented were considered relevant. Furthermore, it checks all the requirements established, including easy assembly, low processing load, simple circuit integration and affordable cost. Thus, this sensor completed the missing feature of the previously tested sensory systems for CPR quality assessment.

Regarding software development, an algorithm was designed to extract features of interest, in order to providing immediate feedback on compressions quality, and metrics of interest for a post-training analysis, including an overall compression score. The designed algorithm proved to be adequate for all the signals acquired from different selected sensors and showed great robustness to all compression parameters variations. Nevertheless, to be considered that, despite of its design to be used for real-time processing, it was only applied to previously acquired sensor data.

Based on the developed work and the above discussion, the recommended sensory system for effective assessment of compressions quality is constituted by an infrared sensor and a pressure sensor.

Recommendations for future work

Regarding the general development of this CPR feedback prototype, future recommended steps are: (i) system implementation and validation in real-time application, and (ii) software integration in an information system with a graphical user interface.

The inclusion of ventilation related measurements in this training prototype would provide a complete assessment of CPR training. Considering all selected systems showed sensibility to detect ventilations, this seems to be an easy extension to include, although further investigation is needed.

Concerning optical fiber macrobending sensor, reported reproducibility issues should be explored in order to create a more robust sensory system, with easy assembly on training manikins. Potentially, a low-cost 3D printed structure would allow optical fiber to maintain a stable base position (maintaining displacement calibration), overcoming the identified limitations. This approach (optical fiber encapsulation) could allow an adaptability different manikin structures, and could inclusively overcome depth overestimation issue.

Concerning the preliminary tests performed with FBG, the encouraging results regarding chest compression detection, with great sensibility and resolution, justify its further exploration in the future. Although FBG sensors do not align with the established requirements for this application, this technology could eventually be used as a validation tool for existing technologies, which is an important development and research topic in this field.

Finally, and considering more long-term developments, prototype testing on continuous training scenarios, prototype testing with an extensive group of users, and prototype integration on different training manikins, are also considered relevant and promote educational validation.

REFERENCES

[1] G. D. Perkins *et al.*, "Basic life support: European Resuscitation Council Guidelines for Resuscitation 2021," *Resuscitation*, vol. 95, pp. 81–99, 2021, doi: 10.1016/j.resuscitation.2021.02.009.

[2] B. Lynch, E. L. Einspruch, G. Nichol, and T. P. Aufderheide, "Assessment of BLS skills: Optimizing use of instructor and manikin measures," *Resuscitation*, vol. 76, no. 2, pp. 233–243, Feb. 2008, doi: 10.1016/j.resuscitation.2007.07.018.

[3] R. Greif *et al.*, "European Resuscitation Council Guidelines 2021 : Education for resuscitation," *Resuscitation*, pp. 1–20, 2021, doi: 10.1016/j.resuscitation.2021.02.016.

[4] J.-T. Gräsner *et al.*, "European Resuscitation Council Guidelines 2021 : Epidemiology of cardiac arrest in Europe," pp. 1–19, 2021, doi: 10.1016/j.resuscitation.2021.02.007.

[5] J. T. Gräsner *et al.*, "Survival after out-of-hospital cardiac arrest in Europe - Results of the EuReCa TWO study," *Resuscitation*, vol. 148, no. December 2019, pp. 218–226, 2020, doi: 10.1016/j.resuscitation.2019.12.042.

[6] Instituto Nacional de Emergência Médica, "Ocorrências Pré-Hospitalates," 2020. https://extranet.inem.pt/stats/?stat=16&mes=11&ano=2020 (accessed Nov. 16, 2021).

[7] G. D. Perkins *et al.*, "European Resuscitation Council Guidelines for Resuscitation 2015. Section 2. Adult basic life support and automated external defibrillation.," *Resuscitation*, vol. 95, pp. 81–99, 2015, doi: 10.1016/j.resuscitation.2015.07.015.

[8] C. Holmgren *et al.*, "Out-of-hospital cardiac arrest: Causes according to autopsy and electrocardiography – Analysis of 781 patients with neither hospital care nor prescribed medication during the preceding two years," *Resuscitation*, vol. 150, no. December 2019, pp. 65–71, 2020, doi: 10.1016/j.resuscitation.2020.02.040.

[9] M. E. H. Ong, G. D. Perkins, and A. Cariou, "Out-of-hospital cardiac arrest: prehospital management," *Lancet*, vol. 391, no. 10124, pp. 980–988, 2018, doi: 10.1016/S0140-6736(18)30316-7.

[10] W. H. Ibrahim, "Recent advances and controversies in adult cardiopulmonary resuscitation," *Postgr. Med J*, vol. 83, no. November 2007, pp. 649–654., 2007, doi: 10.1136/pgmj.2007.057133.

[11] D. E. Niles *et al.*, "Prevalence and hemodynamic effects of leaning during CPR," *Resuscitation*, vol. 82, no. SUPPL. 2, pp. S23–S26, 2011, doi: 10.1016/S0300-9572(11)70147-2.

[12] C. Sá-Couto and A. Nicolau, "General Public's Knowledge Regarding Basic Life Support: A Pilot Study with a Portuguese Sample," *Acta Médica Port.*, vol. 32, no. 2, pp. 111–118, 2019.

[13] A. Cheng *et al.*, "Resuscitation Education Science: Educational Strategies to Improve Outcomes From Cardiac Arrest: A Scientific Statement From the American Heart Association," *Circulation*, vol. 138, no. 6, pp. e82–e122, Aug. 2018, doi: 10.1161/CIR.0000000000000583.

[14] R. Greif *et al.*, “European Resuscitation Council Guidelines for Resuscitation 2015. Section 10. Education and implementation of resuscitation,” *Resuscitation*, vol. 95, pp. 288–301, 2015, doi: 10.1016/j.resuscitation.2015.07.032.

[15] European Ressuscitation Council, “ERC Course Rules,” 2017. [Online]. Available: https://cms.erc.edu/sites/5714e77d5e615861f00f7d18/assets/5a7da3174c84862202cfb056/Course_Rules_VS20171215_V3.1.pdf.

[16] M. Halm and C. Crespo, “Acquisition and Retention of Resuscitation Knowledge and Skills: What’s Practice Have to Do With It?,” *Am. J. Crit. Care*, vol. 27, no. 6, pp. 513–517, Nov. 2018, doi: 10.4037/ajcc2018259.

[17] V. González-Salvado *et al.*, “Training adult laypeople in basic life support. A systematic review,” *Rev. Española Cardiol. (English Ed.*, vol. 73, no. 1, pp. 53–68, 2020, doi: 10.1016/j.rec.2018.11.013.

[18] L. P. Roppolo, T. Saunders, P. E. Pepe, and A. H. Idris, “Layperson training for cardiopulmonary resuscitation: When less is better,” *Curr. Opin. Crit. Care*, vol. 13, no. 3, pp. 256–260, 2007, doi: 10.1097/MCC.0b013e32814db81f.

[19] G. D. Perkins, “Simulation in resuscitation training,” *Resuscitation*, vol. 73, no. 2, pp. 202–211, May 2007, doi: 10.1016/j.resuscitation.2007.01.005.

[20] C. Sá-Couto, A. M. Ferreira, D. Almeida, A. Nicolau, and P. Vieira-Marques, “Evaluation of skills acquisition using a new low-cost tool for CPR self-training,” *Porto Biomed. J.*, vol. 3, no. 1, p. e8, Aug. 2018, doi: 10.1016/j.pbj.0000000000000008.

[21] C. Hansen, C. Bang, M. Stærk, K. Krogh, and B. Løfgren, “Certified Basic Life Support Instructors Identify Improper Cardiopulmonary Resuscitation Skills Poorly: Instructor Assessments Versus Resuscitation Manikin Data,” *Simul. Healthc.*, vol. 14, no. 5, pp. 281–286, 2019, doi: 10.1097/SIH.0000000000000386.

[22] A. Nicolau, I. Jorge, P. Marques, and C. Sá-Couto, “Influence of training feedback devices on CPR skills acquisition and retention: a systematic review and meta-analysis,” *PROSPERO 2021 CRD42021240953*, [Online]. Available: https://www.crd.york.ac.uk/prospero/display_record.php?ID=CRD42021240953.

[23] J. Gruber, D. Stumpf, B. Zapletal, S. Neuhold, and H. Fischer, “Real-time feedback systems in CPR,” *Trends Anaesth. Crit. Care*, vol. 2, no. 6, pp. 287–294, 2012, doi: 10.1016/j.tacc.2012.09.004.

[24] Heart and Stroke Foundation of Canada, “Use of Feedback Devices in Resuscitation Training Courses,” 2020. https://cpr.heartandstroke.ca/s/article/Use-of-Feedback-Devices-in-Resuscitation-Training-Courses?language=en_US (accessed Dec. 28, 2020).

[25] J. Yeung, R. Meeks, D. Edelson, F. Gao, J. Soar, and G. D. Perkins, “The use of CPR feedback/prompt devices during training and CPR performance: A systematic review,” *Resuscitation*, vol. 80, no. 7, pp. 743–751, Jul. 2009, doi: 10.1016/j.resuscitation.2009.04.012.

[26] M. An, Y. Kim, and W. K. Cho, “Effect of smart devices on the quality of CPR training: A systematic review,” *Resuscitation*, vol. 144, no. July, pp. 145–156, 2019, doi: 10.1016/j.resuscitation.2019.07.011.

[27] Simulaids, “Simulaids Econo VTA (Visual Training Assistant) CPR Trainer,” 2020. https://simulaids.co.uk/product/econo-vta-visual-training-assistant-cpr-trainer/ (accessed Dec. 22, 2020).

[28] Simulaids, “Simulaids Adult Brad VTA Manikin with CPR feedback,” 2020. https://simulaids.co.uk/product/adult-brad-vta-with-cpr-feedback/ (accessed Dec. 22, 2020).

[29] Prestan, “Ultralite Prestan,” 2020. https://www.prestanproducts.com/products/cpr-training-manikins/ultralite-manikin/ (accessed Dec. 21, 2020).

[30] Prestan, “Professional Adult Manikin,” 2020. https://www.prestanproducts.com/products/cpr-training-manikins/professional-adult-manikin/ (accessed Dec. 21, 2020).

[31] Prestan, “Professional Adult Series 2000 Manikin,” 2020. https://www.prestanproducts.com/products/cpr-training-manikins/professional-adult-series-2000-manikin/?back=products (accessed Dec. 21, 2020).

[32] 3B Scientific, “BasicBilly+,” 2020. https://www.3bscientific.com.es/pt/simulador-de-suporte-basico-a-vida-basicbilly-tom-de-pele-clara-8000951-p72-light-3b-scientific-basicbilly,p_157_31950.html (accessed Dec. 20, 2020).

[33] Laerdal Medical, “Littel Anne QCPR,” 2020. https://laerdal.com/products/simulation-training/resuscitation-training/little-anne-qcpr/ (accessed Dec. 22, 2020).

[34] Laerdal Medical, “SkillGuide,” 2020. https://laerdal.com/products/simulation-training/resuscitation-training/skillguide/ (accessed Dec. 22, 2020).

[35] BT Inc, “SMART CPR Training Model, Sherpa X,” 2018. http://www.btinc.co.kr/seem2_feature_en/ (accessed Dec. 23, 2020).

[36] Aero Healthcare, “Brayden Pro,” 2021. http://braydenmanikins.com/pro/ (accessed Dec. 23, 2020).

[37] HeartiSense, “HeartiSense Kit,” 2015. https://www.heartisense.com/eng/cpr_works/kit (accessed Dec. 22, 2020).

[38] N. W. Caleb Ho, Johnny Ho, Alan Huang, “A Portable and Scalable Interactive Manikin System,” 2007.

[39] D. M. González-Otero, S. R. de Gauna, J. M. Ruiz, J. J. Gutiérrez, P. Saiz, and M. Leturiondo, “Audiovisual Feedback Devices for Chest Compression Quality during CPR,” in *Resuscitation Aspects*, InTech, 2017, pp. 77–96.

[40] M. I. Tiwana, S. J. Redmond, and N. H. Lovell, “A review of tactile sensing technologies with applications in biomedical engineering,” *Sensors Actuators, A Phys.*, vol. 179, pp. 17–31, 2012, doi: 10.1016/j.sna.2012.02.051.

[41] E. McAdams and C. Gehin, “Force Measurements,” in *Comprehensive Biomedical Physics: Physics of Physiological Measurements*, 1st ed., A. Brahme, Ed. United Kingdom: Elsevier B.V., 2014, pp. 127–137.

[42] M. Sainio *et al.*, “Effect of mattress and bed frame deflection on real chest compression depth measured with two CPR sensors,” *Resuscitation*, vol. 85, no. 6, pp. 840–843, 2014, doi: 10.1016/j.resuscitation.2014.03.009.

[43] A. Nicolau, “Development and validation of a low-cost tool for CPR self-training,” Dissertation presented to obtain Master’s Degree in Biomedical Engineering to Universidade do Porto, Faculdade de Engenharia, 2018.

[44] Y. Kokubo, I. Maeda, S. Hibino, and K. Minami, “Evaluation system for chest compression training ‘Shinnosuke-kun,’” *SEI Tech. Rev.*, no. 84, pp. 172–177, 2017.

[45] S. R. De Gauna, D. M. González-Otero, J. Ruiz, and J. K. Russell, “Feedback on the rate and depth of chest compressions during cardiopulmonary resuscitation using only accelerometers,” *PLoS One*, vol. 11, no. 3, pp. 1–17, 2016, doi: 10.1371/journal.pone.0150139.

[46] S. Boussen *et al.*, “Using an inertial navigation algorithm and accelerometer to monitor chest compression depth during cardiopulmonary resuscitation,” *Med. Eng. Phys.*, vol. 38, no. 9, pp. 1028–1034, 2016, doi: 10.1016/j.medengphy.2016.05.001.

[47] S. R. De Gauna, D. M. González-Otero, J. Ruiz, J. J. Gutiérrez, and J. K. Russell, “A Feasibility Study for Measuring Accurate Chest Compression Depth and Rate on Soft Surfaces Using Two Accelerometers and Spectral Analysis,” *Biomed Res. Int.*, vol. 2016, 2016, doi: 10.1155/2016/6596040.

[48] Y. T. Song and Y. Chee, “The development of feedback monitoring device for CPR,” *Proc. Annu. Int. Conf. IEEE Eng. Med. Biol. Soc. EMBS*, no. January 2015, pp. 3294–3297, 2011, doi: 10.1109/IEMBS.2011.6090894.

[49] F. Gohier, K. Dellimore, and C. Scheffer, “Development of a smart backboard system for real-time feedback during CPR chest compression on a soft back support surface,” *Proc. Annu. Int. Conf. IEEE Eng. Med. Biol. Soc. EMBS*, pp. 346–349, 2013, doi: 10.1109/EMBC.2013.6609508.

[50] A. Kandori, Y. Sano, Y. Zhang, and T. Tsuji, “A simple accurate chest-compression depth gauge using magnetic coils during cardiopulmonary resuscitation,” *Rev. Sci. Instrum.*, vol. 86, no. 12, 2015, doi: 10.1063/1.4938158.

[51] S. Lee *et al.*, “Development of Smart-Ring-Based Chest Compression Depth Feedback Device for High Quality Chest Compressions: A Proof-of-Concept Study,” *Biosensors*, vol. 11, no. 2, p. 35, 2021, doi: 10.3390/bios11020035.

[52] C. J. Centen, “Optical Techniques for the Measurement of Chest Compression Depth and other parameters during CPR,” *United States Patent No. 10,335,346 B2*. 2019, [Online]. Available: https://patents.google.com/patent/US10543147B2/en.

[53] C. Loconsole *et al.*, “RELIVE: A Markerless Assistant for CPR Training,” *IEEE Trans. Human-Machine Syst.*, vol. 46, no. 5, pp. 755–760, 2016, doi: 10.1109/THMS.2016.2586756.

[54] Y. Kim, B. G. Yu, J. H. Oh, and T. W. Kim, “Novel chest compression depth measurement sensor using IR-UWB for improving quality of cardiopulmonary resuscitation,” *IEEE Sens. J.*, vol. 17, no. 10, pp. 3174–3183, 2017, doi: 10.1109/JSEN.2017.2680454.

[55] B. G. Yu, J. H. Oh, Y. Kim, and T. W. Kim, “Accurate measurement of chest compression depth using impulse-radio ultra-wideband sensor on a mattress,” pp. 1–8, 2017, doi: 10.1371/journal.pone.0183971.

[56] T. Klosiewicz, M. Puslecki, R. Zalewski, M. Sip, and B. Perek, “Assessment of chest compression quality - A systematic review,” *Disaster Emerg. Med. J.*, vol. 5, no. 1, pp. 49–56, 2020, doi: 10.5603/DEMJ.a2020.0010.

[57] H. J. J. M. Berden, N. H. J. Pijls, F. F. Willems, J. M. A. Hendrick, and J. F. Crul, “A scoring system for basic cardiac life support skills in training situations,” *Resuscitation*, vol. 23, no. 1, pp. 21–31, 1992, doi: 10.1016/0300-9572(92)90159-A.

[58] C. A. Graham and N. F. Lewis, “A scoring system for the assessment of basic life support ability,” *Resuscitation*, vol. 43, no. 2, pp. 111–114, 2000, doi: 10.1016/S0300-9572(99)00135-5.

[59] R. Anderson, A. Sebaldt, Y. Lin, and A. Cheng, “Optimal training frequency for acquisition and retention of high-quality CPR skills: A randomized trial,” *Resuscitation*, vol. 135, no. August 2018, pp. 153–161, 2019, doi: 10.1016/j.resuscitation.2018.10.033.

[60] Y. Lin, A. Cheng, V. J. Grant, G. R. Currie, and K. G. Hecker, “Improving CPR quality with distributed practice and real-time feedback in pediatric healthcare providers – A randomized controlled trial,” *Resuscitation*, vol. 130, no. May, pp. 6–12, 2018, doi: 10.1016/j.resuscitation.2018.06.025.

[61] C. Buléon *et al.*, “Impact of a feedback device on chest compression quality during extended manikin CPR: a randomized crossover study,” *Am. J. Emerg. Med.*, vol. 34, no. 9, pp. 1754–1760, 2016, doi: 10.1016/j.ajem.2016.05.077.

[62] R. Barcala-Furelos *et al.*, “Can surf-lifeguards perform a quality cardiopulmonary resuscitation sailing on a lifeboat? A quasi-experimental study,” *Emerg. Med. J.*, vol. 34, no. 6, pp. 370–375, 2017, doi: 10.1136/emermed-2016-205952.

[63] C. Abelairas-Gómez, E. Rey, V. González-Salvado, M. Mecías-Calvo, E. Rodríguez-Ruiz, and A. Rodríguez-Núñez, “Acute muscle fatigue and CPR quality assisted by visual feedback

devices: A randomized-crossover simulation trial," *PLoS One*, vol. 13, no. 9, pp. 1–14, 2018, doi: 10.1371/journal.pone.0203576.

[64] A. López-González, M. Sánchez-López, A. Garcia-Hermoso, J. López-Tendero, J. Rabanales-Sotos, and V. Martínez-Vizcaíno, "Muscular fitness as a mediator of quality cardiopulmonary resuscitation," *Am. J. Emerg. Med.*, vol. 34, no. 9, pp. 1845–1849, 2016, doi: 10.1016/j.ajem.2016.06.058.

[65] P. S. Martin, A. M. Kemp, P. S. Theobald, S. A. Maguire, and M. D. Jones, "Does a more 'physiological' infant manikin design effect chest compression quality and create a potential for thoracic over-compression during simulated infant CPR?," *Resuscitation*, vol. 84, no. 5, pp. 666–671, 2013, doi: 10.1016/j.resuscitation.2012.10.005.

[66] R. M. Sutton *et al.*, "First quantitative analysis of cardiopulmonary resuscitation quality during in-hospital cardiac arrests of young children," *Resuscitation*, vol. 85, no. 1, pp. 70–74, 2014, doi: 10.1016/j.resuscitation.2013.08.014.

[67] Laerdal, "CPR scoring explained," p. 12, 2015, [Online]. Available: https://www.laerdal.com/us/support/scoring.

[68] C. Sa-Couto, A. Nicolau, R. Marques-Costa, and P. Vieira-Marques, "CPR personal trainer: A low-cost training tool with objective feedback," *Resuscitation*, vol. 130, no. 2018, p. e107, Sep. 2018, doi: 10.1016/j.resuscitation.2018.07.224.

[69] I. Sousa, "Gamifying autonomous CPR training," Thesis presented to obtain Master's Degree in Medical Informatics to Universidade do Porto, Porto, Portugal, 2019.

[70] PTRobotics, "HC-SR04 Ultrasonic Ranging Module," 2021. https://www.ptrobotics.com/sensor-ultrasom/4783-hc-sr04-ultrasonic-ranging-module-4pin.html (accessed May 12, 2021).

[71] PTRobotics, "Sharp GP2Y0A51SK0F Analog Distance Sensor," 2021. https://www.ptrobotics.com/sensores-opticos/4260-sharp-gp2y0a51sk0f-analog-distance-sensor-2-15cm.html (accessed May 12, 2021).

[72] PTRobotics, "VL6180X Time-of-Flight Distance Sensor," 2021. https://www.ptrobotics.com/sensores-opticos/3797-vl6180x-time-of-flight-distance-sensor-carrier-with-voltage-regulator-regulador-de-voltagem.html (accessed May 13, 2021).

[73] PTRobotics, "Triple Axis Accelerometer - ADXL335," 2021. https://www.ptrobotics.com/acelerometros/601-triple-axis-accelerometer-breakout-adxl335.html (accessed May 14, 2021).

[74] PTRobotics, "Triple Axis Accelerometer - MMA8452Q," 2021. https://www.ptrobotics.com/acelerometros/9364-modulo-acelerometro-triplo-eixo-mma8452q-com-headers-sparkfun-.html (accessed May 14, 2021).

[75] PTRobotics, "Triple Axis Accelerometer & Gyro - MPU-6050," 2021. https://www.ptrobotics.com/acelerometros/3639-triple-axis-accelerometer-gyro-mpu-6050.html (accessed May 15, 2021).

[76] Sharp, "Distance Measuring Sensor Unit GP2Y0A51SK0F Data Sheet, Sheet No. OP13007EN." [Online]. Available: https://global.sharp/products/device/lineup/data/pdf/datasheet/gp2y0a51sk_e.pdf.

[77] PTRobotics, "Round Force-Sensitive Resistor (FSR) Interlink 402," 2021. https://www.ptrobotics.com/sensor-de-pressao/3629-round-force-sensitive-resistor-fsr-interlink-402.html (accessed May 27, 2021).

[78] PTRobotics, "Square Force Sensitive Resistor (FSR) Interlink 406," 2021. https://www.ptrobotics.com/sensor-de-pressao/3629-round-force-sensitive-resistor-fsr-interlink-402.html (accessed May 27, 2021).

[79] Interlink Technologies, “FSR 402 Data Sheet, Sheet No. 30-81794,” pp. 1–4, 2013, [Online]. Available: http://www.interlinkelectronics.com/FSR402short.php.

[80] Interlink Technologies, “FSR 406 Data Sheet, Sheet No. 30-73258.” pp. 1–4, 2013, [Online]. Available: www.interlinkelectronics.com.

[81] M. A. Zawawi, S. O’Keffe, and E. Lewis, “Intensity-modulated fiber optic sensor for health monitoring applications: A comparative review,” *Sens. Rev.*, vol. 33, no. 1, pp. 57–67, 2013, doi: 10.1108/02602281311294351.

[82] A. Argyros, *Structure, properties and characteristics of optical fibres*, vol. 2. Woodhead Publishing Limited, 2009.

[83] M. A. Mentzer, “Fiber optic sensors,” *Photonic Devices Syst.*, vol. 2, no. 6, pp. 247–277, 2017, doi: 10.1201/9780203743515.

[84] P. Roriz, O. Frazão, A. B. Lobo-Ribeiro, J. L. Santos, and J. A. Simões, “Review of fiber-optic pressure sensors for biomedical and biomechanical applications,” *J. Biomed. Opt.*, vol. 18, no. 5, p. 050903, 2013, doi: 10.1117/1.jbo.18.5.050903.

[85] H. Di, Y. Xin, and J. Jian, “Review of optical fiber sensors for deformation measurement,” *Optik (Stuttg).*, vol. 168, pp. 703–713, 2018, doi: 10.1016/j.ijleo.2018.04.131.

[86] M. M. Patil and O. Prohaska, “Fiber optic sensor for joint angle measurement,” *IEEE/Engineering Med. Biol. Soc. Annu. Conf.*, vol. 10, no. pt2, pp. 803–804, 1988, doi: 10.1109/iembs.1988.95055.

[87] W. J. Yoo *et al.*, “Development of respiration sensors using plastic optical fiber for respiratory monitoring inside MRI system,” *J. Opt. Soc. Korea*, vol. 14, no. 3, pp. 235–239, 2010, doi: 10.3807/JOSK.2010.14.3.235.

[88] H. Kopola, O. Mantylä, M. Mäkiniemi, K. Mähönen, and K. Virtanen, “An instrument for measuring human biting force,” vol. 2331, pp. 149–155, 1994.

[89] A. Grillet *et al.*, “Optical fiber sensors embedded into medical textiles for healthcare monitoring,” *IEEE Sens. J.*, vol. 8, no. 7, pp. 1215–1222, 2008, doi: 10.1109/JSEN.2008.926518.

[90] J. De Jonckheere *et al.*, “OFSETH: Smart medical textile for continuous monitoring of respiratory motions under magnetic resonance imaging,” *Proc. 31st Annu. Int. Conf. IEEE Eng. Med. Biol. Soc. Eng. Futur. Biomed. EMBC 2009*, pp. 1473–1476, 2009, doi: 10.1109/IEMBS.2009.5332432.

[91] A. S. Silva, A. Catarino, M. V. Correia, and O. Frazão, “Design and characterization of a wearable macrobending fiber optic sensor for human joint angle determination,” *Opt. Eng.*, vol. 52, no. 12, p. 126106, 2013, doi: 10.1117/1.oe.52.12.126106.

[92] C. Davis, A. Mazzolini, J. Mills, and P. Dargaville, “A new sensor for monitoring chest wall motion during high-frequency oscillatory ventilation,” *Med. Eng. Phys.*, vol. 21, no. 9, pp. 619–623, 1999, doi: 10.1016/S1350-4533(99)00094-6.

[93] A. T. Augousti, F. X. Maletras, and J. Mason, “Improved fibre optic respiratory monitoring using a figure-of-eight coil,” *Physiol. Meas.*, vol. 26, no. 5, pp. 585–590, 2005, doi: 10.1088/0967-3334/26/5/001.

[94] L. Bilro, J. Lemos Pinto, J. Oliveira, and R. Nogueira, “Gait monitoring with a wearable plastic optical sensor,” *Proc. IEEE Sensors*, no. November, pp. 787–790, 2008, doi: 10.1109/ICSENS.2008.4716559.

[95] H. Di, S. Sun, and Y. Che, “Respiration measurement using fibre-optic deformation sensor,” *J. Mod. Opt.*, vol. 64, no. 6, pp. 639–645, 2017, doi: 10.1080/09500340.2016.1255367.

[96] J. K. Sahota, N. Gupta, and D. Dhawan, “Fiber Bragg grating sensors for monitoring of physical parameters: a comprehensive review,” *Opt. Eng.*, vol. 59, no. 06, p. 1, 2020, doi:

10.1117/1.oe.59.6.060901.

[97] P. Roriz, L. Carvalho, O. Frazão, J. L. Santos, and J. A. Simões, “From conventional sensors to fibre optic sensors for strain and force measurements in biomechanics applications: A review,” *J. Biomech.*, vol. 47, no. 6, pp. 1251–1261, 2014, doi: 10.1016/j.jbiomech.2014.01.054.

[98] G. Wehrle, P. Nohama, H. J. Kalinowski, P. I. Torres, and L. C. G. Valente, “A fibre optic Bragg grating strain sensor for monitoring ventilatory movements,” *Meas. Sci. Technol.*, vol. 12, no. 7, pp. 805–809, 2001, doi: 10.1088/0957-0233/12/7/309.

[99] M. F. Domingues *et al.*, “Energy-Aware Wearable E-Health Architecture Using Optical FBG Sensors for Knee Kinematic Monitoring,” *2018 IEEE Glob. Commun. Conf. GLOBECOM 2018 - Proc.*, pp. 1–6, 2018, doi: 10.1109/GLOCOM.2018.8647425.

[100] S. Umesh, S. Padma, S. Asokan, and T. Srinivas, “Fiber Bragg Grating based bite force measurement,” *J. Biomech.*, vol. 49, no. 13, pp. 2877–2881, 2016, doi: 10.1016/j.jbiomech.2016.06.036.

[101] C. Hong, Y. Yuan, Y. Yang, Y. Zhang, and Z. A. Abro, “A simple FBG pressure sensor fabricated using fused deposition modelling process,” *Sensors Actuators, A Phys.*, vol. 285, pp. 269–274, 2019, doi: 10.1016/j.sna.2018.11.024.

[102] DigiKey, “Industrial Optical Fibers IF-E93,” 2021. https://www.digikey.pt/products/pt/optoelectronics/fiber-optics-transmitters-discrete/116?k=IFE93 (accessed May 29, 2021).

[103] Mouser Eletronics, “Broadcom/Avago HFBR-EUS100Z,” 2021. https://pt.mouser.com/ProductDetail/Broadcom-Avago/HFBR-EUS100Z?qs=jT9z6tsiFNmu8uqseWtCnQ%3D%3D (accessed May 29, 2021).

[104] DigiKey, “Industrial Fiber Optics IF-D91B,” 2021. https://www.digikey.pt/products/pt/optoelectronics/fiber-optics-receivers/117?k=IF D91B (accessed May 29, 2021).

[105] G. K. Palshikar, “Simple Algorithms for Peak Detection in Time-Series.” pp. 1–13, 2009.

APPENDICES

A. CIRCUITS ASSEMBLY

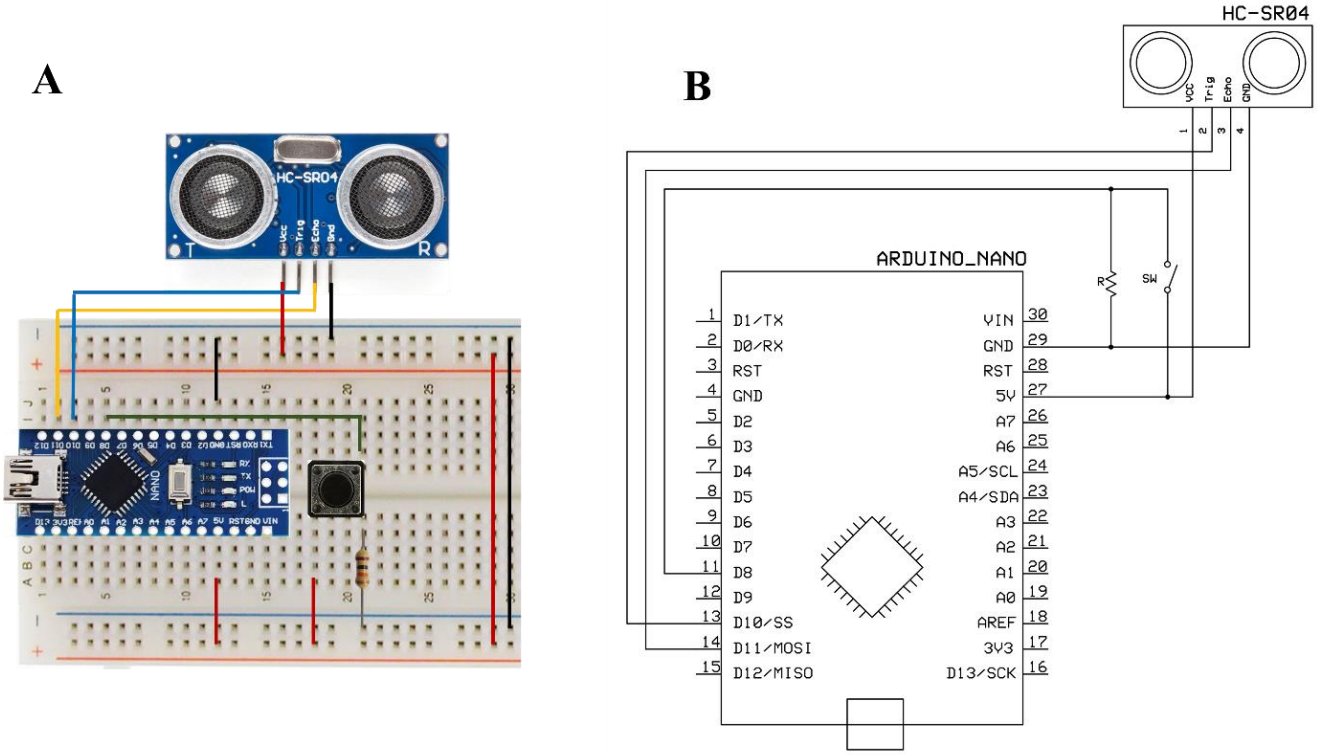

Figure A.1. Ultrasonic sensor HC-SR04 circuit assembly on the breadboard (A) and respective circuit schematic (B), with R = 1 kΩ.

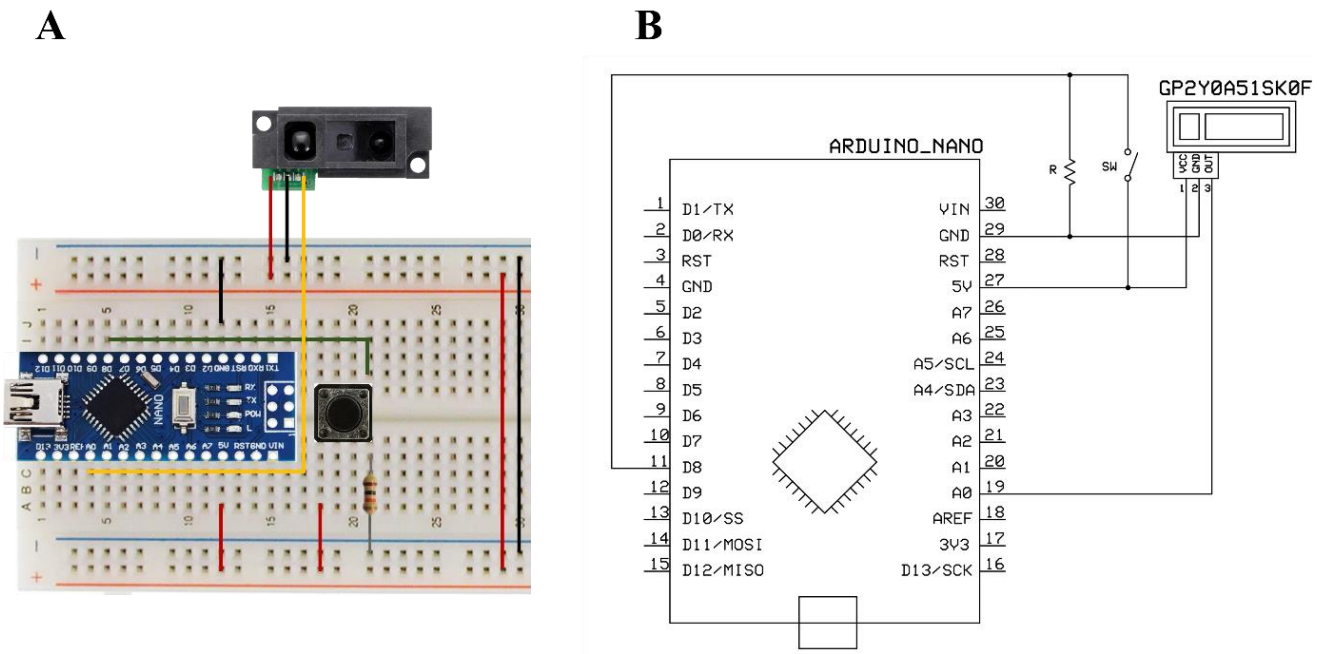

Figure A.2. Analog infrared sensor GP2Y0A51SK0F circuit assembly on the breadboard (A) and respective circuit schematic (B), with R = 1 kΩ.

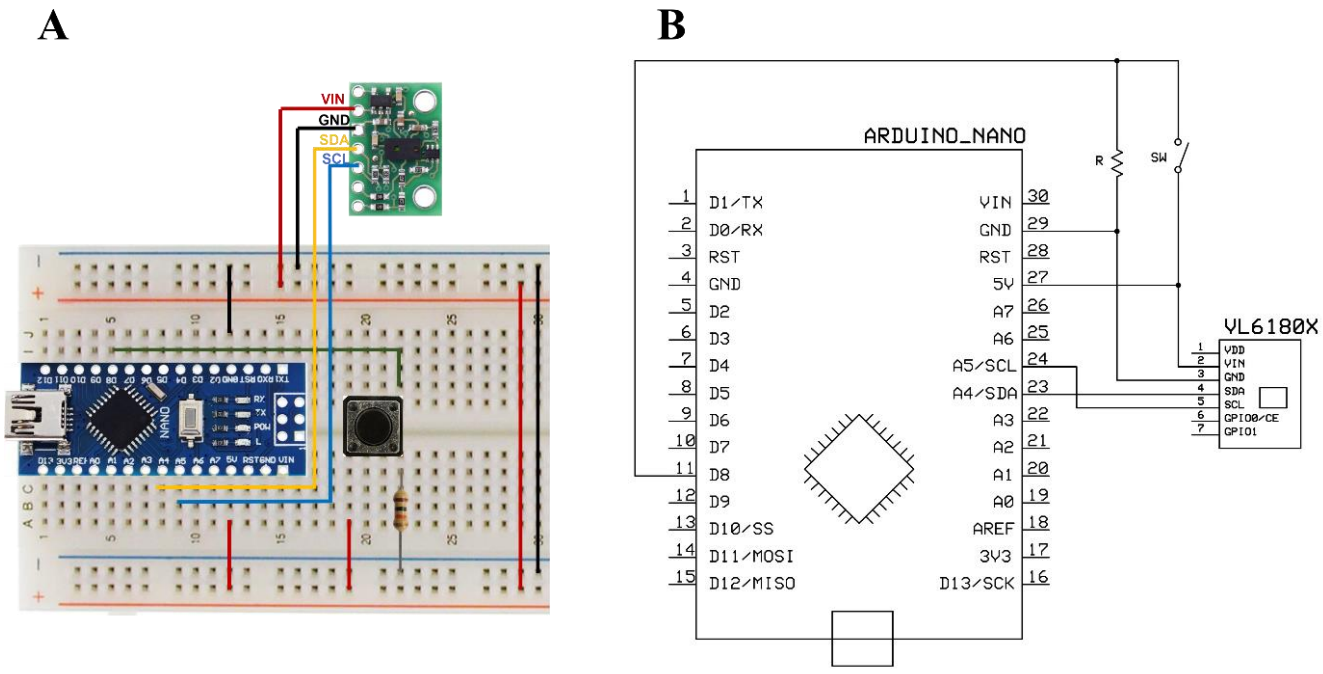

Figure A.3. Digital infrared sensor VL6180X circuit assembly on the breadboard (A) and respective circuit schematic (B), with R = 1 kΩ.

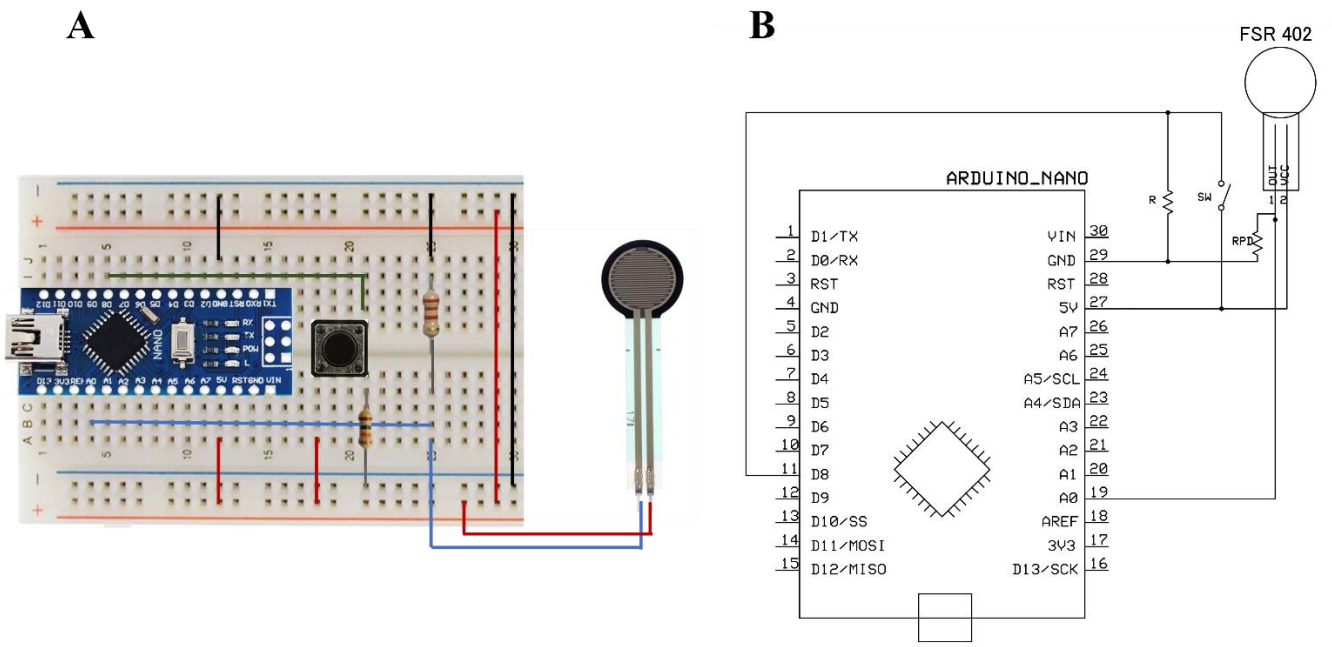

Figure A.4. Analog pressure sensor FSR 402 circuit assembly on the breadboard (A) and respective circuit schematic (B), with R = 1 kΩ and RPD = 2.2 kΩ.

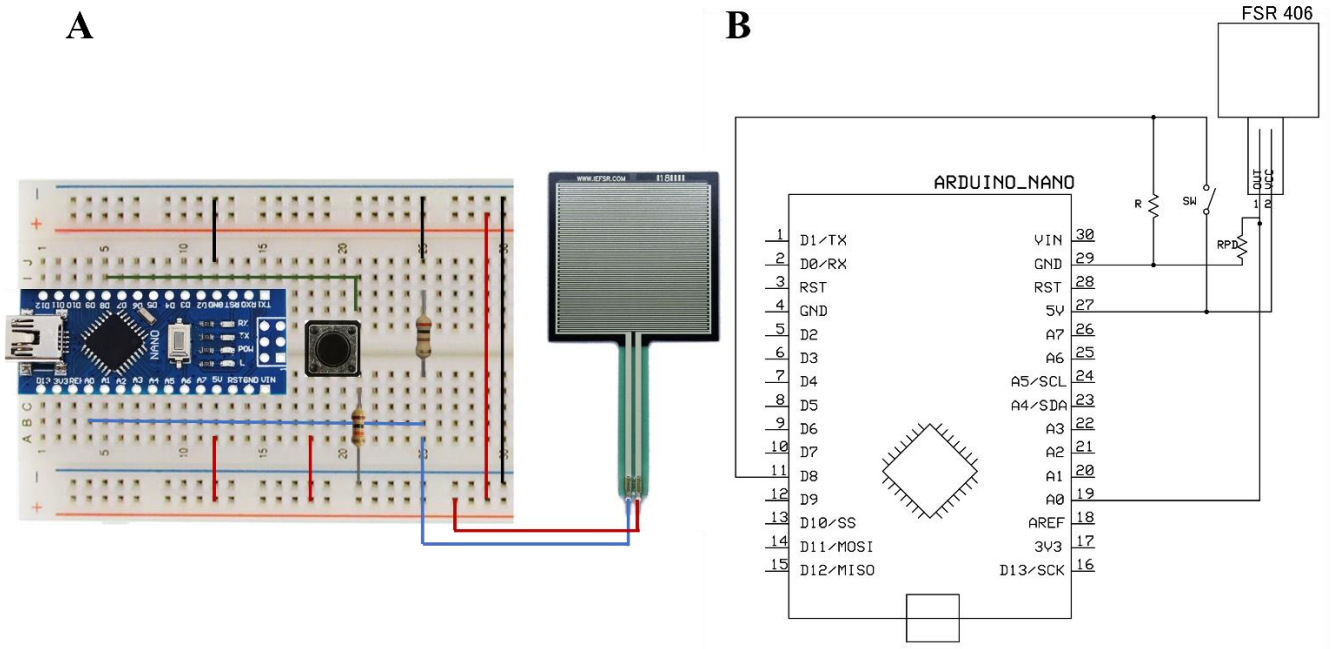

Figure A.5. Analog pressure sensor FSR 406 circuit assembly on the breadboard (A) and respective circuit schematic (B), with R = 1 kΩ and RPD = 0.2 kΩ.

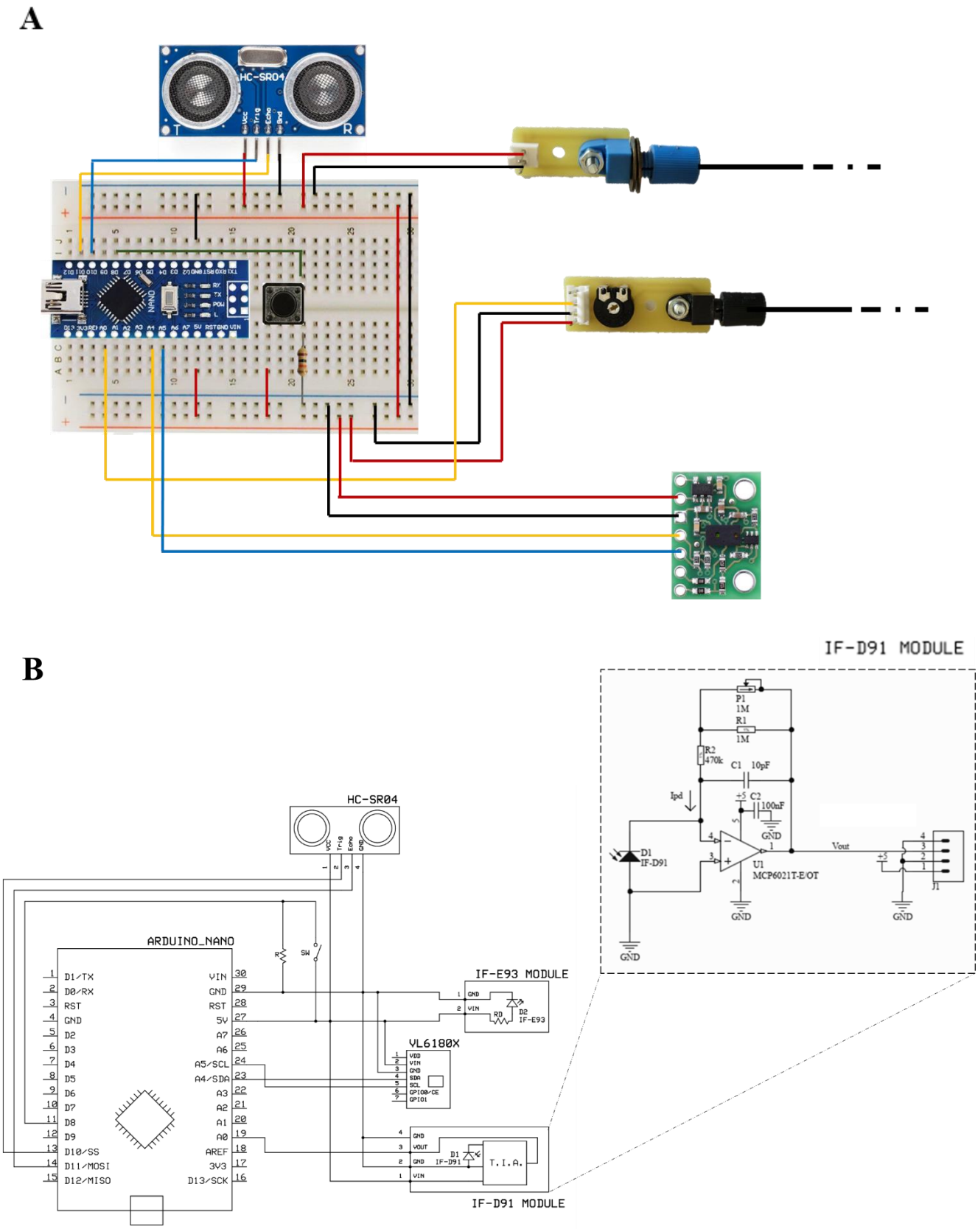

Figure A.6. Ultrasonic sensor HC-SR04, digital infrared sensor VL6180X and optical fiber macrobending sensor with LED source IF-E93 and photodetector IF-D91 circuit assembly on the breadboard (A) and respective circuit schematic (B), with R = 1 kΩ, RD = 75Ω and RPD = 2.2 kΩ. A photodetector IF-D91 module transamplifier impedance circuit is available, with component values discriminated on the circuit schematic.

B. SENSOR TESTING PROTOCOLS

Test Protocol I – Sensor Response to Compressions

For each sensor, perform three different acquisitions:

1. Wait until signal stabilization (about 5 seconds);
2. Perform 10 to 15 correct chest compressions;
3. Allow signal stabilization.

Test Protocol II – Sensor Response to Variations in Compressions Components

For each sensor, for each compression parameter to be tested, perform three different acquisitions:

1. Wait until signal stabilization (about 5 seconds);
2. Perform 10 to 15 compressions of each parameter variation* tested;
3. Perform 5 second pauses between parameter variants (or wait until signal stabilization);
4. At the end of the acquisition, allow signal stabilization.

***Compression parameters and respective tested variants:**

1. Hand position:
    a. Correct hand position (middle of the chest)
    b. Incorrect hand position
2. Compression depth:
    a. Shallow compressions (< 5 cm)
    b. Correct compression depth (5 to 6 cm)
    c. Deep compressions (> 6 cm)
3. Compression rate:
    a. Low compression rate (60 to 70 compressions per minute)
    b. Correct compression rate (100 to 120 compressions per minute)
    c. High compression rate (130 to 140 compressions per minute)
4. Chest Recoil
    a. Correct chest recoil (full decompression)
    b. Incorrect chest recoil

Test Protocol III – Pressure Sensor Response to Hand Position

For each sensor, perform three different acquisitions:

1. Wait until signal stabilization (about 5 seconds);
2. Perform 10 to 15 compression with correct hand position (middle of the chest);
3. Wait 5 seconds for signal stabilization;
4. Preform 10 to 15 compressions with incorrect hand position in different chest places, with 5 second pauses in between:
    a. Bellow correct hand position (stomach)
    b. Above correct hand position (top of sternum)
    c. On the right of correct hand position (right ribs)
    d. On the left of correct hand position (left ribs)
5. Allow signal stabilization.

Calibration Protocol for Optical Fiber Macrobending Sensor

Perform different acquisitions:

1. Wait until signal stabilization (about 5 seconds);
2. Perform 30 compressions with the corresponding variation parameter*;
3. Allow signal stabilization;
4. Wait for physical recovery before repeat acquisition.

***Compression parameters variations to be included:**

a. correct compressions – preform 3 acquisitions;
b. shallow compressions (< 5 cm) – perform 2 acquisitions;
c. deep compressions (> 6 cm) – perform 2 acquisitions;
d. incorrect recoil – perform 2 acquisitions.

Test Protocol IV – Protocol for Sensor Comparative and Quantitative Analysis

Perform two different acquisitions:

5. Wait until signal stabilization (about 5 seconds);
6. Perform two sets of 30 compressions with the corresponding variation parameter*;
7. Perform 20 to 30 second pauses between compression sets;
8. Allow signal stabilization;
9. Wait for physical recovery before repeat acquisition.

***Compression parameters variations to be included:**

a. correct compressions;
b. shallow compressions (< 5 cm);
c. deep compressions (> 6 cm);
d. low compression rate (< 100 compressions per minute)
e. high compression rate (> 120 compressions per minute)
f. incorrect recoil;
g. incorrect hand position

Training Protocol

For every training acquisition:

1. Wait until signal stabilization in the beginning (about 5 seconds);
2. Perform full CPR training, with 6 sets of compression and ventilations in a 30:2 ratio;
3. At the end of the acquisition, allow signal stabilization;
4. Wait for physical recovery between different acquisitions.

C. TESTED ALGORITHMS FOR PEAK DETECTION

Several algorithms for peak detection were tested while studying the most adequate alternative for this application needs.

A similar, yet more commonly, used maxima detection algorithm, that compared a data point *n* depth with the two left neighbors and the two right neighbor data points was tested, with similar results to the used algorithm, although slightly more robust to erroneous detection of signal roughness peaks. Pre-compression events were equally incorrectly detected, implying the use of the timeout technique to isolate compression maxima peaks. Thus, it showed no great advantage in comparison with the used algorithm, being this chosen since it required fewer neighbor points for maxima detection.

Alternatively to more standard maxima detection algorithms, and inspired in the results obtained by Palshikar [105], three different peak functions which capture the "spikiness" of a data point *n* in the local context were also tested. "Spikiness" values above a certain threshold were considered peaks. Different number of neighbors and different "spikiness" threshold values were taken into consideration for a strengthened peak detection. Despite of the mathematical differences, all three algorithms were immune to erroneous detection of peaks due to signal roughness and pre-compression events. On the other hand, they identified not only maxima peak points but also the surrounding neighbors as "peaks" with adequate "spikiness" values. This shows the inadequacy of these approaches for the available data. Once more, using the peak timeout technique, this problem was solved, with the selection of the maximum peak per compression. Nevertheless, the computational load associated with the use of these expressions is certainly bigger than the computational load of the selected algorithm and might be inadequate for a real-time implementation.

Thus, none of these approaches seems to bring additional advantage or optimization to the selected algorithm for compression peak detection.

2021

INÊS ISABEL CANELAS NUNES JORGE

DEVELOPMENT OF AN OBJECTIVE MEASUREMENT SYSTEM FOR QUALITY ASSESSMENT OF CHEST COMPRESSIONS DURING CPR

NOVA SCHOOL OF SCIENCE & TECHNOLOGY